Mapping of causes for increase in dissolved natural organic matter in a Czech watershed

Martine Carlson

Master thesis
Lektorprogrammet
30 credits

Department of Chemistry
Faculty of Mathematics and Natural Sciences
UNIVERSITY OF OSLO

[June/2021]

Mapping of causes for increase in dissolved natural organic matter in a Czech watershed.

2021

Mapping of causes for increase in dissolved natural organic matter in a Czech watershed

Martine Carlson

http://www.duo.uio.no/

Trykk: Reprosentralen, Universitetet i Oslo

Abstract

Dissolved organic matter (DNOM) is a mixture of heterogeneous hydrophobic and hydrophilic organic molecules that is ubiquitous in surface waters. It is formed from biodegradation of plant and microbial remains. DNOM differs in molecule size, polarity, light absorbing qualities, and bioavailability. This DNOM has a great impact on the water chemistry and the aquatic ecosystems living there by affecting the acidity, as well as transport of heavy metals and organic pollutants. Moreover, drinking water treatment plants (DWTP) that uses surface waters as a source of raw water are greatly affected by DNOM as it causes taste and odour problems as well as formation of harmful disinfection by-products in purification processes.

There has been an increasing concentration of DNOM in surface waters over the past decades in many regions with acid soils. The drivers of this increase is known to be decrease in acidic rain, alternation in precipitation pattern and increased temperature. Also, catchment characteristics are found to highly influence the amount and quality of DNOM in surface waters and the effect of the drivers of increased DNOM.

Increasing concentrations of DNOM causes the DWTP to have to adapt their raw water purification processes by increasing the coagulant and disinfection doses. It may even be necessary to modify the purification process in the treatment plants in order to adjust to the changes in raw water quality. Monitoring of the changes in the water quality is therefore key to generate the knowledge and awareness that is needed in order to sustain drinking water quality.

In this thesis, the temporal and spatial differences in the amount and quality of DNOM in runoff from catchments in the southeast of The Czech Republic are assessed. Moreover, data on the regional temporal drivers for changes in DNOM have been data mined and compiled and the spatial differences in the catchment characteristic are addressed.

The aim of this thesis is to reveal the temporal and spatial differences between the amount and quality of DNOM, as well as the physicochemical characteristics, of raw water samples collected from a set of catchments used as raw water sources in the Czech Republic. This is achieved by studying changes in the regional drivers (e.g., amount of biomass, temperature, precipitation and sulphur deposition) at the sites as well as the spatial difference sin catchment characteristics.

Preface

This master thesis has been carried out at the Department of Chemistry, Univercity of Oslo, in 2021. First and foremost, I would like to express my deepest gratitude to my supervisor Proffesor Rolf D. Vogt for his valuable comments and unique patience. I am especially grateful for Camille Carpart for helping me with R and always having such a good sprit. I would like to thank our Czech partners for collecting and sending water samples for the purpose of this thesis. I am also gratefull to Susanne Jørntvedt Jørgensen for her help with coordinating and assisting any lab questions and Berit Kåsa for analyzing the DOC and ToN in the water samples recived.

Table of Contents

Abbreviations

DNOM	Dissolved natural organic matter
DOC	Dissolved organic carbon
DWARF	Drinking water avareness for the future
DWTP	Drinking water treatment plants
HCl	Hydrochloric acid
HMW	High Molecular Weight (>100 kDa)
HS	Humic substance
LMW	Low Molecular Weight (<100 kDa)
NDVI	Normalized difference vegetation index
NetCDF	Network Common Data Form
NIR	Near-infrared
NOM	Natural organic matter
PAR	Photosynthetically active radiation
pH	Negative logarithm of H^+ ions activity in solution
Red	Infrared r
S	Sulphur
SAR	Specific Absorbance Ratio
SOM	Soil organic matter

sUVa	Specific absorbance at 254 nm
sVISa	Specific absorbance at 400 nm
TotN	Total Nitrogen
TotP	Total Phosphor
UiO	University of Oslo
UV	Ultraviolet
UV-Vis	Ultra Violet and Visible range
VIS	Visible

List of Tables

List of Figures

Mapping of causes for increase in dissolved natural organic matter in a Czech watershed

1. Introduction

Over the past decades here has been observed an increase in colour in many surface waters in Eastern North America as well as central Europe (Erlandsson et al.,2008; Skjelkvåle et al., 2005; Worrall et al. 2003). This increase has been found to be mainly due to increased concentrations of dissolved natural organic matter (DNOM) (Eikebrokk et al., 2004; Hongve et al., 2004; Monteith et al., 2007; Skjerkvåle et al., 2003). DNOM is a heterogenous mixture of hydrophobic and hydrophilic organic molecules of aromatic and aliphatic carbon, encompassing a wide range of molecule size, polarity, light absorbing qualities, and bioavailability. It has great impact on the water chemistry and the aquatic ecosystems by affecting the acidity, as well as transport of heavy metals and organic pollutants (Matilainen et al., 2011). DNOM is in addition a source of nutrients and energy for heterophilic bacteria. The DNOM quality controls the extent to which DNOM is bioavailable for microorganisms. The degree to which DNOM is consumed by microorganisms depend on its size and structure. When addressing the quality of DNOM it is useful to distinguish between high molecule weight (HMW) and low molecule weight (LMW) moieties. HMW humic DNOM consist of more aromatic DNOM with longer conjugated double bonds than LMW DNOM. LMW is more oxygenated and hydrogen saturated. This LMW DNOM is thus more bioavailable for microorganisms and easier biodegradable than HMW DNOM. The HMW DNOM is on the other hand more responsible for most of the colouring of surface waters.

Moreover, DNOM affects the raw water quality for drinking water treatment plants (DWTP) by causing taste and odour problems, in addition to promoting formation of harmful disinfectant by-products (Reckhow and Singer, 1990) and biological growth in water distribution networks (i.e., fouling, Eikebrokk et al., 2004). Due to this the level and quality of DNOM are important factors in development and operation of water treatment processes. The increasing concentrations of DNOM causes the DWTP to have to adapt their raw water purification processes by increasing the coagulant and disinfection doses (Eikebrokk et al., 2004). It may even be necessary to modify the purification process in the treatment plants in order to adjust to the changes in raw water quality. Monitoring of the changes in the water

quality is therefore key to generate the knowledge and awareness that is needed in order to sustain drinking water quality

DNOM in dystrophic surface waters is manly derived from the watershed (i.e., allochthonous) while in eutrophic lakes the main DNOM fraction is produced in the lake (i.e., autochthonous). The origin of allochthonous DNOM is mainly degradation products of plant, animal, microbial remains and excretion. The quantity and quality of DNOM in dystrophic surface waters is thus mainly controlled by the amount and type of biomass in the watershed. The amount of biomass is found to be increasing in the many boreal and nemoral regions due to climate change (longer growing season), accumulation of reactive nitrogen and increase atmospheric CO_2, as well as land-use change. The flushing of DNOM is governed by amount and intensity of precipitation, by dictating the flow regime in the catchment, and by the water chemistry governing the solubility of DNOM. Elevated ionic strength due to e.g. carbonates in the soil (i.e., hard water) decreases its solubility. The past decrease in acid rain has led to a substantial decrease in ionic strength as well as loss of labile aluminium, which acted as a precipitating agent of the DNOM. The observed increases in DNOM quantity and changes in quality in surface water, is thus mainly governed by the increased biomass and precipitation amount and intensity, as well as decreased acid rain loading. The relative importance of these drivers is determined by catchment characteristics (Fikstvedt, 2021). There is therefore a need to link DNOM quantity and quality to both the changing regional pressures as well as catchment characteristics in order to understand and predict future trends in DNOM. This is a prerequisite for the DWTP enabling them to adjust water treatment efficacy (Vogt et al., 2004; Hongve et al., 2004).

Summing up, in order to understand the change in DNOM concentration and quality in surface waters over time there is need to know how its main drivers (i.e., climate change, amount of biomass, loading of sulphur deposition) have been changing. There is also a need to recognize important catchment characteristics governing the impact of these changes.

1.1 Aim of study

This thesis work is an integral part of the project “Drinking Water Readiness for the Future (DWARF)” within the KAPPA program financed through EEA and Norway Grants. The project is inspired from a cooperation among water basin authorities, drinking water producers and Czech and Norwegian research partners for drinking water readiness for the future.

The aim of this thesis is to reveal the temporal and spatial differences between the amount and quality of DNOM, as well as the physicochemical characteristics, of raw water samples collected from a set of catchments used as raw water sources in the Czech Republic. This is achieved by studying changes in the regional drivers (e.g., amount of biomass, temperature, precipitation and sulphur deposition) at the sites as well as the spatial difference sin catchment characteristics.

2. Theory

2. 1 Dissolved natural organic matter (DNOM) characteristics

Natural organic matter (NOM) is used as a common denominator for all forms of natural organic biomass. Dissolved natural organic matter (DNOM) is limited to the fraction of NOM that is found in the aqueous phase and passes through a 0.45µm membrane filter. DNOM is ubiquitously in surface waters and in soil- and groundwater (Bolan et al., 2011; Vogt et al., 2004). DNOM is a heterogeneous mixture of hydrophobic and hydrophilic organic molecules of aromatic and aliphatic carbon (Matilainen et al., 2011). The relatively hydrophobic fraction, generally accounting for more than 50% of the DNOM in surface waters, is commonly referred to as humic substance (HS) that consists mainly of a complex mix of uncharacterizeable compounds. This high molecular weight and aromatic DNOM is more coloured and is thus mainly responsible for the "browning" of surface waters (Clark et al., 2010; Gjessing, 2013). The remaining DNOM is the non-humic fraction that is made of more identifiable organic compounds such as carbohydrates, lipids, carboxylic acids, amino acids, proteins and hydrocarbons.

The distinguishable non-humic portion of the DNOM constitutes the fulvic moieties of the DNOM pool. DNOM that is bioavailable for heterogeneous microorganisms undergo biodegradation reaction and may be completely mineralized or partly oxidized forming proteins, carbohydrates and lipids that have lower molecule weight (Gjessing, 2013). Likewise, the humic moieties of DNOM, that absorbs radiation due to conjugated double bond chromophores, may be photo-oxidized (i.e., photo bleached) to smaller, less aromatic and more hydrophilic and saturated organic compounds.

The degradation products and metabolic bi-products, as well as more recalcitrant polymers such as lignin, can again undergo various synthesis reactions forming larger molecules that are more

robust and resistant to further microbial degradation. This again forms the humic part of DNOM.

The dissolution from NOM to DNOM in soil depends on the structure of the DNOM molecule as well as the chemical properties of the soil solution. Small saturated and polar NOM molecules are more hydrophilic and thus more soluble in water compared to larger aromatic NOM molecules. Moreover, the solubility of DNOM is controlled by its content of weak acid functional groups. Proteolysis of these weak acids renders the DNOM negatively charged. This increases the solubility due to that the negatively charged molecules are more polar and thus more hydrophilic. The charge depends on pH and the level of trivalent cations in the solution (Clark et al., 2010). If the pH in the soil solution is relatively low, the degree of proteolysis is low. In addition, a low pH increases the dissolution of aluminium and iron in the soil solution. Protolyzed negatively charged DNOM form complexation with trivalent cations. This reduces the hydrophilicity and the solubility of DNOM in water.
The negative charge on DNOM is balanced by a diffuse layer of polyvalent cations around the molecule. This positively charged outer- and negatively charged inner layer of the molecule is referred to as the diffused double layer (DDL) (Håland, 2017). The thickness of the DDL layer affect the solubility of DNOM. This is controlled by the ionic strength of the soil solution. Increased ionic strength reduces the thickness of the DDL layer and reduces thereby the repulsion between the molecules allowing for a greater flocculation and thus decreased solubility (de Wit et al., 2007; Håland, 2017; Vogt et al., 2004).

2.1.1 Chromophoric DNOM

The change in watercolour is due to DNOM´s chromophores qualities that enable it to absorb light. Chromophoric (i.e., coloured) DNOM (CDNOM) consist of many aromatic rings and aliphatic chains constructed by conjugated double bonds that absorb ultraviolet (UV= λ10-400nm) and visible (Vis= λ310-1100nm) wavelengths of the electromagnetic spectrum.

DNOM absorbance in the UV and Vis spectra is mainly caused by different lengths of conjugated double bonds. Single carbon-carbon double bonds (C=C) adsorb UV radiation at λ180 nm. The absorption wavelength increases with increasing length of the conjugated chain, stretching way up into the Vis spectra. In addition aromatic carboxylic groups and phenolic groups absorb UV radiation at λ205 nm, and λ270 nm, respectively. The specific UV

absorbance (sUVa) is referring to the normalized UV absorbance achieved by a unit amount of DOC (Abs@λ254nm/mg C L^{-1}) and varies according to the aromaticity and size of DNOM. Likewise, the specific Vis absorbance (sVISa) is referring to the absorbance in the Vis part of the spectra relative to the amount of DOC (Abs@λ254nm /mg C L^{-1}). I.e., this proxy is referring to the CDNOM that absorb light in the visual part of the spectra. HMW DNOM commonly has high sUVa and sVISa and are coloured. Vice versa LMW has low sUVa and sVIS, and is less coloured.

The specific absorbance ratio (SAR = Abs@λ254nm/Abs@λ400nm) is controlled by the molecule size. LMW CDNOM is known to have relatively high absorbance in the lower wavelength (i.e., blue shift) and has high SAR values. On the other hand, HMW CDNOM has relatively higher absorbance at longer wavelength (i.e., red shift) and thus a low SAR value. The reason for this is that as the length of the conjugated double bonds increases the absorbance also occurs at longer wavelength. Long conjugated double bonds are associated with increased aromaticity and molecule weigh.

Light absorption by CDNOM causes darkening of surface waters by inhibiting light from reaching lower part of the water column. Reduction in the amount and depth of photosynthetically active radiation (PAR 400 – 700 nm) available for phototropic aquatic organisms causes a reduction in the autotrophic activity. As a consequence of this there will be a decrease in primary production. Moreover, this forces the phototrophic organisms upward through the water column. In addition, when the colour becomes darker the water temperature rises due to the adsorption of the radiation energy. This can cause longer and stronger summer stratification of surface water lakes. (Arrigo & Borwn, 1996; Nima et al., 2019)

2.2 Catchment characteristics

A catchment is defined as a morphological landscape enclosure confined by where water that flows out at a given point is collected, with the highest point always on the edge of the catchment. Water flows in the catchment according to gravity, from the highest point in the landscape to the lowest. Depending on the porosity of the soil and its water saturation the percolating rainwater finds different flow-paths down into and through the soil and ends up into the watercourse. Catchments vary in size and shape and can be divided into sub-catchments, meaning smaller sub-units contributing with surface water tributaries within the catchment. The

vegetation type, soil cover and properties, bedrock geology, land use, water resident time, and catchment size influences the amount and quality DNOM that is exported from the soil organic matter (SOM) to surface waters (Sepp et al., 2019).

2.2.1 Type of vegetation cover

Surface waters draining catchments that have a high coverage of swamps, bogs and peat land are usually rich in DNOM. Catchments with forest cover have dense biomass and therefor also much NOM for degradation. This provides potentially more DNOM for transport from the terrestrial landscape to surface waters (Finstad et al., 2016; Larsen et al., 2011). Much of this DNOM is nevertheless sorbed to mineral soil along its flow-path towards the watercourse. The water in streams draining coniferous forest cover have higher concentrations of DNOM compared to deciduous forests (Sepp et al., 2019). Change in land use from outfield grazing to forest increases the biomass and thus the amount of available NOM for degradation and thereby the export of DNOM.

The Czech Republic has a high forest coverage. The forests have been expanding during the second half of the 20th century due to long term afforestation of infertile cropland. In 2015 33.8% of the Czech territory consisted of forest, of which 72.3 % of the forest cover was coniferous forest and 26.6 % broadleaved forest (*Ministry of the Environment of the Czech Republic, 2017).*

2.2.2 Soil organic matter (SOM)

The soil is differenced in six horizontal layers that generically differs from each other in terms of mineral- and organic matter content, density, colour, texture, structure, and thickness (Figure 1). The density generally increases downwards in the layers as the soil get more packed (Sciencefact, 2021).

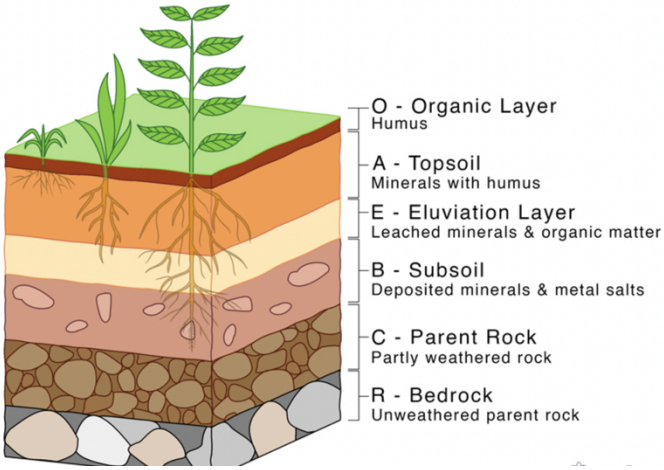

Figure1: Soil layers (From: https://www.sciencefacts.net/soil-horizons.html)

The decomposition of dead plant and biomass naturally starts in the organic layer (O) as this layer is rich in fresh organic matter. Topsoil (A) is the mineral layer beneath the O layer with

the most organic matter. An important aspect of this A layer is its density as it is relatively porous and therefore more exposed for sub-lateral runoff flow during periods with much and intense precipitation (Sciencefact, 2021). Water that flows sub-laterally through the O and A soil layers to surface waters is usually referred to as surface runoff. This flow-path conduit a high content of DNOM from the soil to surface waters due to less sorption to mineral soil. The amount and quality of DNOM that is transported to surface waters is thus depending on the flow paths in the catchment, which is governed by precipitation pattern and seasonally fluctuations.

2.3 Drivers for changes in DNOM concentration

The increase of DNOM in surface waters are to found to be governed by previous decrease in acidic rain (de Wit et al., 2007; Finstad et al., 2016; Garmo & Skancke et al., 2018; Skjelkvåle et al., 2003, 2008), changes in climate factors such as increase intensity and amount of precipitation (Hongve et. al., 2004) and increased biomass (Laesen et al., 2011a).

2.3.1 Decreased acid deposition

Emissions of sulphur dioxide and nitrogen oxides was a huge environmental problem in the second half of the 20th century, mainly because it led to acidic rain containing sulphuric and nitric acid. These strong mineral acids had a strong impact on aquatic ecosystems in rivers and lakes, as well as in forest and soil. In acid soil with poor buffering capacity the acid rain stimulated the release of toxic inorganic aqueous aluminium (EEA, 2011). In the water systems the acid rain caused a decrease in DNOM, as well as loss of acid neutralization capacity and nutrients.

There is a strong correlation between decrease sulphur deposition and increased DNOM concentration in surface waters that have been exposed to acidic rain (Finstad et al., 2016; Garmo & Skancke, 2018). Furthermore, the highest increase is found in surface waters that has had the largest decrease in acid deposition. This is caused by an increased solubility of the DNOM due to a combination of increased charge density of the DNOM and reduced ionic strength of the soil solution (de Wit et al., 2007; Ekström et al., 2011; Haaland et al., 2010; Monteith et al., 2007). Humic charge density is affected by the complexation of trivalent metal cations and protons to weak acid binding sites. When the acid deposition decreased the dissolution of the trivalent Al metal cations decreased along with the H^+-ions in the soil

solution. This led to a reduction in occupation of metal cations and protons to weak organic acid binding sites (Monteith et al., 2007) and thereby to a higher charge density of the DNOM, causing it to be more hydrophilic and thus more soluble. The decline in acid deposition lead also to a reduction in ionic strength because there are less ions in the solution, mainly due to the loss of the sulphate ion that was the major anion during acidic rain epochs. Decreased ionic strength leads to an increased repulsion between the DNOM molecules by stimulating increase thickness of the DDL (de Wit et al., 2007; Vogt et al., 2004). As a result of this the solubility of DNOM increases. This is especially the case for the less soluble moieties of DNOM. These fractions are often higher in molecule weight and more aromatic with a lower density of week acid functional groups. The decrease in sulphur emission has subsided and is no longer considered a present strong driver for increased concentration of DNOM in surface waters (Finstad et al., 2016)

2.3.2 Climate changes

Emissions of greenhouse gases causes the temperature to increase, this furthermore causes changes in the precipitation pattern and increased seasonal fluctuations. In addition, the changes in climate has expanded the growing season in the boreal and nemoral biomes. This leads to increased terrestrial biomass that subsequently is decomposed to DNOM. This contribute to the increase of DNOM in surface waters.

2.3.2.1 Increased temperature

According to the Global Climate Report (NOAA, 2020) the global temperature has increased by +0.08 ^{o}C per decade between 1880 to 1981, and by +0.18 ^{o}C since 1981. The Czech Republic is in the Temperate and humid continental climate region in the northern hemisphere. The lowest temperatures are found in the regions with mountains along the norther, eastern and south-western borders. While the warmest region is found in the lowlands along the south-western borders.

In humid climates, as in the Czech Republic, the temperature is a key factor for plant growth since a higher annual temperature causes a longer growing season (Larsen et al., 2011b). A longer growing season leads to more terrestrial carbon fixation, thereby a larger biomass density, also known as greening (Finstad et al., 2016). Increased temperature has also led to

elevated treelines, where forest limits are moving up so that the forests are expanding towards higher altitudes (Forsgren et al., 2015). Moreover, increasing winter-temperature at higher latitudes affects if the precipitation falls as snow or rain, in addition to alternation in the soil frost duration. Hence, affecting the pattern of leaching and watershed runoff. An increasing temperature also increases the rate of the decomposition reactions. This speeds up the transformation of plant- and microbial remains to NOM. With more available plant remains and a higher decomposition rate more terrestrial fixed carbon can be transported to surface waters as DNOM (Eikebrokk et al., 2004).

3.3.2.2 Alternation in precipitation pattern

The water cycle is highly depending on the air temperature, since higher temperature causes more water to evaporate as well as warmer air has the ability to hold more water vapour. As a consequence of global warming the precipitation pattern is becoming more intense with more flooding and short-term heavy rainfall as well as more severe droughts. This causes regions of the world that already have heavy rainfall to get wetter as well as the areas that have dry air and drought is at risk of becoming drier and warmer (IPCC, 2020). The alternation in precipitation pattern is therefore a strong indicator for global warming.

The flux of DNOM from the terrestrial landscape to surface waters increases with more intense precipitation and heavy flooding. This change is caused by the changes in water flow-path in the catchment as the soil gets saturated with water and thereby the runoff from soil to surface waters increases. As described in Chapt. 2.2.2 the soil profile gets denser downwards in the soil layers. This makes the upper organic rich O and A layers better conduits for the DNOM rich water facilitating sub-lateral transport from the terrestrial landscape to surface waters, thereby bypassing the absorptive capacity of the deeper mineral soil layer (Haaland et al., 2010).

2.4 Data Analysis

2.4.1 Normalized Difference Vegetation Index (NDVI)

Normalized Difference Vegetation Index (NDVI) is a graphical indicator that determines the fraction of radiation mainly absorbed for photosynthesis as a measure for the fraction of vegetation cover, generally referred to as greenness. This is thus a proxy for the density of biomass on the earth surface. The remote satellite monitoring is based on the sensing of distinct wavelength of visible red (λ620–750 nm) and near-infrared (λ800 to 2500 nm) sunlight reflected

by plants. Chlorophyll, the pigment in plant leaves that also makes them appear green absorb visible red light that is used in photosynthesis. On the other hand, the cell structure of the plant leaves reflects near-infrared (NIR) light. By measuring the intensity of red and NIR radiation coming off the Earth it is possible to quantify the photosynthetic capacity of the vegetation in a given pixel (e.g., of 1 km^2). The calculation of one NDVI value for the pixel is given from Equation (3) (The Earth Observatory, 2000).

(3) $NDVI = \frac{(NIR-Red)}{(NIR+Red)}$

NDVI calculation is always a number between plus one and minus one. A value close to zero indicates no vegetation (rock or bare soil) while a value close to plus one indicates the highest possible density of green leaves. Negative values are due to clouds, water and or snow. Where there is dense vegetation the reflected radiation in NIR wavelength is much greater than in the Red wavelength. If there is very little difference between NIR and Red reflected, then the vegetation is likely sparse and may consist of grassland, tundra or dessert (The Earth Observatory, 2000).

2.4.2 Statistical analysis – Loess regression

Loess regression is a non-parametric statistic approach that relaxes the linear assumptions of conventional regression methods. Instead it focuses on a fitted curve. Non-parametric regression is a category of regression analysis in which the predictor does not take a predetermined form but is constructed according to information obtained from the data.

This regression method fits multiple regressions in a local neighbourhood, and the fitted points are estimated based on the whole curve rather than one particular estimate. Loess regression is resourceful if the X variables are bound in a specific range and the dataset is large. The curve shows the moving average, a calculation for analysing data points by making a series of averages of different subsets of the whole dataset. A moving average is often used for time series data to smoot out short-term fluctuations and mark long-term trends or cycles.

(Prabhakaran, 2017)

3. Material and Method

The catchments that are studied in this thesis belong to the Otava River Blanice watercourses that are located in the southwest Bohemian region. All of the sampling points are along the

main river or tributaries to the rivers. Figure 2 points out the location of the sampling points. From the map one can see that Pisek, Černíčský potok, Volšovkou and Locenice are located along the Otava River and Putim and Podedvory are located along the Blanice River. The arrows indicate direction of water flow.

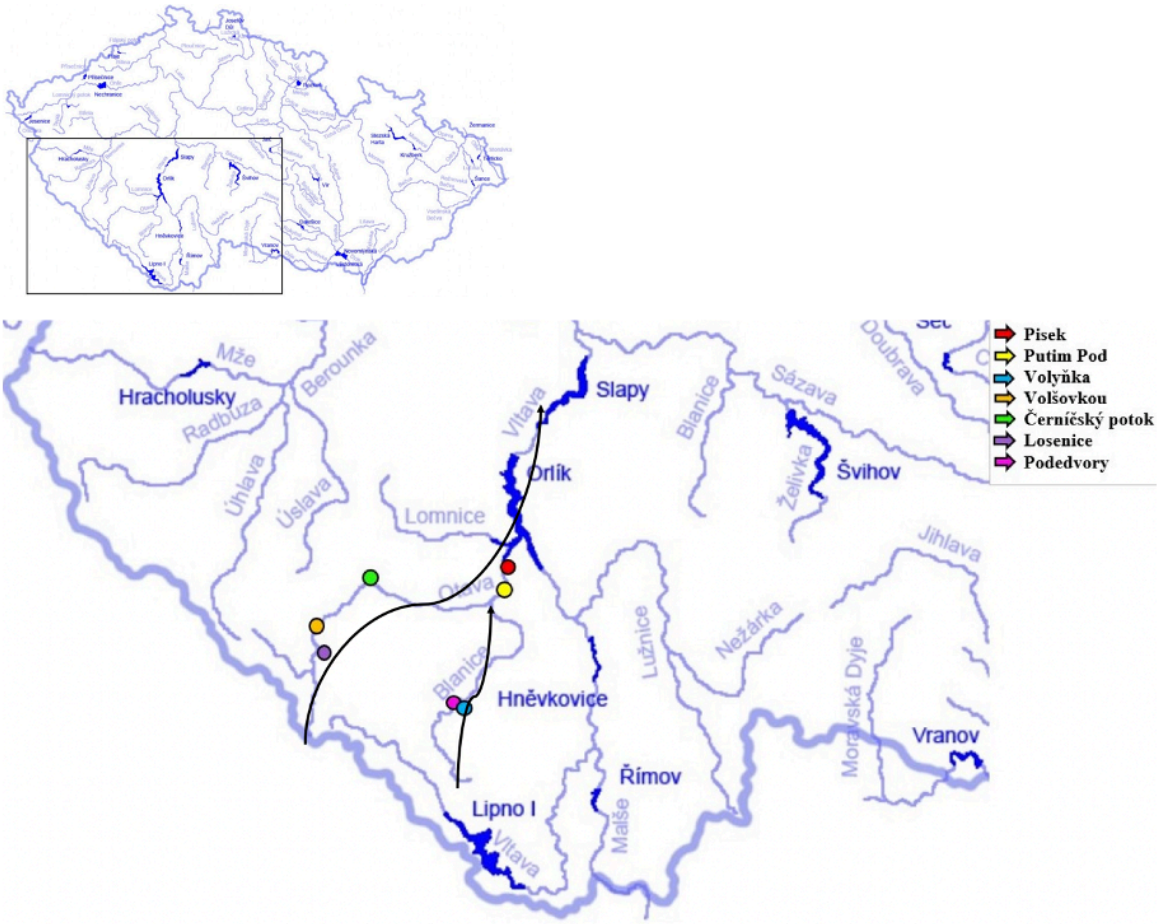

Figure 2: Sampling points in the Otava catchment along the Otava- and Blanice river.

The study in this thesis includes: 1) data mining for changes in drivers governing DNOM increase (i.e., sulphur deposition, temperature and precipitation, and biomass) over time; and 2) assessing temporal trend in previous water chemistry data sets, new results of the chemical analysis of water samples collected in 2021; as well as 3) comparing the water chemistry in the studied Czech catchment to lakes in southeast Norway.

3.1 Data mining for changes in DNOM drivers

3.1.1 Sulphur deposition

Data of temporal trends in estimated deposition of Sulphur (S) and Nitrogen in The Czech Republic was downloaded from the European Monitoring and Evaluation Program (EMEP, 2005, 2011, 2020). This is a co-operative program monitoring of long-range transmission of air pollutants in Europe. This scientifically based and policy driven program is under the Convention of Long-range Transboundary Air Pollution (CLRTAP) for solving the transboundary air pollution problems.

3.1.2 Temperature and precipitation

Climate maps of the Czech Republic as well as annual temperature and rainfall for the regions South Bohemia and Plzeň were downloaded from Czech Hydrometeorological Institute (CHMI, 2021). The aim was to get an overview over spatial differences in climate and the temporal climate development in The Czech Republic as well as locally in the regions of the sub-catchments in Otava.
Maps for the years from 1981-2010 are compiled with maps for each year from 2011-2020 in order to assess the development in annual temperature and precipitation.

3.1.3 Biomass

The Copernicus Global Land Service is a European flagship program of Earth Observation that monitors changes on continental biomass by monitoring biophysical variables describing the state, dynamism and the distribution of terrestrial vegetation (Copernicus, 2021a). As an integral part of this surveillance, they use NDVI as described in Chapt. 2.4.1 (Copernicus, 2021b). The NDVI indexes were used as a proxy for vegetation cover to detect if the biomass density had changed over time in the catchments.

The NDVI data are in the form of NetCDF files (i.e., .nc files) that contain NDVI data for the whole world. There are three NetCDF data files that are generated each month, finalized on the 1th, 11th and 21th, i.e. a total of 36 files a year. Each NDVI product covers accumulated observations for a period of 10 days, up to the 10th, 20th and the last day of the month. If there are three or more observations from the last 10 days, then only observations from these 10 days are used (Tavares et al., 2020). Otherwise, observations from the last 16 days were used. In the NetCDF file all the NDVI values are linked to coordinates as decimal degrees from the World Geodetic System 84 (WGS 84) (Bruno Smets et al., 2020: Fikstvedt, 2021).

Trends in vegetation density over time was assessed by studying the NDVI data in months of the year where the vegetation cover is found to be most dense; i.e., June, July and August (Finstad et al., 2016). Thus, nine NetCDF files were extracted for each year from 2000 to 2019. This resulted in 174 files in the time period 2000 to 2020. The NetCDF files divides the world into pixels with a 300m x 300m and 1000m x 1000m resolution. The $1km^2$ was downloaded in this case because the 300m x 300m was not available for the time period 1999-2016. The NDVI data was processed in the statistic program R-studio. This program is an integrated development environment for the R-langue that is well suited for making data analysis scripts, reports, graphs and more (R-studio, 2021). In R-studio R packages can be downloaded based on the required analysis. These packages are collections of functions and data sets that increase the power of R by improving existing base R functionalities, or by adding new ones. Several R packages were downloaded in the R-script, but most importantly the package "ncdf4" was downloaded to R-studio so that the netCDF could be read by R-studio and the NDVI data could be accessed.

The catchments that are included in this thesis had a shapefile (.shp) of the polygons in the catchments and the catchment outlines. The number of polygons in the shapefiles included in this analysis varied from 1 to 115. The sum of these polygons makes up the area within the shapefile. Due to how the shapefiles varied in the number of polygons the R-script was made to extract NDVI data for every year from 2000 to2020 (i.e., 9 files a year, a total of 180 files), and take the mean of every year in every polygon. Figure 3 shows as an example the shapefile of the watershed of Černíčský potok, which contained 5 polygons representing 5 cub-catchments. The mean of all the five polygons was bind together in one table including the standard derivation for each year. The combined mean of all polygons was so on plotted with a Loess regression to show the time trend in NDVI development over 20 years.

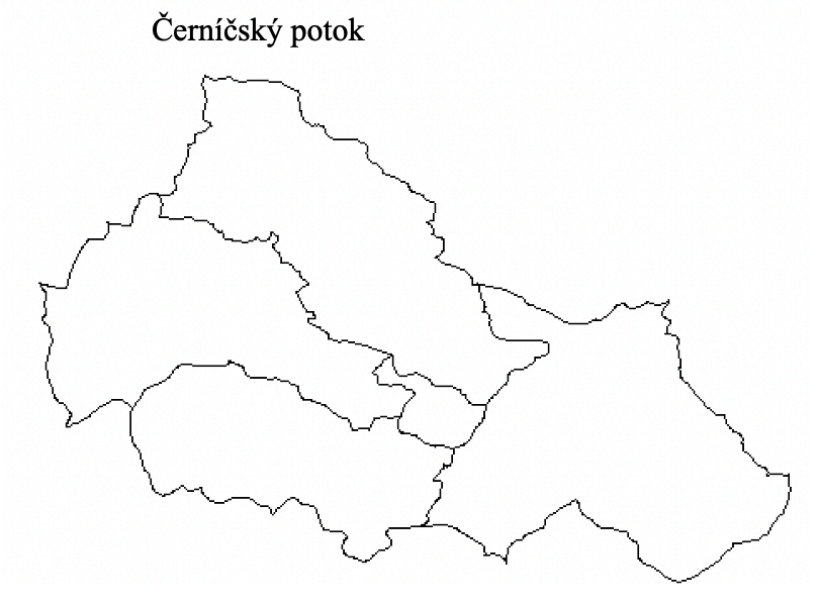

Figure 3: Shape of Černíčský potok catchment including the lines that show the 5 polygons constituting the catchment..

3.2 Assessing temporal trends in water chemistry

3.2.1 Old monitoring data

The old monitoring data were used to study temporal longer, trends as well as seasonal fluctuations. The old data were compiled with data generated from fresh samples (Chapt. 3.2.2) in an attempt to study a longer time trend. The old data was combined in a excel sheet, and the min, quartiles (25% and 75%), median was calculated for the chemical parameters that was of interest, these are used to compare the water chemistry of the surface waters in the Otava-catchment in chapter 4.2.2 and 4.3.2 and with the 100-lakes Project. The same calculations of 25%, median and 75% quartile was done for the 100-Lakes Project.

3.2.2 Analysis of fresh water samples

The 17 water samples that were received from the Czech Republic were delivered in 0.5L flask and had been filtrated through a 0.4 μm filter at the sample site. These samples were analysed for biodegradability of the DNOM, DOC, Total N and UV-Vis spectra. Combining these recent data with the older monitoring data allowed a comparison of the data.

3.2.2.1 Sample preparation

Upon arrival to the University of Oslo they were stored in the dark at 10 °C. Further sample preparation was done according to analysis requirements described in the following.

3.2.2.2 Biodegradation

The analysis was carried out at the Section for Environmental chemistry, Dept. of Chemistry, University of Oslo (UiO), using SensorDish® Reader to measure the O_2 concentration in the samples.

At day 0, asap. after sample arrival to UiO, the samples were prepared by filtrating trough a 0.2 μm syringe filter to remove most of the bacteria and filled into 30 mL containers. The syringe was flushed with the sample and the container was washed with filtrated samples as well as Type 1 water (ultra pure water) to remove any impurities. At day 1 the inoculum was prepared. The incubation starts at day 4 were the bacterial community goes through four phases:

1. “Lag phase” where the bacterial community adapts to the new environment.
2. “Exponential growth” where the bacterial community grows due to cell division.
3. “Stationary growth” where the amount of cell derived from metabolism is balanced by the number of cell deaths.
4. “Death phase” where cell death exceed cell growth.

During the “exponential growth” phase the bacteria uses oxygen and the concentration of O_2 in the water samples decreases. The slope of the oxygen concentration curve relates to the respiration rate of the bacterial community. This provides a proxy of degradation rate of DNOM and thus the biodegradability of the DNOM. (Crapart et al., 2021).

3.2.2.3 Dissolved Organic Carbon (DOC) and Total Nitrogen (TotN)

The DOC concentration is used as a proxy for DNOM in the water samples because it is the main component in DNOM, constituting about 50 w/w%. The analysis was measured at the Department of Bioscience, UiO, adhering to the ISO 8245 (1999) method.

The samples is deliverd to the combustion furnace with purified air. The samples undergoes a combustion trough heating up to 680C with a platinum catalyst. It undergoes a decomposition reaction when it converts to carbondioxide and NO gas. Then, the CO2/NO generated is cooled and dehumidified and sendt to the detectore. The concentration of the TC/TN in the samples are so on compared to a calibration curve. The standards making the calibration curve were made in the range of the ToTN og DOC from the old monitoring data from 2000-2006.

3.3.4 UV-Vis Absorbency

Ultraviolet-Visible (UV-Vis) spectroscopy is used to measure the absorbance of the DNOM In the water samples over the ultraviolet and visible part of the spectra. A Shimadzu UV-1800 UV-Visible Spectrophotometer with 1 cm quartz cuvettes was used to measure the spectrum of absorbance for the water samples. The wavelength (λ) was scanned from 200 nm to 800 nm. To background correct the spectrophotometer prior to the analysis one scanning with both cuvettes was filled with Type 1 water, moreover one of the cuvettes was filled with Type 1 water during the analysis as a reference. Values of absorbency at $\lambda = 254$ and $\lambda = 400$ were used to calculate sUVa, sVISa and SAR as described in Chapt. 2.1.1).

4. Results and discussion

The results of the data analysis and experimental laboratory work explained in Chapt. 3 "Materials and methods" are presented and discussed in this chapter. The time trends in regional factors that control the DNOM increase are presented, i.e. sulphur deposition, temperature and precipitation.

For each catchment area, the characteristics and development of biomass over time is presented. To achieve a better perspective of the catchment, some key parameters of their surface water chemistry are compared to results from a 100-Lakes Project studying surface waters in southeast Norway.

At the onset of this study, an important goal was to assess the trends of DNOM in surface waters, however only a limited number of catchments have monitoring data with proxies for this parameter, and only over a limited period of time. This made this difficult. However, the datasets of the three main catchments (i.e., Pisek, Volšovkou and Blanice Podedvory) have DOC data. This only made it possible to say something about changes in season from 2000-2006 and compare the levels of DOC to the water sample taken at January 18. 2021.

The spatial comparisons analysis of water chemistry is based on the monitoring data from 2000 to 2006. This temporal frequency of these dataset varied in extent between the catchments. This sets restraints for the assessment. Due to the lack of old data the results from the experimental lab work (UV-vis, TotN and biodegradability) are not included, though the result of these analysis are attached in the Appendix. The dataset from Czechia and 100-Lakes Project are provided in Appendix.

4.1 Time trends in drivers for increased DNOM concentration

4.1.1 Acid rain deposition

Temporal trends in deposition of Sulphur (S) and Nitrogen (N) in the Czech Republic are shown in Figure 4 (EMEP, 2005, 2014, 2020). The strong decline in acid deposition lasted until the turn of the century. By 2000 the S deposition had decreased by 83%, from 483 in 1980 to 83 Gg S in 2000. During the last 20 years the S deposition has decreased an additional 8% to a total of 91%. The same trends are seen for reduced and oxidized N, though the decrease are not so strong (i.e., 57 and 50%, respectively).

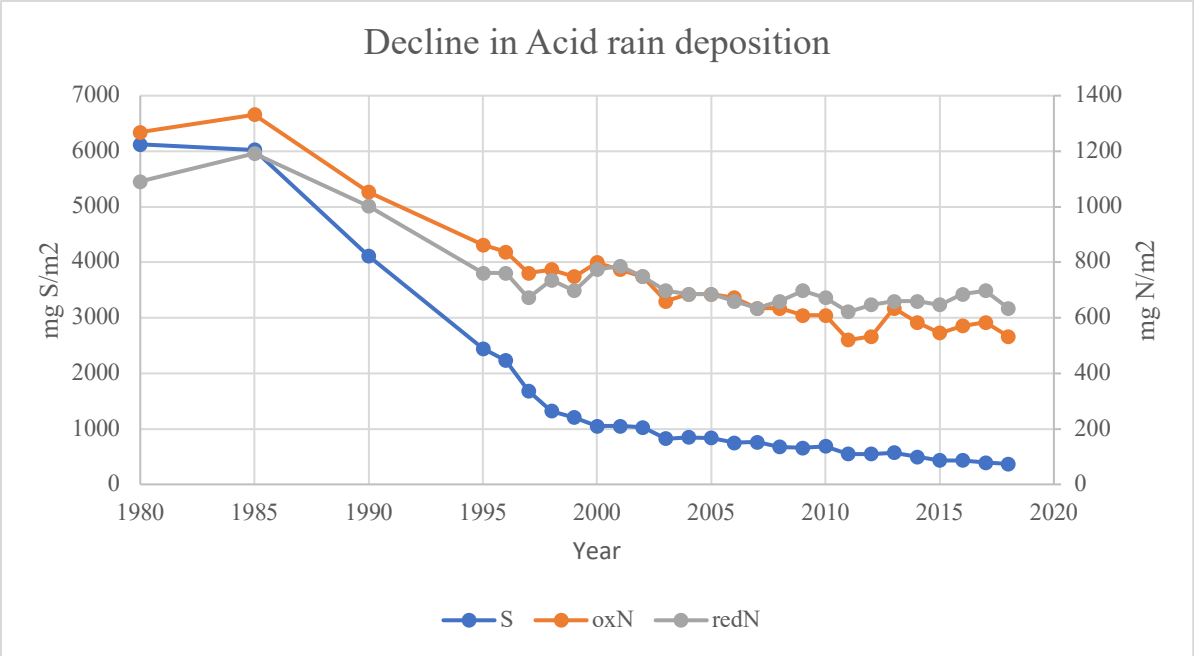

Figure 4:Decrease in Sulphur (S) and oxidized and reduced Nitrogen (N) deposition in Czech republic (EMP, 2005, 2014, 2020)

Figure 5 shows the spatial distribution in deposition of oxidised sulphur (mg S/m^2) (top), oxidised nitrogen (mg N/m^2)(middle) and reduced nitrogen (mg N/m^2)(lower) in Czechia (EMEP, 2020).

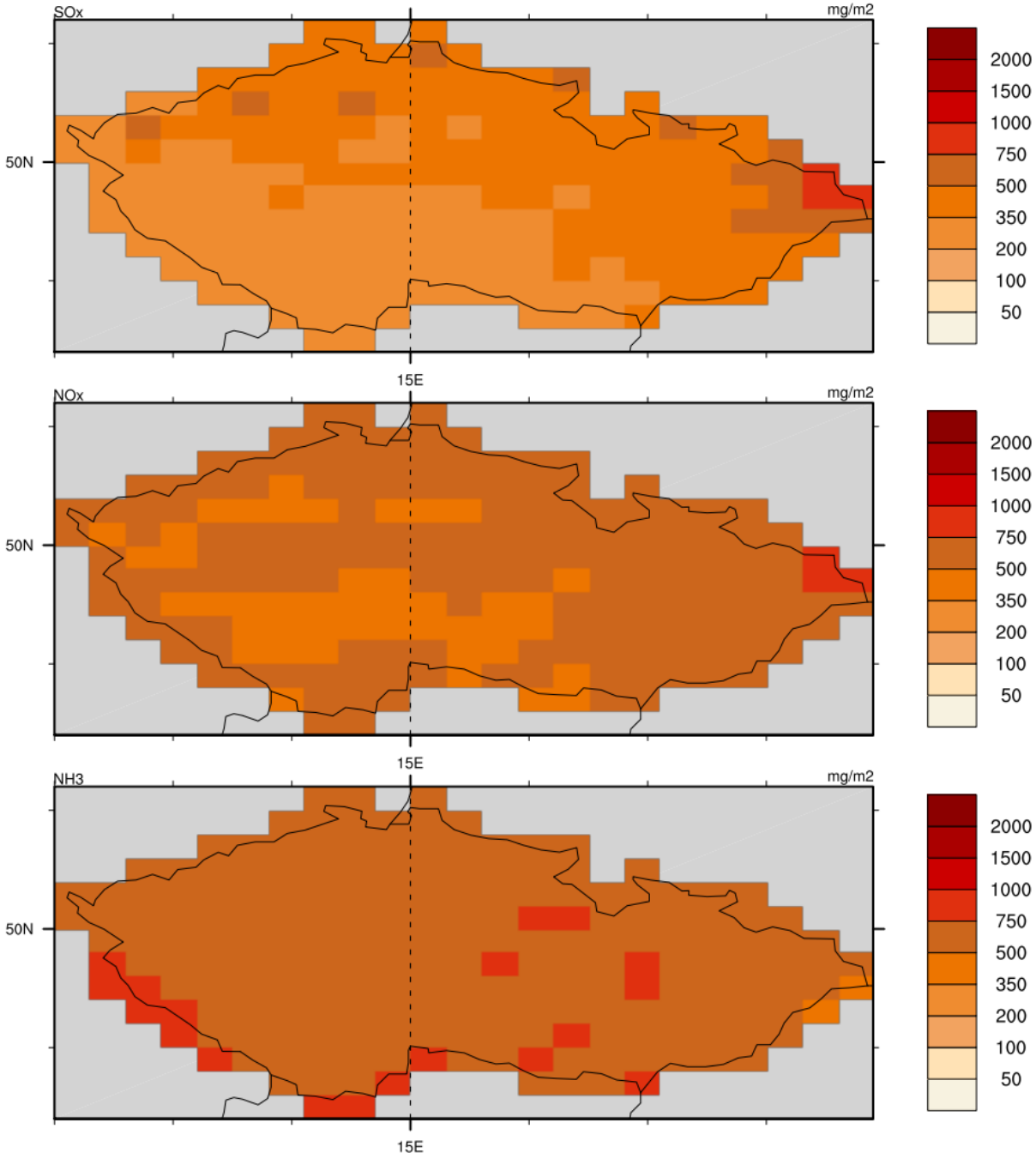

Figure 5:Spatial distribution in deposition of oxidised sulphur (mg S/m^2) (top), oxidised nitrogen (mg N/m^2)(middle) and reduced nitrogen (mg N/m^2)(lower) in Czechia (EMEP, 2020).

Sulphur deposition in Czechia is lowest in the study region (between 200 – 350 mg S/m^2 in 2018), though the deposition of oxidized (500 to 750 mg N/m^2) and especially reduced N (750 – 1000 mg N/m^2) is high along the border to Germany and Austria. For comparison the S, oxidized N and reduced N deposition in Birkenes, southernmost Norway, receiving the highest acid rain loading in Norway, was in 2012 measured to 448 mg S/m^2, 756 mg N/m^2 and 648 mg N/m^2, respectively, implying rather similar acid rain loading.

4.1.2 Temperature and precipitation

The average annual rainfall in The Czech Republic varies spatially between 450 mm to 1250 mm during the time period 1981-2010 and by years from 2011 – 2020, as shown in Figure 6. The darkness of the colour in the map answers to the amount of precipitation, i.e. the darker the colour the more precipitation in that graphical area that period or year. Apparently, the annual amount of precipitation varies and there was no significant development from 2010 – 2019. On the other hand, it is clear that 2013 and 2017 were exposed to more rainfall, while 2015 and 2018 were dryer years. In 2020, the amount of precipitation was high, especially in regions in southeast, in north and at one area in the middle. This indicates that the areas that had the most precipitation in 1981 to 2010 were even wetter in 2020.

The mean annual temperature varies spatially within the Czech Republic from 2 °C to 11 °C from 1981 – 2010. The year-to-year variation from 2011 to 2019 is show in Figure 7 From the figure it is clear that the temperature has increased over time. From 1980-2010, compared to 2011, 2012 and 2013 the colour is gradually getting darker. However, from 2013 to 2014 the temperature seems to rise significantly. This development continues to 2020, which indicates that the annual air temperature is rising in The Czech Republic.

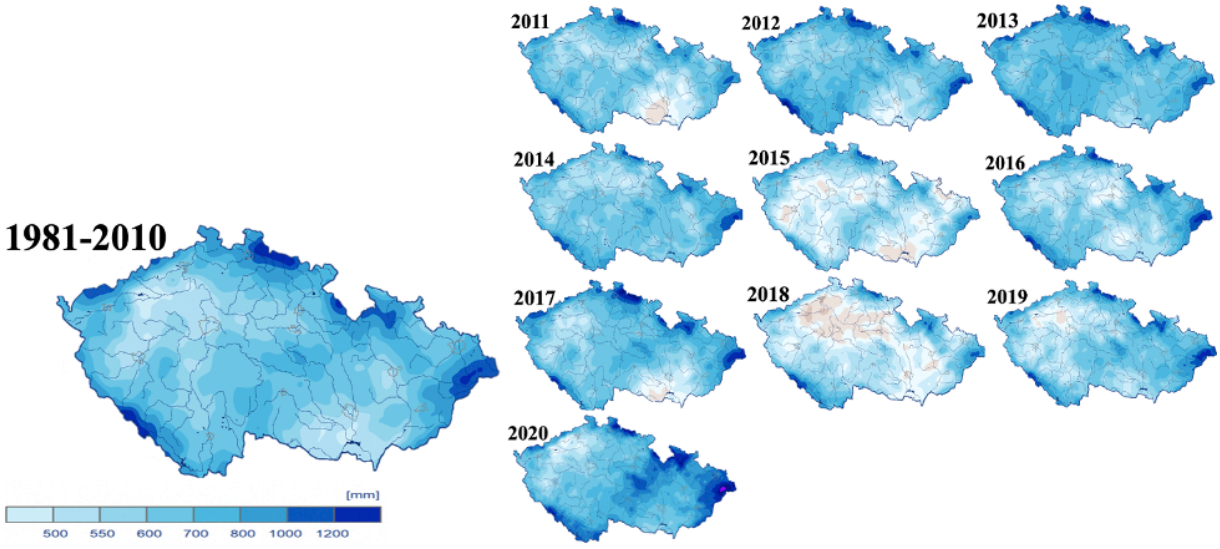

Figure 6: Climate maps of rainfall in The Czech Republic (CHMI, 2020).

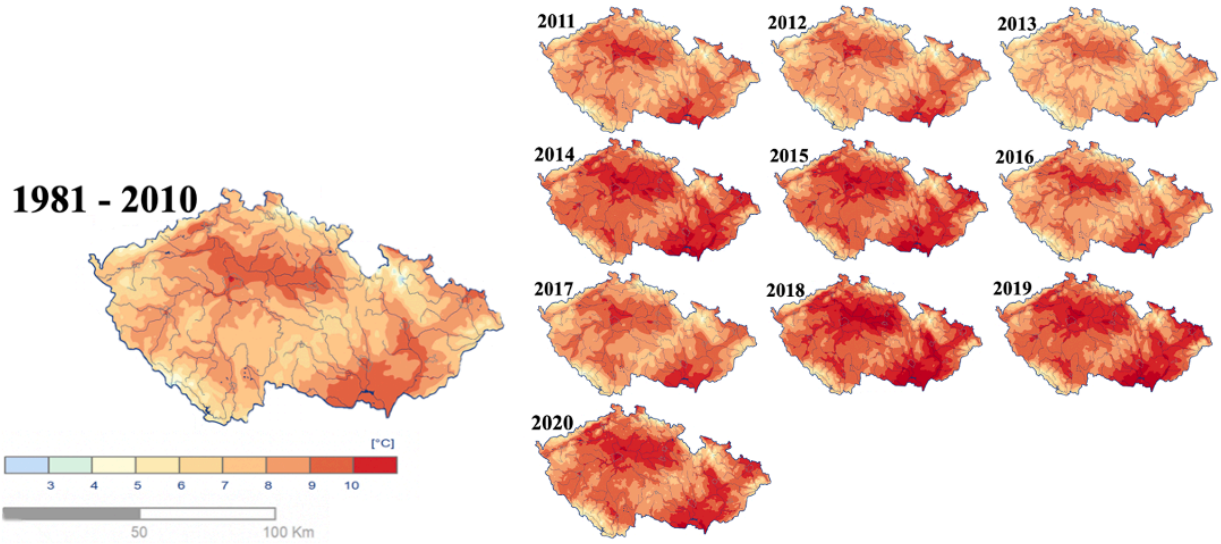

Figure 7 Climate maps of temperature in The Czech Republic (CHMI, 2020).

Figure 8 presents the annual rainfall from 1980 to 2020 in the region South Bohemia and Plzeň. The development of average rainfall over the last forty years does not indicate an increase. However, the temperature shows an increase for both regions (Figure 9).

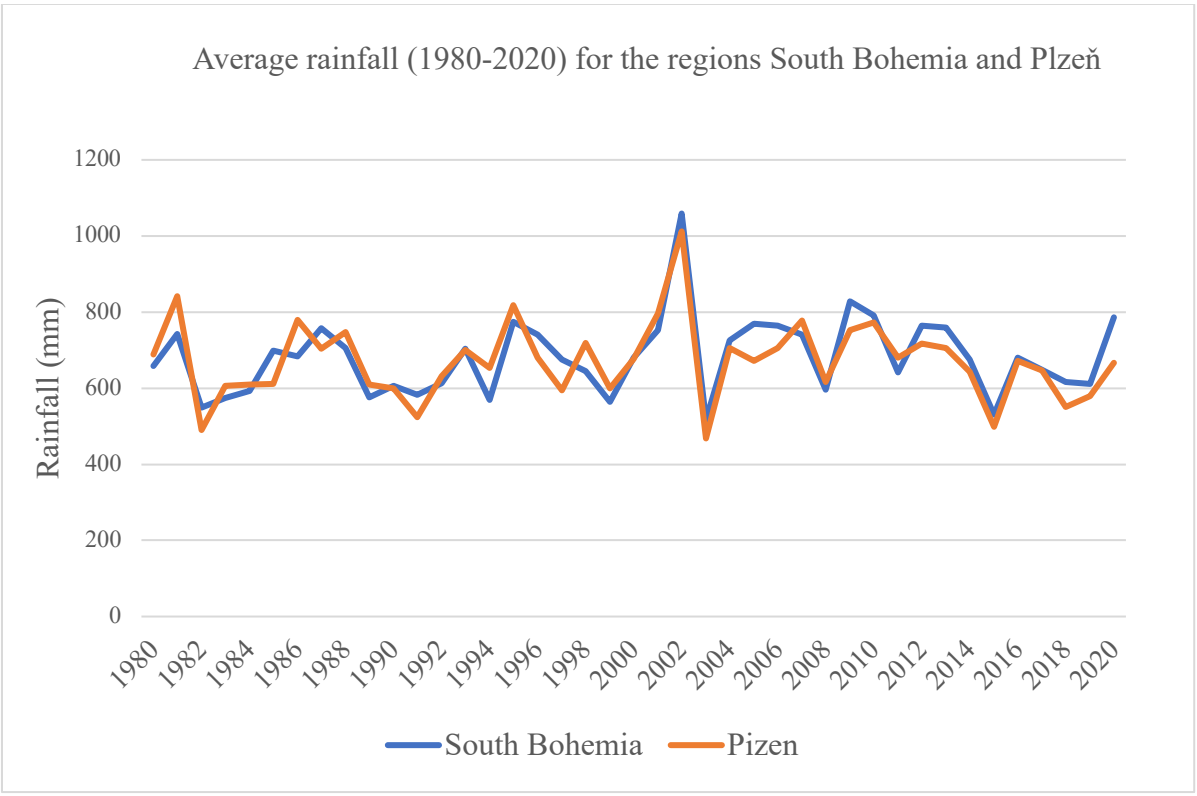

Figure 8: Average rainfall from 1980-2020 in the region South Bohemia and Plzeň (CHMI, 2020).

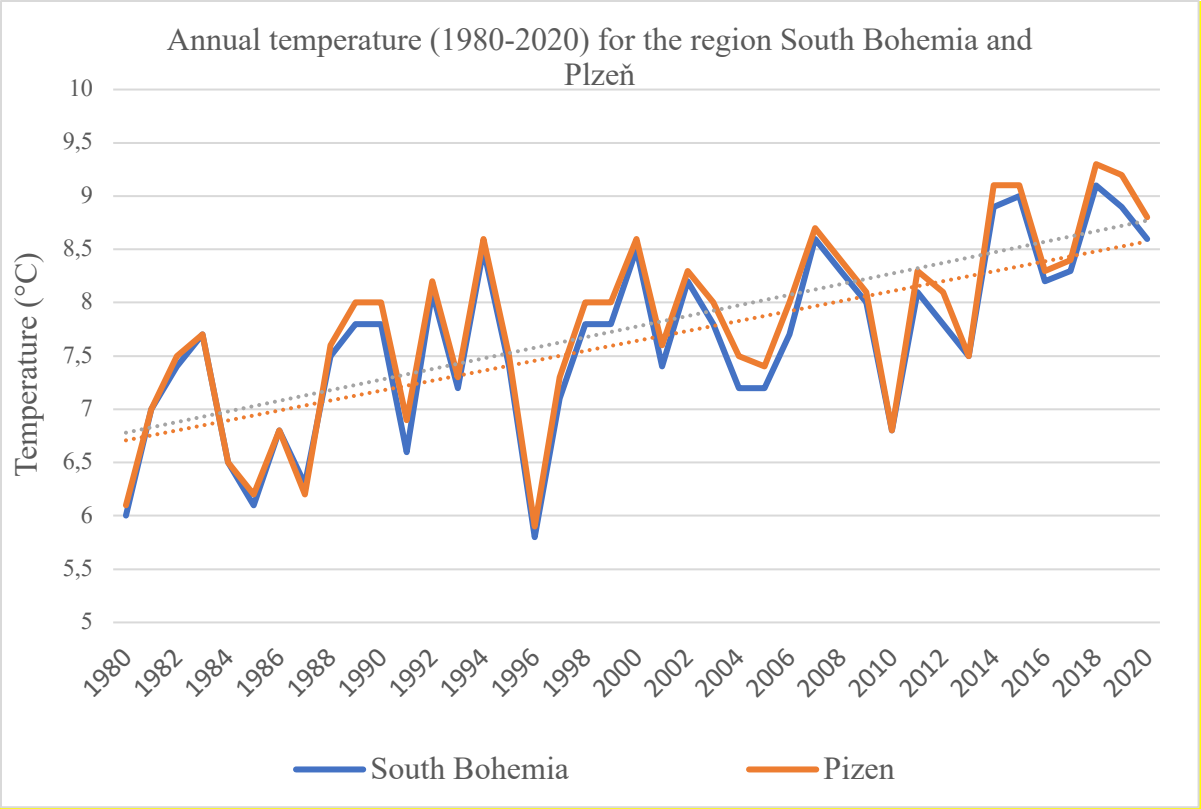

Figure 9: Average temperatures from 1980-2020 in the region South Bohemia and Plzeň (CHMI, 2020)

Summing up, both Sulphur- and reactive nitrogen deposition in Czech is greatly reduced during the last 40 years, although of which the studied region has the lowest sulphur deposition in Czechia. The temperature was found to have a significant increasing trend, however there was no indication of any specific seasonal changes. The amount and intensity of rainfall do not show any temporal trends.

4.2 Catchments characteristics

The compiled data on the studied catchments from the data mining are described in this chapter. All of the sampling points of the Otava catchment lies within a range of 922 square kilometers and are all tributaries to Otava River. However, quantitative analysis of their land composition cover shows that there are wide spatial difference in the land-use composition between the catchments. Although data exists, due to the limited time period, analysis of temporal difference was not within the scope of this study. In order to achieve some understanding of the water chemistry in the surface waters of the catchments only the key chemical parameters (i.e., pH, alkalinity, SO_4^{2-}, Ca^{2+}, total N and total P) were assessed. Importantly, the project is in an early phase and therefore the spatial comparison of the parameters is limited to the average, min, max, median, and quartiles.

Figure 10 shows the outlines of all the sub-catchments to Otava catchment, this illustrates the shape of the catchments. Also, the small lines within each catchments indicates the number of polygons (as described in 3.1.3). Figure 12a to 12gdisplay pie charts of the relative land cover composition, regarding forest, cropland, grassland, water and urban land. (Copernicus, 2019).

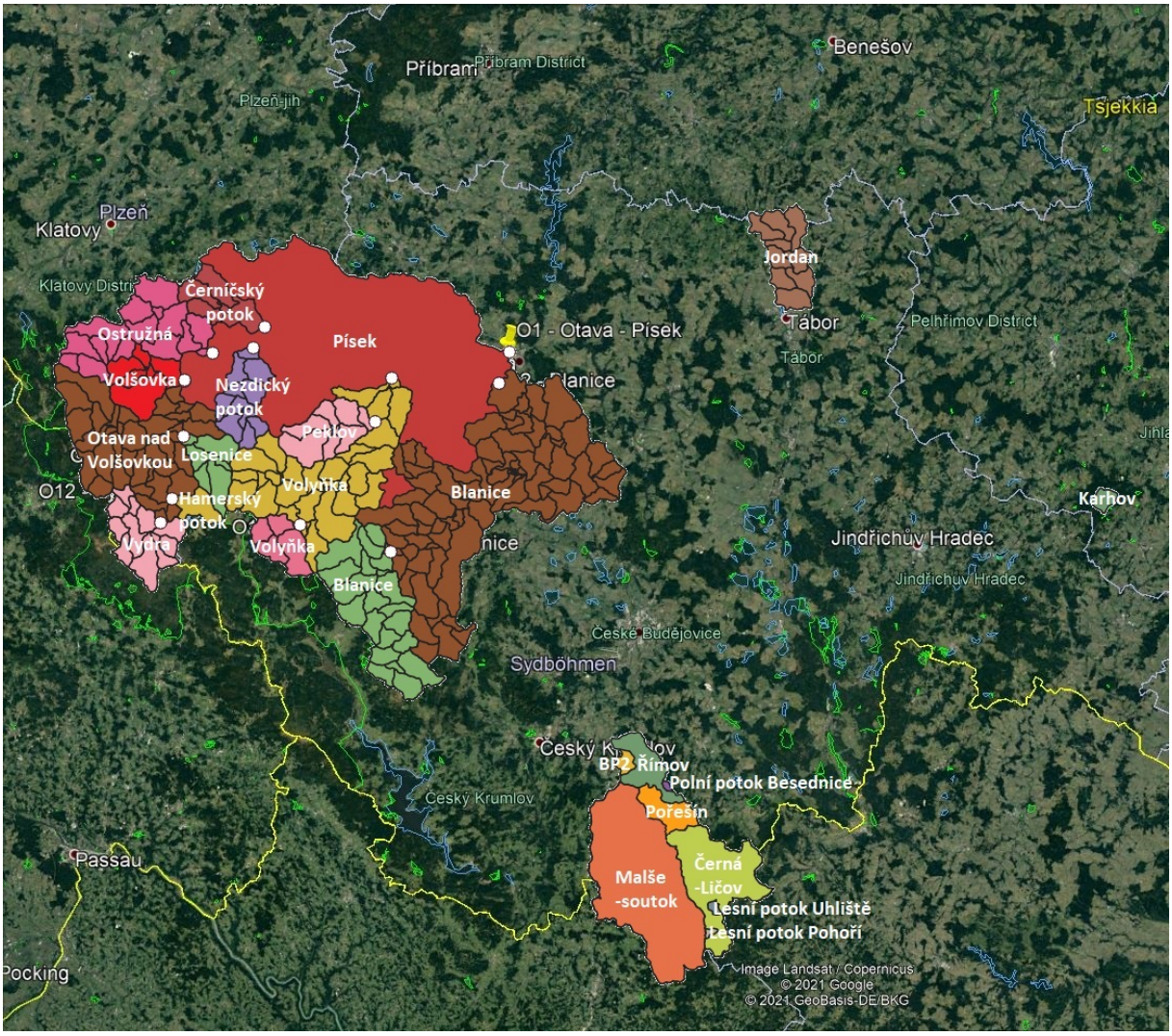

Figure10: The scape of the catchments outlines as well as polygons for all the sub-catchments in Otava.

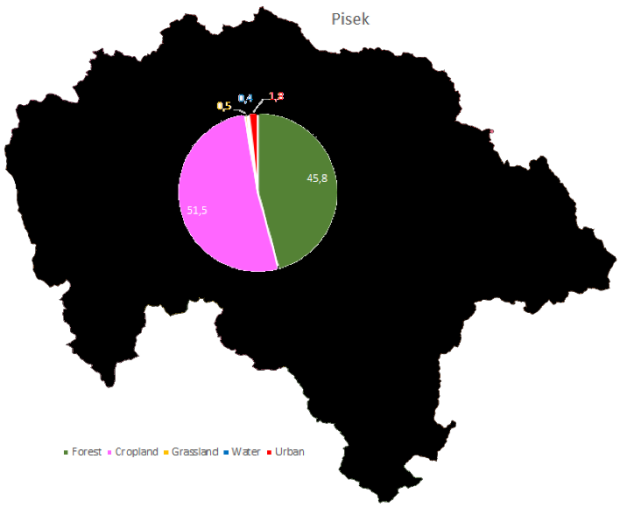

Figure 11a: Land cover composition in the entire Otava catchment.

Otava - Pisek nad sampling site is located just west of the city center of Pisek, one of the last city's the Otava river runs through before it merges with the larger Vltava river. This catchment covers thus the entire watershed of Otova and Blanice watercourse. This high order river has a high coverage of cropland (51.5%). The rest is forest (45.8%). The surface water has the highest Ca^{2+} concentration, almost 5 times higher than the low order Volšovka - Červené Dvorce and over 2 times more than the low order Blanice - Podedvory, as presented in Table 1.

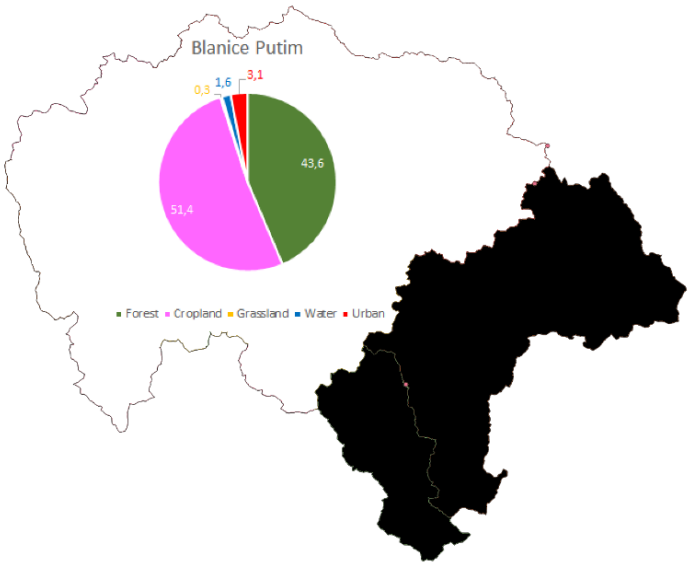

Figure 11b: Land cover composition in Blanice Putim catchment.

Blanice Putim pod comprises the entire Blanice watercourse, including the Blanice – Podedvory sub catchment. The sampling point is at the mouth of the watercourse where Blanice river meets Otava river. The Blanice watershed accounts for about a third of the Pisek catchment, Land-use composition is thus similar to Pisek, with domination of cropland (51.4%) and forest (43.6%). This similarity is mainly

order of these two watercourses.

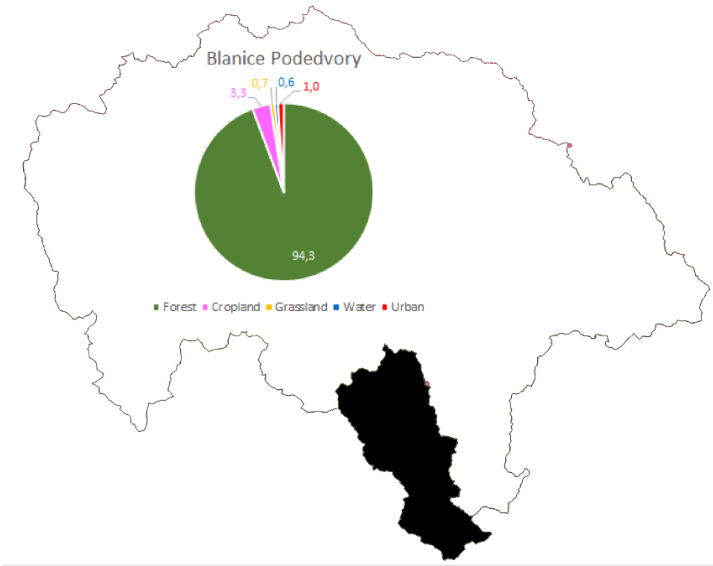

Figure11c: Land cover composition in Blanice Podedvory catchment.

Blanice Podedvory is the upper part of Blanice river. This catchment differs from the lower part of the river (i.e., Blanice Putim) with a much higher forest cover (94.3%). Of all the catchment, Blanice Podedvory has the highest amount of forest cover.

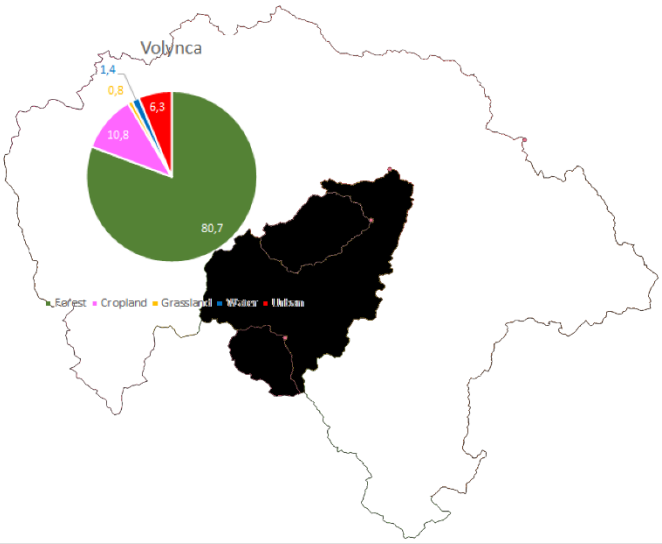

Figure 11d: Land cover composition of Volyňka - Strakonice catchment.

Volyňka - Strakonice is located in the lower part of the Otava river including thesub-catchments Peklov - Nemětice and Volyňka - Vimperk nad. The catchment has a land composition dominated by forest (80.7%). Although relatively scattered, this catchment has the highest percentage cover of urban land (6.3%).

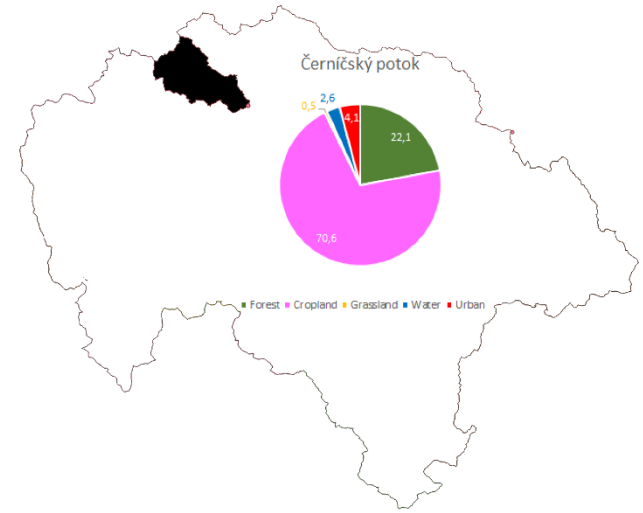

Figure 11e: Land cover composition of Černíčský potok catchment.

Černíčský potok – Bojanovice, has the highest coverage of cropland (70.6%) of all the catchments. The catchment is located in the Otava river lowland, representing one of the first tributaries to Otava river. The water chemistry in the runoff from this sub-catchment has the highest values in regards to all key chemical parameters, compared to the other Otava catchments (Table 1). The concentration of sulfate is -stream, and over 2 times higher than found in main Pisek river. This is mainly due to high evapotranspiration in the cropland fields.

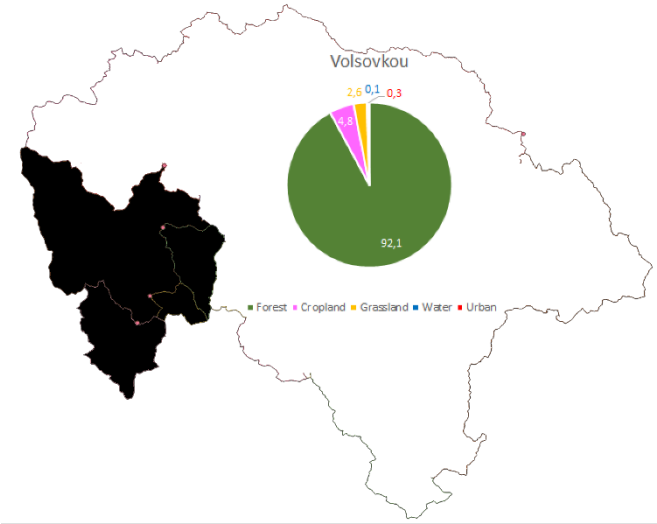

Figure 11f: Land cover composition in Volšovkou catchment.

Otava - nad **Volšovkou** (Červené Dvorce) is located in the Otava river north of Losenice, and just south of the city Sušice. The catchment has a land coverage dominated by forest (92.1%) and has the lowest concentration of Ca^{2+} and nitrogen in the water chemistry.

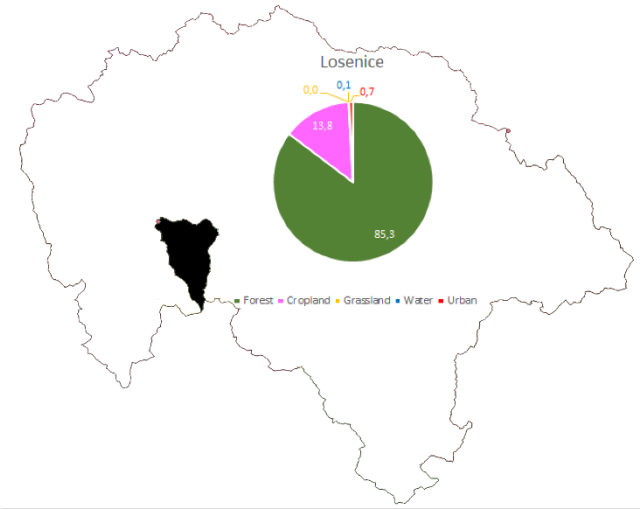

Figure 11g: Land cover composition of Losenice catchment.

Losenice is a sub-catchment of Otava - nad Volšovkou, located south of Volšovkou in the river of the town Rejštejn. Locenice lies near the head catchment of the Otava river. The catchment has a high forest coverage (85.3%), as well as some cropland (13.8%).

The quartiles (Table 1) are used to illustrate the spred ın the varıables, sınce thıs removes 25% of the upper (75%) and lower scale (25%), and so removes any outliers and makes the remaining 50% of the data more generic. In order to set the levels of the chemical parameters from the Czech catchments in a familiar context they were compared to the levels found in the 100-lakes project in Norway. This provides information regarding how the catchments in the Czech Republic are similar or different compared to our familiar lakes found southeastern Norway.

Table 1: Quartiles and means of key chemical parameters (i.e., pH, alkalinity, sulfate, calcium, nitrogen and phosphate) from monitoring data between 2000-2006 for the catchment in Czechia

and the same parameters from the spatial variation in the 100-Lakes Project. The same table including min max is provided in in Appendix. “Table1A“ denote no data.

		Otava - Písek	Blanice - Putim pod	Volyňka	Černíčský potok	Volšovkou	Losenice	Podedvory	100-Lakes
pH	25%	7.70	7.70	7.75	8.10	7.50	7.40	7.60	5.95
	Median	7.50	7.50	7.60	7.80	7.10	7.20	7.50	6.50
	75%	7.30	7.30	7.40	7.78	7.10	7.10	7.30	6.70
Alkanility (mmol/L)	25%	0.67	-	0.94	-	0.19	-	0.38	0.09
	Median	0.830	-	1.00	-	0.250	-	0.440	0.153
	75%	0.96	-	1.10	-	0.31	-	0.53	0.256
SO_4^{2-} (mg/L)	25%	17.0	-	-	37.0	5.5	-	-	1.516
	Median	21.0	-	-	43.5	7.0	-	-	2.22
	25%	28.0	-	-	97.8	9.00	-	-	3.725
Ca^{2+} (mg/L)	Median	9.73	-	-	-	2.00	-	4.00	1.475
	25%	14.0	-	-	-	2.80	-	4.50	2.44
	Median	18.0	-	-	-	4.00	-	7.00	4.635
TotN (mg/L)	25%	2.03	2.26	2.67	2.84	1.06	1.23	1.59	0.1845
	Median	2.39	2.73	3.13	3.44	1.26	1.50	1.86	0.27
	75%	3.22	3.26	3.73	4.95	1.59	1.77	2.23	0.4225
TotP (mg/L)	25%	0.08	0,11	0.09	0.10	0.03	0.04	0.03	0.0055
	Median	0.10	0.13	0.11	0.150	0.03	0.06	0.032	0.0089
	75%	0.13	0.19	0.16	0.24	0.04	0.07	0.05	0.0147

Compared to the Norwegian surface waters all catchments in Otava have a higher pH value ($8 > pH > 7$) compared to the southeastern Norwegian lakes, especially Černíčský potok that had a pH of 8.10. This is significantly different from the pH in 100-Lakes Project, where median is 6.50, and the quartiles vary from 5.95 - 6.70, i.e. slightly on the more acidic side of the pH scale. Likewise, the median alkalinity is higher in Pisek and Blanice Podedvory compared to what we find in our local surface waters in Norway. For Volšovkou the alkalinity is about the same as the 75% quartile of Norway. This can be seen in connection with pH, since the alkalinity is the capacity of water to resist acidification. In waters with pH above 6.3 this alkalinity is basically made up of a high bicarbonate (HCO_3^-) concentration. The levels of SO_4^{2-} and Ca^{2+} in the three Otava catchments that have data for these parameters indicate that the concentrations are higher than in Norway. In fact, the median sulphate value in Pisek is almost 10 times higher than the median found in the 100-lakes project. This is also the same for Ca^{2+} and TotN. The highest concentration of Ca^{2+} in Otava (Pisek) is almost 6 times higher than found in Norway. The high levels of HCO_3^- (based on alkalinity) and Ca^{2+} imply that there is easy weatherable carbonates in the soils. The largest differences between the Czech and Norwegian sites are in the levels of nutrients. The TotP concentrations are much higher in in

the Czech sites, where the highest median value found in Černíčský potok (0.15) is almost 17 times higher than the highest median value in the Norwegian lakes. The highest median value for TotN (Černíčský potok) is likewise almost 13 times higher. This clearly shows that the studied Czech watersheds are strongly influenced by agricultural activities and/or sewage.

4.3 Time trend analysis

4.3.1 NDVI

Temporal changes in biomass, based on NDVI data for the years 2000 to 2019, are presented for each catchment in this chapter. The Loess regression technique creates a smooth regression line based on the moving average of each year. The vertical lines for each point indicate the standard derivation of the set of NDVI measurement that year, this includes all the measurements in the polygons (see 3.1.3) of the catchment. Temporal changes in biomass, based on NDVI data for the years 2000 to 2019, are presented for each catchment in this chapter. The Loess regression technique creates a smooth regression line based on the moving average of each year. The vertical lines for each point indicate the standard derivation (STD) of the set of NDVI measurement that year, this includes all the measurements in the polygons (see 3.1.3) of the catchment. This means that the STD in data for each polygon in the catchment is determined and so on the spread between the polygons are found. These STD values are combined and make up for the average spread in the whole catchment for each year. For example, Černíčský potok has five polygons (see 3.1.1), for each polygon there are NDVI measurements at the 1st, 11th and 21th of the months June, July and August. This makes up for 9 files a year and a total of 180 NDVI observations for every polygon from 2000-2019. To combine the data of the 180 observations the average NDVI and the standard derivation for each year is found for all the polygons. To find the NDVI for the whole catchment the NDVI measurements from all the polygons are combined, the standard derivation is so on also calculated from the standard derivations from each polygon, this leads to the standard derivation shown as vertical lines for each point.

The NDVI increases in all the catchments between 2000 and 2010, based on the positive increase of the moving average (i.e., blue lines in Figs. 12 – 18). A slight exception is for Volšovkou that peaks in 2007. After 2010 the trends in biomass differ more between the catchments. The biomass in Pisek, Volyňka and Černíčský potok decreases slightly until 2019. While for the catchments Blanice Putim Pod, with its upper sub-catchment Blanice Podedvory, Volšovkou and Losenice, the biomass increases again from around 2012 to 2019. There are no

clear differences in the watershed characteristics between these two different NDVI trends since 2012.

Quartiles and median value of NDVI from year 2000-2019 for the catchments is presented in Table 1. Losenice and Blanice Podedvory is the two catchments with the highest quartile and mean NDVI value, thus the highest vegetation density. These catchments have a forest cover of 85% and 94%, respectively.

Table 2: Median and quartile NDVI values of the watersheds from 2000-2019.

	Písek	Blanice Putim	Volyňka	Černíčský potok	Volšovkou	Losenice	Blanice Podedvory
25%	0.654	0.639	0.665	0.632	0.685	0.709	0.708
Median	0.682	0.665	0.691	0.668	0.708	0.728	0.729
75%	0.610	0.688	0.714	0.691	0.735	0.756	0.754

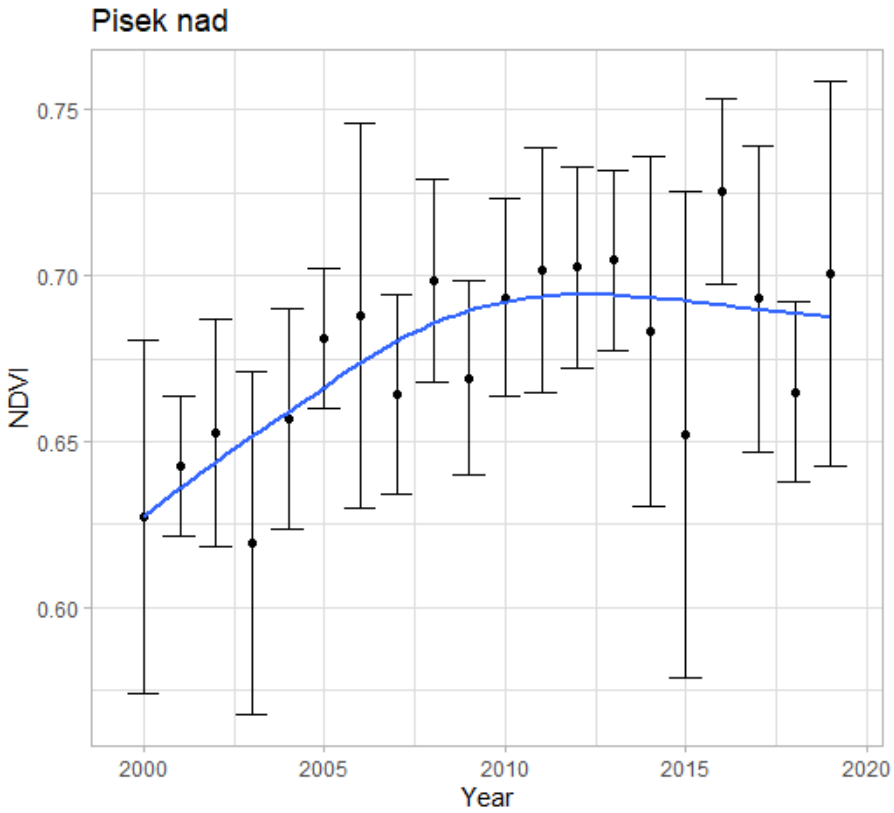

Figure 12: NDVI for Pisek nad from 2000-2019.

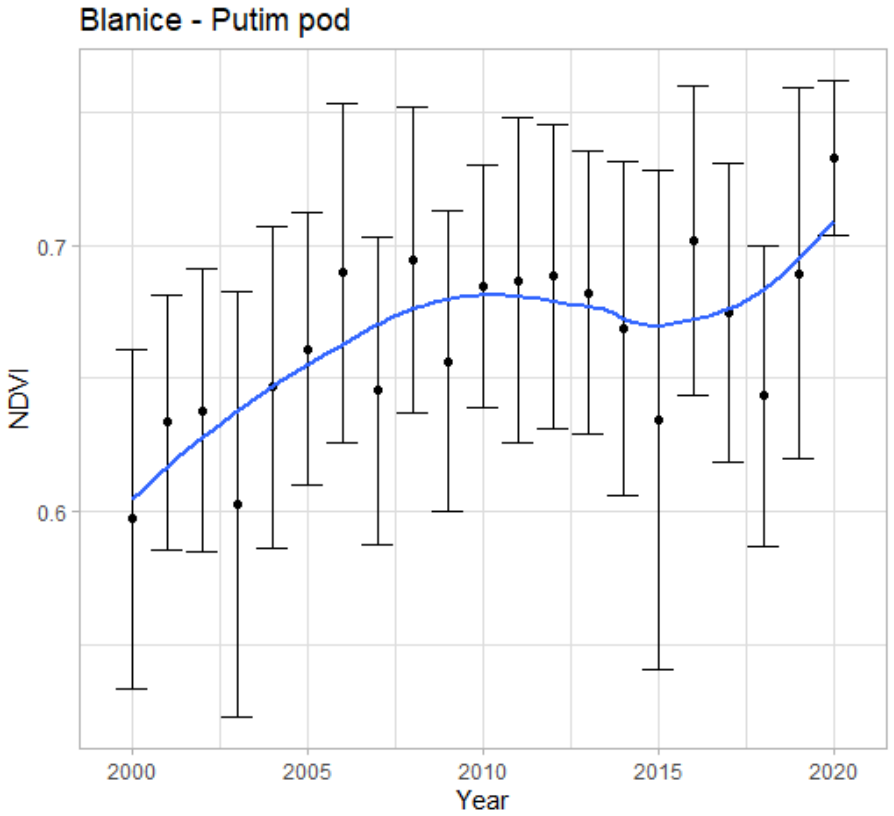

Figure 13: NDVI for Blanice Putim Pod from 2000-2019.

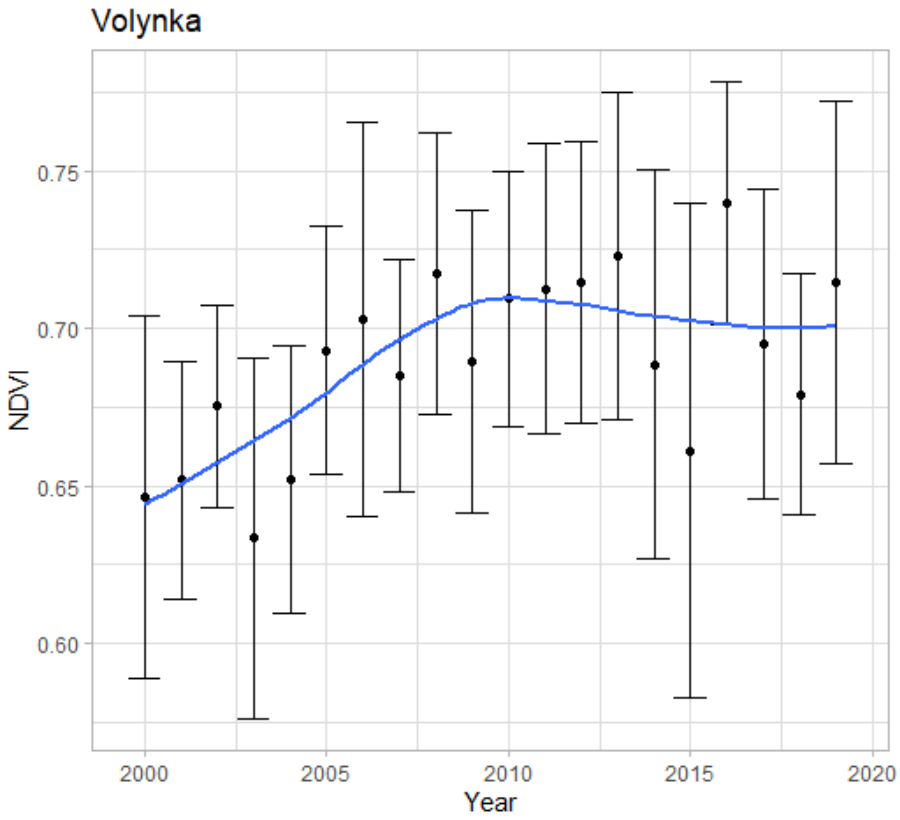

Figure 14: NDVI for Volynka from 2000-2019

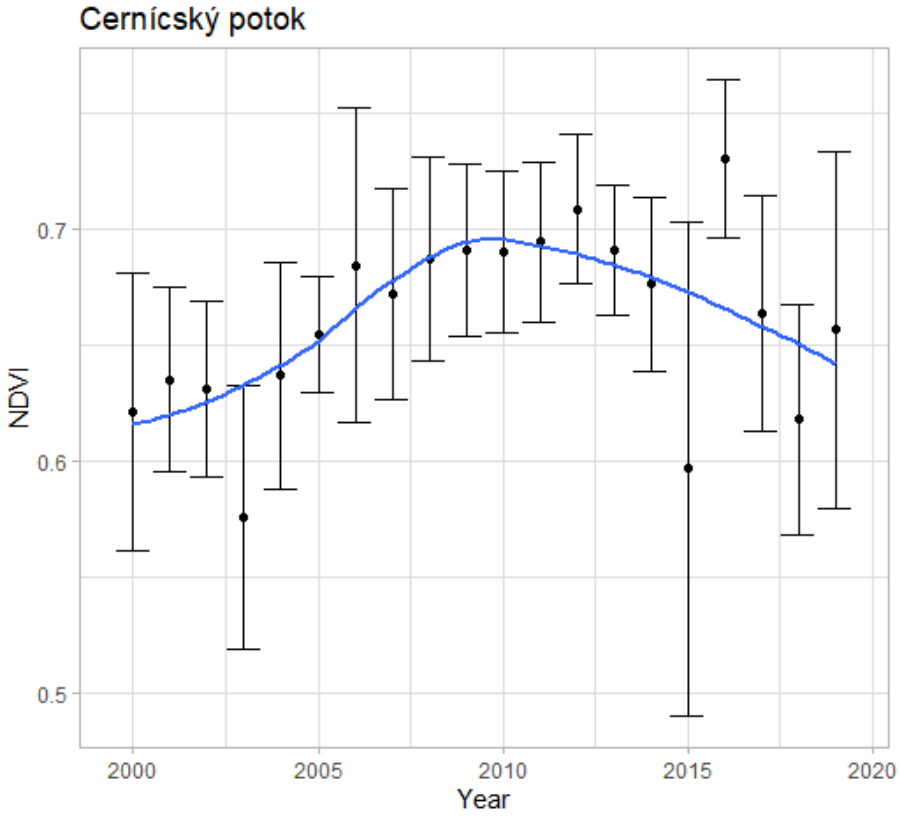

Figure 15: NDVI for Černíčský potok from 2000-2019.

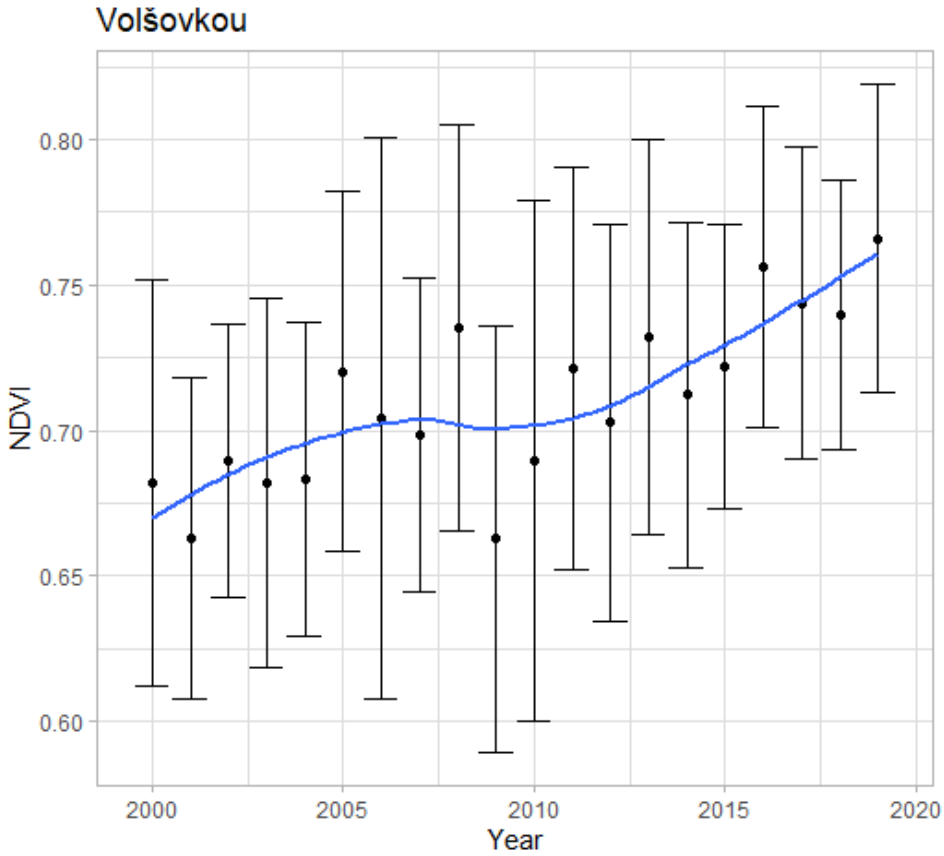

Figure 16: NDVI for Volšovkou from 2000-2019.

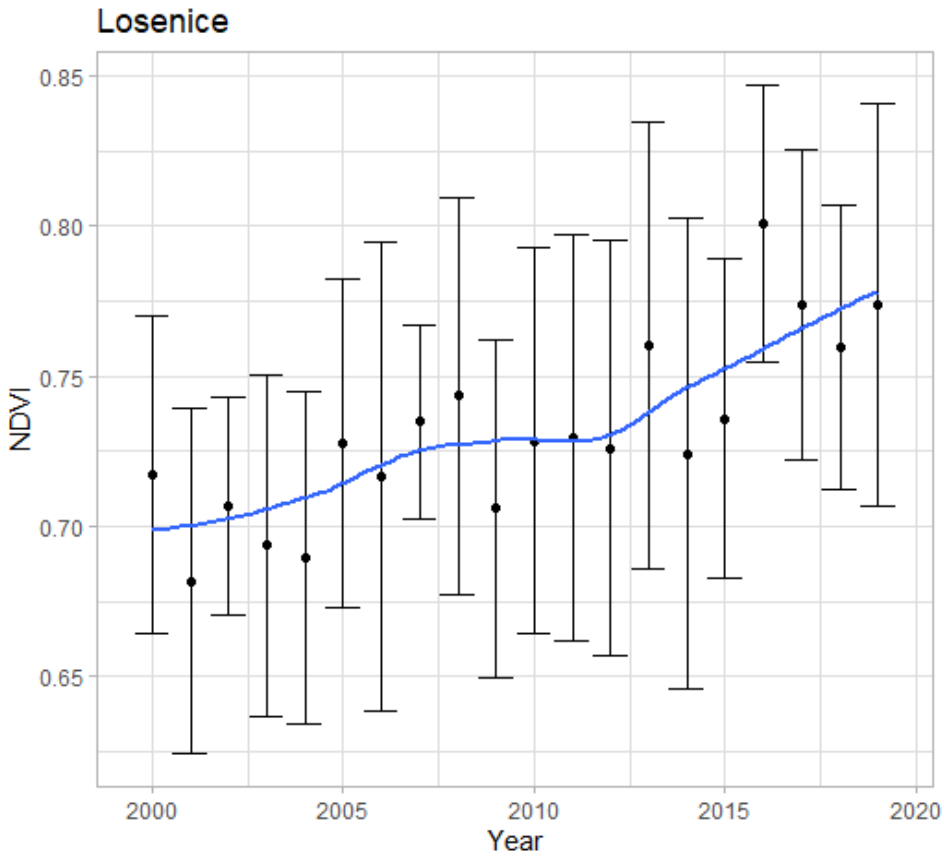

Figure 17: NDVI for Locenice from 2000-2019.

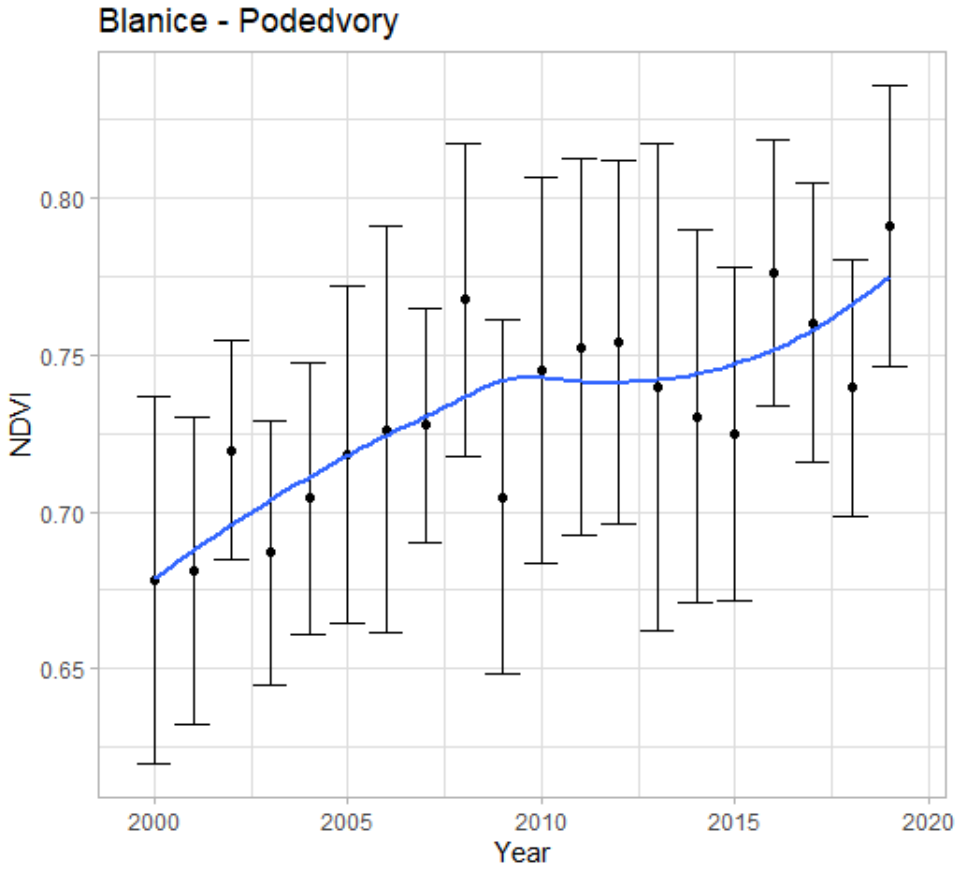

Figure 18: NDVI for Blanice Podedvory from 2000-2019.

To sum up, all of the catchments show an overall increasing trend in biomass from 2000-2010. Differences in temporal trends in biomass do not appear to be governed by the catchment characteristics assessed in this study.

The highest biomass are found in the mainly forested Blanice Podedvory and Losenice.

The causes for changes in vegetation density are not well documented, but it is likely to be linked to higher air temperature (Figure 9), accumulation of N and changes in land use. The amount of vegetation growth is affected by the increasing temperature, as it lengthens the growing season leading to more vegetation. Increased biomass causes the SOM pool to increase and be available for degradation and possible leaching of more DNOM in surface waters.

4.3.2 Water chemistry

The Czech waterworks monitor the water chemistry in the runoff from the watersheds described in Chapt 4.2. These data that were presented in Table 1 had been compiled by our Czech partners for the period from 2000 to 2006. Of the studied sites only Pisek, Volšovkou and Blanice Podedvory had data for DOC. In addition the DOC concentration of the water samples taken in the Czech Republic in January 2021 are presented in Table 2. This provides DOC data

to the catchments that have no current DOC data (Table 1). As seen in Table 2 the DOC concentration varies from 1.64 mg C/L in Losenice to 6.30 mg C/L in Černíčský potok. The high levels at Černíčský potok is likely due to that agriculture accounts for more than 75% of the catchment area. There are also large differences in evapotranspiration between the mountainous Losenice and the Černíčský potok lowland, causing dilution in Losenice and up concentration in Černíčský potok.

Table 3: Measured DOC concentration (mg C/L) of the water samples taken 21.January 2021.

	Písek	Blanice Putim	Volyňka	Černíčský potok	Volšovkou	Losenice	Blanice Podedvory
DOC	3.43	4.96	4.52	6.30	2.24	1.64	3.23

Considering the large seasonal fluctuations any time-trend based analysis would be unreliable due to the limited duration of the monitoring data. The median and quartile DOC concentrations at the three watersheds with DOC data are compared to the DOC levels in the Norwegian lakes from the 100-Lakes Project (Table 3). The DOC concentrations of the new sample from Pisek, Blanice Podedvory and Volšovkou collected in January 2021 are compared to the DOC concentrations in the runoff from these catchments in January to February 2000 to 2006 (Figures 24 and 25).

Table 4: Median and quartile DOC concentrations (mg C/L) of the watersheds with DOC monitoring data and 100-Lakes Project

DOC	Písek	Volšovkou	Blanice Podedvory	100-Lakes
25%	4.85	2.80	3.83	4.44
Median	6.10	4.65	5.45	7.32
75%	7.70	5.60	6.20	11.0

For the three catchments that have DOC data from 2000-2006 (Table 3) their median DOC concentrations are ranked as Pisek > Blanice Podedvory> Volšovkou. The relatively high levels at Pisek may be due to anthropogenic input from agriculture, comprising more than half of the watershed, and sewage due to several large villages with this large watershed. The variation

between the 25% and 75% quartile in Table 3 reflect the amplitude of seasonal fluctuations in DOC concentration. Smallest variation is found at Blanice Podedvory, which is a headwater catchment dominated by 94% forest. The 25% quartile DOC concentration in Pisek is higher compared to the 100-lakes 25% quartile; otherwise, the overall DOC concentrations are lower in the Otava catchments compared to the 100-lakes.

Only Blanice Putim and Volyňka have DOC concentrations in 2021 (Table 2) that are within the ranges of the median values of the monitored DOC concentrations in 2000-2006 presented in Table 3. Volsovkou and Losenice have a lower DOC concentration in 2021 than the 25 quartile values in 2000-2006. The concentration of the water sample of Černíčský potok (Table 2) is higher than the median DOC concentrations found in 2000-2006, but in the range of the values in 100-lakes.

From the Figure 19, Figure 20 and Figure 21 it is clear that the DOC concentration of the water samples taken in 2021 is lower than the seasonally average DOC concentrations in January-February 2000-2006 at the three catchments with DOC monitoring data.

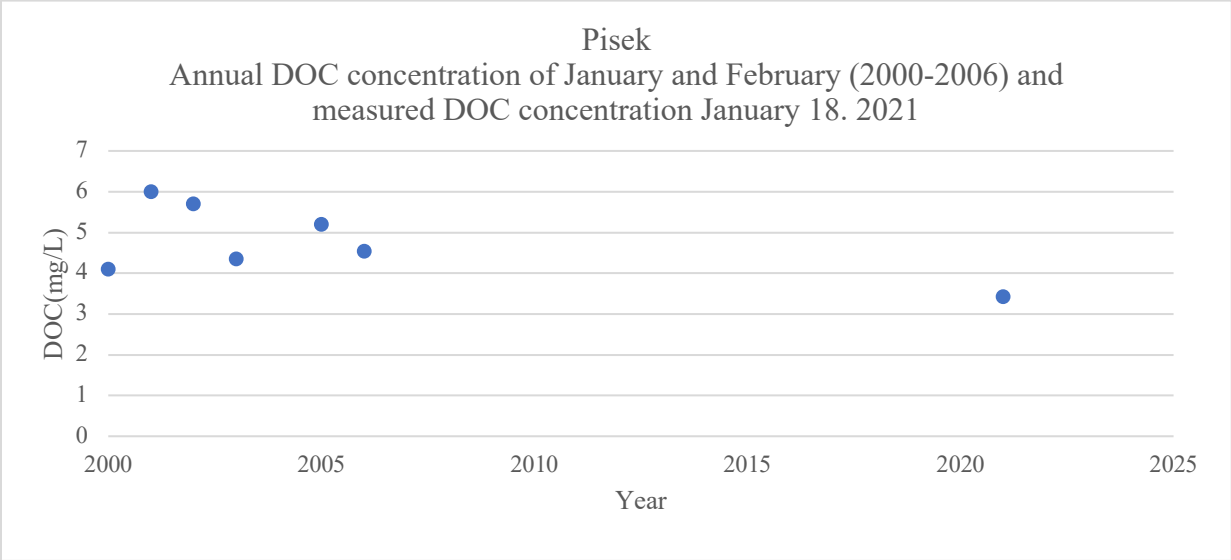

Figure 19: Annual DOC concentration in January-February (2000-2006) and measured DOC concentration January 18.2021 Pisek.

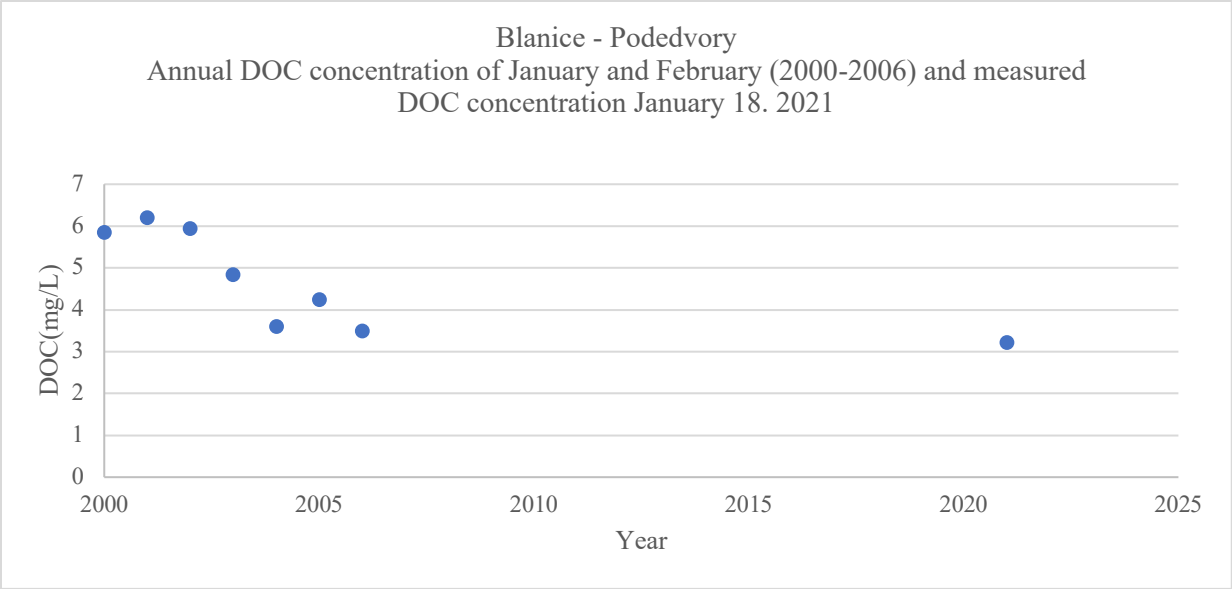

Figure 20: Annual DOC concentration in January-February (2000-2006) and measured DOC concentration January 18.2021 Blanice Podedvory.

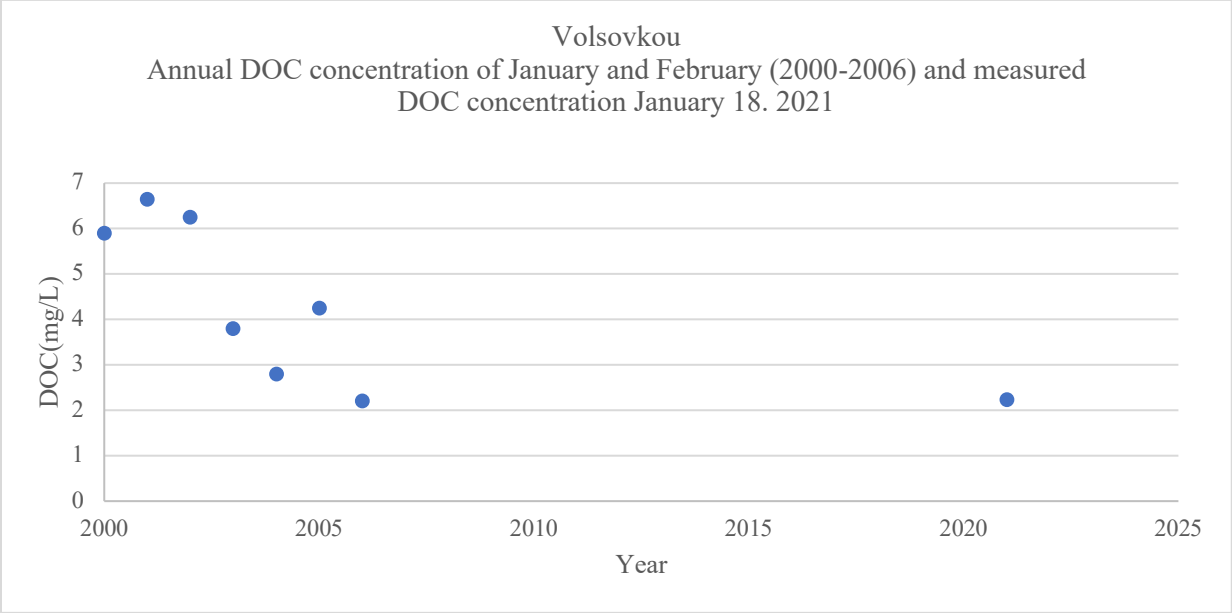

Figure 21: Annual DOC concentration in January-February (2000-2006) and measured DOC concentration January 18.2021 Volsovkou.

To sum up, the DOC levels in the runoff from the Czech catchments are somewhat lower than what we find in our local surface waters. The spatial variation in levels of DOC appear to be mainly governed by the fraction of agricultural land-use in the watersheds. This may also reflect a higher evapotranspiration and thus up-concentration in the lowland regions. Based on the existing data there is no cause to conclude that the levels of DNOM in the studied Czech surface

waters has increased – rather the opposite. This we may speculate can be due to decreased loss of manure through surface runoff from agriculture, as well as improved sewage treatment.

5. Conclusion

The study of long term trends in drivers of DNOM increase showed that there from 2000 to 2020 have been a significant decrease in acid rain loading, as well as an increase in temperature and in biomass. Based on this one would expect to see an increase in the levels of DNOM in the runoff from the studied catchments. On the contrary, none of the DNOM proxies (e.g., DOC, Colour or UV absorbance, nor COD_Mn) indicate any increase in DNOM. This may be due a too limited record of monitoring data (i.e., only 6 years) with large seasonal fluctuations. Still, the water samples from 2021 also support that there has been no increase in DNOM.
The pH in these surface waters are slightly alkaline, indicating the presence of carbonates in the soil. This is supported by relatively high levels of Calcium. This generates high ionic strength renders a low solubility of the DNOM. The amount of DNOM leached from these non-acid forest soils is thus expected to be low. The main sources of DNOM are then instead anthropogenic runoff from agriculture and possibly sewage from stormflow or network leakage. The apparent decline in DNOM may thus be due to improved agricultural management and sewage network renovation.

5.1 Future work

To get a more complex picture of the water chemistry and the concentration and quality of DNOM in the Otava catchment there is need for more data of physical and chemical parameters of the surface waters and more water samples taken for this purpose. There is need to look at the catchments characteristic in more detail, due to how the catchments characteristics affect the DNOM and its quality greatly. This project is thus only in a starting phase, there is ongoing work with our Czech partners to get more information and hopefully better understanding of the chemical and physical parameters affecting DNOM concentrations in the surface waters in the Otava catchment so that the DWTP can gain knowledge about changes in raw water quality.

References

Arrigo, K. R., & Brown, C. W. (1996). Impact of chromophoric dissolved organic matter on UV inhibition of primary productivity in the sea. *Marine Ecology Progress Series, 140*(1-3), 207-216.

Bolan, N. S., Adriano, D. C., Kunhikrishnan, A., James, T., McDowell, R., & Senesi, N. (2011). Dissolved Organic Matter: Biogeochemistry, Dynamics, and Environmental Significance in Soils. *Advances in agronomy, 110*, 1-75.

Bruno Smets, Jonathan Leon Tavares, Carolien Toté, & Wolters, E. (2020). *Copernicus Global Land Operations.*

Carpart, C., Andersen, T., Hessen., D. O., Valiente, N., Vogt, R.D. (2021). *Favtors Governing Biodegradability of Dissolved Natural Organic Matter in Lake Water*. Submitted: 2021

Clark, J.M., Bottrell, S.H., Evans, C.D., Monteith, D.T., Bartlett, R., Rose, R., . . . Chapman, P.J. (2010). The importance of the relationship between scale and process in understanding long-term DOC dynamics. *Science of the Total Environment, 408*(13), 2768-2775. doi:10.1016/j.scitotenv.2010.02.046

Copernicus (2019). *Global land cover*. Copernicus Land Monitoring Service. Retrieved on June 14, 2021 from: https://lcviewer.vito.be/2019

Copernicus (2021a). *Home.* CGLS. Retrieved on June 14, 2021 from: https://land.copernicus.eu/global/

Copernicus (2021b). *Vegetation*. CGLS. Retrieved on June 14, 2021 from: https://land.copernicus.eu/global/themes/vegetation

Czech Hydrometeorological Institute (2019). Territorial air temperature. CHMI Portal. Retrieved from: https://www.chmi.cz/historicka-data/pocasi/uzemni-teploty?l=en

Czech Hydrometeorological Institute (2019). Territorial precipitation. CHMI Portal. Retrieved from: https://www.chmi.cz/historicka-data/pocasi/uzemni-teploty?l=en

de Wit, H. A., Mulder, J., Hindar, A., & Hole, L. (2007). Long-Term Increase in Dissolved Organic Carbon in Streamwaters in Norway Is Response to Reduced Acid Deposition. *Environmental Science & Technology, 41*(22), 7706-7713. doi:10.1021/es070557f

Earth Observing System (2021). NDVI. Retrieved on June 14, 2021 from: https://eos.com/ndvi/

Eikebrokk, B., Vogt, R. D., & Liltved, H. (2004). NOM increase in Northern European source waters: discussion of possible causes and impacts on coagulation/contact filtration processes.

Ekström, S.M., Kritzberg, E.S, Kleja, D.B, Larsson, N., Nilsson, P.A., Graneli, W., & Bergkvist, B. (2011). Effect of Acid Deposition on Quantity and Quality of Dissolved Organic Matter in Soil–Water. *Environmental Science & Technology, 45*(11), 4733-4739.

EMEP (2005). Emission Data reported to LRTAP Convention and NEC Directive Initial review for HMs and POPs. Retrieved on June 14, 2021 from https://www.emep.int/publ/reports/2005/emep_technical_1_2005.pdf

EMEP (2011). Transboundary particulate matter in Europe. Retrived from https://projects.nilu.no/ccc/reports/emep4-2011.pdf

EMEP (2020). Earlier reported EMEP MSC-W modelled air concentrations and depositions. Retrieved on June 14, 2021 from https://www.emep.int/

Erlandsson, M., Buffam, I., Fölster, J., Laudon, H., Temnerud, J., Weyhenmeyer, G.A. and Bishop, K. (2008). Thirty-five years of synchrony in the organic matter concentrations of Swedish rivers explained by variation in flow and sulphate. Global Change Biology, 14: 1191-1198. doi:10.1111/j.1365-2486.2008.01551.x

European Environment Agency (2011). Air quality in Europe – 2011 report – nr.12. Retrieved from: https://www.eea.europa.eu/publications/air-quality-in-europe-2011

Fisktvedt, D. (2021). *Effect of regional pressures and source characteristics on DNOM quality of relevance for drinking wate*[i]*r plants.* Master thesis. UiO

Finstad, A. G., Andersen, T., Larsen, S., Tominaga, K., Blumentrath, S., de Wit, H., & Hessen, D. O. (2016). From greening to browning: Catchment vegetation development and reduced S-deposition promote organic carbon load on decadal time scales in Nordic lakes.

Forsgren, E., Aarrestad, P. A., Gundersen, H., Christie, H., Friberg, N., Jonsson, B., . . . Ødegaard, F. (2015). Klimaendringenes påvirkning på naturmangfoldet i Norge

Garmo, Ø. A., & Skancke, L. B. (2018). Overvåking av langtransportert forurenset luft og nedbør. Årsrapport – Vannkjemiske effekter 2017; Monitoring long-range transboundary air pollution. Water chemical effects 2017.

Gjessing, E. T. (2013). Coloured materials in surface water in the sub Arctic Zone: An overview of its formation, properties and environmental changes. *Natural Science, 5*(3), 400-410. doi:10.4236/ns.2013.53053

Haaland, S., Hongve, D., Laudon, H., Riise, G., & Vogt, R. D. (2010). Quantifying the Drivers of the Increasing Colored Organic Matter in Boreal Surface Waters. *Environmental Science & Technology, 44*(8), 2975-2980. doi:10.1021/es903179j

Hongve, D., Riise, G., & Kristiansen, J. F. (2004). Increased colour and organic acid concentrations in Norwegian forest lakes and drinking water – a result of increased precipitation? *Aquatic Sciences, 66*(2), 231-238. doi:10.1007/s00027-004-0708-7

Håland, A. (2017). *Characteristics and Bioavailability of Dissolved Natural Organic Matter in a Boreal Stream during Storm Flow.* Master thesis. UiO

Intergovernmental Panel on Climate Change. (2021). Methodology Report on Short-lived Climate Forcers. IPPC. Retrieved on June 14, 2021 from: https://www.ipcc.ch/report/methodology-report-on-short-lived-climate-forcers/

Larsen, S., Andersen, T., & Hessen, D.O. (2011a). Climate change predicted to cause severe increase of organic carbon in lakes.(Report). *Global Change Biology, 17*(2), 1186-1192.

Larsen, S., Andersen, T., & Hessen, D. O. (2011b). Predicting organic carbon in lakes from climate drivers and catchment properties. *Global Biogeochemical Cycles, 25*(3), doi:10.1029/2010GB003908

Matilainen, A., Gjessing, E. T., Lahtinen, T., Hed, L., Bhatnagar, A., & Sillanpää, M. (2011). An overview of the methods used in the characterisation of natural organic matter (NOM) in relation to drinking water treatment. *Chemosphere, 83*(11), 1431-1442. doi:https://doi.org/10.1016/j.chemosphere.2011.01.018

Ministry of the Environment of the Czech Republic (2017). Seventh National Communication of the Czech Republic under the United Nations framework convention on climate change. Retreived on June 14, 2021 from: https://unfccc.int/files/national_reports/annex_i_natcom_/application/pdf/17589243_czech_republic-nc7-br3-1-nc7_br3_cze.pdf

Monteith, D. T., Stoddard, J. L., Evans, C. D., de Wit, H. A., Forsius, M., Høgåsen, T., . . . Vesely, J. (2007). Dissolved organic carbon trends resulting from changes in atmospheric deposition chemistry. *Nature, 450*(7169), 537-540. doi:10.1038/nature06316

Nima, C., Frette, Ø., Hamre, B., Stamnes, J. J., Chen, Y.C., Sørensen, K., . . . Erga, S. R. (2019). CDOM Absorption Properties of Natural Water Bodies along Extreme Environmental Gradients. *Water, 11*(10). doi:10.3390/w11101988

NOAA (2021). National Centers for Environmental Information, State of the Climate: Global Climate Report for Annual 2020, published online January 2021. Retrieved on June 14, 2021 from https://www.ncdc.noaa.gov/sotc/global/202013.

Prabhakaran S. (2017). *Loess regression and smoothing with R*. http://r-statistics.co/. Retrieved on June 14, 2021 from: http://r-statistics.co/Loess-Regression-With-R.html

Reckhow, D. A. and Singer, P. C. (1990). Chlorination by-products in drinking waters: From formation potentials to finished water concentrations. J. Am. Water Works Assoc. 82(4): 173–180.

Science facts.net (2021). Soil Horizons. Science Facts. Retrieved on June 14, 2021 from: https://www.sciencefacts.net/soil-horizons.html

Sepp, M., Kõiv, T., Nõges, P., Nõges, T. (2019). The role of catchment soils and land cover on dissolved organic matter (DOM) properties in temperate lakes. Elevier.

Skjelkvåle, B. L., Rognerud, S., Fjeld, E., Christensen, G.N. & Røyset, O. (2008). Nasjonale innsjøundersøkelse 2004-2006, Del I: Vannkjemi. Status for forsuring, næringssalter og metaller. In: Norsk institutt for vannforskning.

Skjelkvåle, B. L. (2003). The 15-year report: Assessment and monitoring of surface waters in Europe and North America acidification and recovery, dynamic modelling and heavy metals (ICP Waters report 73/2003).

Skjelkvåle, B.L., Stoddard, J.L., Jeffries, D.S., Tørseth, K., Høgåsen, T., Bowman, J., . . . Worsztynowicz, A. (2005). Regional scale evidence for improvements in surface water chemistry 1990–2001. *Environmental Pollution, 137*(1), 165-176.

Vogt, R.D., Akkanen, J., Andersen, D.O., Brüggemann, R., Chatterjee, B., Gjessing, E., . . . Zsolnay, Á. (2004). Key site variables governing the functional characteristics of Dissolved Natural Organic Matter (DNOM) in Nordic forested catchments. *Research across Boundaries, 66*(2), 195-210. doi:10.1007/s00027-004-0710-0

Worrall, F., Harriman, R., Evans, C., Watts, D., Adamson, C., Neal, J., . . . Stevens, T. (2004). Trends in Dissolved Organic Carbon in UK Rivers and Lakes. *Biogeochemistry, 70*(3), 369-402.

6.Appendix

Data Availability Statement: The data from the 100-lakes project in this study is available on the open access : https://osf.io/r39ng/?view_only=d1b8c4c2c68c4ca59bb4c78a817fc64b.

6.1 Experimental lab-work

Table A1: Result of the experimental lab-work of the waters samples for the Czech Republic.

Description	Date	Catchment	DOC mg/L	TN/mg/L	RR	tmax_h	BdgT	ox_initial	Abs. 254	Abs. 400
Písek	18.01.2021	Otava river catchment	3,426	2,291	0,58473625	15,406375	3,119	301,29562	0,13	0,017
Putim pod	18.01.2021	Otava river catchment	4,960	3,208	0,99002506	15,0303333	2,62033333	243,777575	0,172	0,018
Volyňka	18.01.2021	Otava river catchment	4,520	4,937	1,094214	14,32025	2,76425	301,29562	0,135	0,013
Peklov	18.01.2021	Otava river catchment	3,287	3,837	1,06264887	16,3911667	3,26275	275,715526	0,107	0,012
Černíčský potok	18.01.2021	Otava river catchment	6,296	2,312	1,00610943	17,1519167	3,57558333	275,715526	0,171	0,015
Nezdický potok	18.01.2021	Otava river catchment	3,100	3,430	0,98958226	16,167125	5,41841667	281,118129	0,101	0,012
Ostružná	18.01.2021	Otava river catchment	2,727	2,736	1,20832197	15,8629167	3,77	281,11813	0,095	0,01
Volšovka	18.01.2021	Otava river catchment	1,958	1,819	1,76509005	13,0565833	2,291	301,29562	0,067	0,008
Volšovkou	18.01.2021	Otava river catchment	2,238	0,870	1,27697156	12,8198333	2,36683333	301,29562	0,113	0,015
Losenice	18.01.2021	Otava river catchment	1,642	1,192	0,9121973	14,33725	3,11091667	301,29562	0,067	0,009
Hamerský potok	18.01.2021	Otava river catchment	2,231	0,460	1,17669301	14,7979167	2,35841667	243,777575	0,122	0,017
Vydra	18.01.2021	Otava river catchment	2,556	0,767	0,04217158	15,2161667	1,85091667	243,777575	0,145	0,022
Volyňka	18.01.2021	Otava river catchment	2,301	0,834	0,94576191	14,9711667	2,51075	275,715526	0,088	0,01
Podedvory	18.01.2021	Otava river catchment	3,228	1,308	1,1275736	14,6500833	2,56125	243,777575	0,136	0,017
Karhov1	19.01.2021	Karhov catchment	12,570	0,894	1,13181861	14,3837083	3,16983333	243,777575	0,553	0,061
Karhov2	19.01.2021	Karhov catchment	9,648	0,808	1,95334765	14,7049167	2,67133333	275,715526	0,454	0,054
Karhov3	19.01.2021	Karhov catchment		10,710	0,831	1,05482946	16,1629583	3,10225	275,715526	0,462

6.2 NDVI raw data

Under is the raw data for the NDVI graphs presented in Figure … - Figure …, with annual NDVI for 2000-2019 including standard derivation for each catchment is presented in Figure 1A and Figure 2A.

Catchment	1. Pisek	STD	2. Putim pod	STD	3. Volyňka	STD
2000	0,6274291	0,05318578	0,5972121	0,06345497	0,6465305	0,05764841
2001	0,6425621	0,02117822	0,6336724	0,04784965	0,6518338	0,03780289
2002	0,6526584	0,03441576	0,6379951	0,05322892	0,6753051	0,03223893
2003	0,6193481	0,05161925	0,6026384	0,07968788	0,6333428	0,05728228
2004	0,6567738	0,03310659	0,6466914	0,06039643	0,6520057	0,04266116
2005	0,6808464	0,02106729	0,6611278	0,05127069	0,6929652	0,03939936
2006	0,687946	0,05808807	0,689692	0,06360932	0,7028445	0,06279181
2007	0,6642235	0,02984546	0,6455786	0,05771567	0,6850126	0,03692051
2008	0,6985072	0,03071264	0,6943947	0,05729552	0,7174334	0,04465194
2009	0,6690919	0,02925206	0,6565058	0,0562312	0,6894813	0,04793313
2010	0,6934195	0,02995313	0,6845897	0,04564042	0,709254	0,04072514
2011	0,7015079	0,03703843	0,6868189	0,06107865	0,7124427	0,04609126
2012	0,7024981	0,03019836	0,6883434	0,05706255	0,7145473	0,04482721
2013	0,7046744	0,02728706	0,6820735	0,05305374	0,7229181	0,05179613
2014	0,6830942	0,05270941	0,6685239	0,06274396	0,6885465	0,06150929
2015	0,6519106	0,07330153	0,6346017	0,0938296	0,6610637	0,07856526
2016	0,7254109	0,02811258	0,7017909	0,05803358	0,7395007	0,03860239
2017	0,6929997	0,04625768	0,674648	0,05625305	0,6951451	0,04908311
2018	0,6648766	0,027091	0,6433931	0,05642293	0,6789682	0,03823937
2019	0,7004836	0,05802212	0,6895186	0,06994832	0,7147606	0,05757157

Figure 1A: Annual NDVI data and standard derivation for the catchments Pisek, Putim Pod and Volynka.

Catchment	5. Černíčský	STD	9. Volšovkou	STD	10. Losenice	STD	14. Podedvo	STD
2000	0,6208832	0,05993455	0,6820992	0,06987419	0,717146	0,05284148	0,6781174	0,05832546
2001	0,6352209	0,03992265	0,6630313	0,0550179	0,6818338	0,05734011	0,6813235	0,04900812
2002	0,6311732	0,03784036	0,6897443	0,0470241	0,7067038	0,03639993	0,7196301	0,03480017
2003	0,5755368	0,05712595	0,6821284	0,06358024	0,6935977	0,05692989	0,6868904	0,0420536
2004	0,636935	0,04908715	0,6833914	0,05400217	0,6895703	0,05547628	0,7042403	0,04307435
2005	0,6546368	0,02513652	0,7203691	0,0620747	0,7276798	0,05474149	0,7181351	0,05358248
2006	0,6843531	0,06780344	0,7042493	0,09637689	0,7166874	0,07782143	0,7261871	0,06493417
2007	0,6721289	0,04582964	0,6982734	0,05388043	0,7347731	0,03249402	0,7275749	0,03738812
2008	0,6875797	0,04406178	0,7355504	0,06978756	0,7435	0,06595436	0,7674858	0,04986699
2009	0,6911714	0,03711527	0,662699	0,07327863	0,7059843	0,05628535	0,7047076	0,05627403
2010	0,6903342	0,03506611	0,6896531	0,08960961	0,7284612	0,06423377	0,7450417	0,06129367
2011	0,69476	0,03451218	0,7213023	0,06893434	0,7294014	0,0674541	0,7525433	0,06006366
2012	0,708839	0,03244655	0,7026386	0,06811823	0,7259987	0,06923445	0,7542506	0,05786202
2013	0,6913194	0,02801272	0,7321402	0,06776767	0,760107	0,07432394	0,7397797	0,07770496
2014	0,67642	0,03760636	0,7122322	0,05935319	0,7242617	0,07853477	0,7304163	0,05934988
2015	0,5965886	0,10667662	0,7219266	0,04883045	0,7359221	0,05312326	0,7249706	0,05306262
2016	0,7306027	0,03393042	0,7563613	0,05529678	0,8007154	0,04611756	0,7760567	0,04242773
2017	0,6635356	0,0507703	0,7436107	0,05359218	0,7738234	0,05191674	0,7601225	0,04445368
2018	0,617791	0,04997603	0,739744	0,04649683	0,7596103	0,04752176	0,7394172	0,04118424
2019	0,6565649	0,07734099	0,7659561	0,05298462	0,7739876	0,06694697	0,7908692	0,04483747

Figure 2A: Annual NDVI data and standard derivation for the catchments CP, Volsovkou, Losenice and Podedvory.

6.3. Land composition cover.

Data for caulated land cover composition is presented in Figur 3A and Figure 4A.

		Blanice Podedvory			Volynca	
		Pix	%		**Pix**	**%**
Red	Urban	85	0,55		1002	4,09
Yellow	Grassland	116	0,75		200	0,82
Green	Forest	14683	94,33		19773	80,73
Cyan	Water	45	0,29		150	0,61
Blue	Water	51	0,33		200	0,82
Magentas	Urban	76	0,49		534	2,18
Midtones	Cropland	509	3,27		2633	10,75
			100,00			100,00
Highlights		59131			128650	
Shadows		925			0	
TOTAL		75460			155208	
		75621			153142	
		161				
		15565			24492	
	Forest		**94,3**			**80,7**
	Cropland		**3,3**			**10,8**
	Grassland		**0,7**			**0,8**
	Water		**0,6**			**1,4**
	Urban		**1,0**			**6,3**
			100,0			100,0

Figure 3A:Raw data for pie chart of land cover composition.

Pisek			Černíčský potok			Losenice	
Pix	%		Pix	%		Pix	%
1068	1,69		522	2,47		127	0,65
314	0,5		112	0,53		8	0,04
28951	45,79		4661	22,08		16587	85,31
106	0,17		184	0,87		8	0,04
143	0,23		369	1,75		12	0,06
64	0,1		349	1,65		12	0,06
32586	51,53		14911	70,64		2689	13,83
	100			100			100
102802			41871			12889	
4315			570			267	
140614			49256			41108	
170349							
63232			21108			19443	
	45,8			22,1			85,3
	51,5			70,6			13,8
	0,5			0,5			0
	0,4			2,6			0,1
	1,8			4,1			0,7
	100			100			100

Figure 4A:Raw data for pie chart of land cover composition.

6.R-script

The R-skript used to extract and calculate NDVI in the Otava catchments:

```
#install packages -----
install.packages("dplyr")
install.packages("ncdf4")
install.packages("raster")
install.packages("sf")
install.packages("stringr")
install.packages("rgdal")
install.packages("writexl")
install.packages("xlsx")
#get packages ----
library(dplyr)
library(ncdf4)
library(raster)
library(sf)
library(stringr)
library(rgdal)
library(ggplot2)
library(RColorBrewer)
library(dplyr)
library(xlsx)
library(openxlsx)
#functions

mean_of_shapefile <- function(catchment_polygon, start_year, stop_year){

 table <- data.frame()


 for (year in start_year:stop_year){
  if (year <= 2011){
   setwd("C:/Martine/")
  } else{
   setwd("~/")
  }
  path1 <- paste("NDVI_data", year, sep = "/") #lag navn til NDVI mappe
  filenames <- list.files(path1, full.names=TRUE) #lag liste over alle filer i mappa

  for (i in 1:length(filenames)){
   ndvi_map <- raster(filenames[i], varname="NDVI") #f?r NDVI representert med et kart
   ndvi <- handle_shapefile(catchment_polygon, ndvi_map) #f?r snitt-NDVI i nedb?rsfeltet
   total_date <- filenames[i]
   total_date <- str_sub(total_date, start = 27, end = 34)
   trow <- c(total_date, ndvi)
   table <- rbind(table, trow)
  }
 }
 colnames(table) = c("Date", "NDVI")
 return(table)
}

handle_shapefile <- function(catchment_polygon, ndvi_map){
 spdf <- as_Spatial(catchment_polygon$geometry,IDs=as.character(catchment_polygon$station_id)) #change of format in some way
 ndvi_vals <- extract(ndvi_map,spdf) #linking the catchment_polygon to the NDVI map
 #print(ndvi_vals)
 ndvi <- mean(ndvi_vals[[1]], na.rm = TRUE) #ta gjennomsnittet og kast NA verdier


return(ndvi)
}
annual_NDVI <- function(catchment_table){
 #transform NDVI elements to numeric
 ndvi <- as.numeric(catchment_table[,2])
 years <- catchment_table[,1] %>% str_sub(0,4) %>% unique()
 NDVI <- c()
 NDVI_SD <- c()
 #make a list where the indexes are every 12th element

 for(i in years){
  l <- grep(i, catchment_table[,1])
  ndvi_mean <- ndvi[l] %>% mean(na.rm = T)
  ndvi_sd <- ndvi[l] %>% sd(na.rm = T)
  NDVI <- append(NDVI,ndvi_mean)
  NDVI_SD <- append(NDVI_SD, ndvi_sd)
 }
 ndvi_df <- data.frame(years,NDVI, NDVI_SD)
 return(ndvi_df)
}


#function for returning NDVI for specific years
```

```
pathS<-"~/catchment_outlines/catchment_outlines/Sampling/odberyHBU.shp"
testS<-st_read(pathS)

#nr.1 Pisek nad
path1<-"~/catchment_outlines/catchment_outlines/1/Otava-O1.shp"
test1<-st_read(path1)

#nr.2 Blanice - Putim Pod
path2<-"~/catchment_outlines/catchment_outlines/2/Otava-O2.shp"
test2<-st_read(path2)

#nr.3 Volyňka
path3<-"~/catchment_outlines/catchment_outlines/3/Otava-O3.shp"
test3<-st_read(path3)

#nr.5 Černíčský potok
path5<-"~/catchment_outlines/catchment_outlines/5/Otava-O5.shp"
test5<-st_read(path5)

#nr. 9 Volsovkou
path9<-"~/catchment_outlines/catchment_outlines/9/Otava-O9.shp"
test9<-st_read(path9)

#nr. 10 Locenice
path10<-"~/catchment_outlines/catchment_outlines/10/Otava-O10.shp"
test10<-st_read(path10)


#nr.14 Blanice - Podedvory
path14<-"~/catchment_outlines/catchment_outlines/14/Otava-O14.shp"
test14<-st_read(path14) #24 deler



#nr.1 Pisek
Otava1_nr1<-test1[1,]

#nr.2 Blanice -Putim Pod
Otava2_nr1<-test2[1,]
Otava2_nr2<-test2[2,]
Otava2_nr3<-test2[3,]
Otava2_nr4<-test2[4,]
Otava2_nr5<-test2[5,]
Otava2_nr6<-test2[6,]
Otava2_nr7<-test2[7,]
Otava2_nr8<-test2[8,]
Otava2_nr9<-test2[9,]
Otava2_nr10<-test2[10,]
Otava2_nr11<-test2[11,]
Otava2_nr12<-test2[12,]
Otava2_nr13<-test2[13,]
Otava2_nr14<-test2[14,]
Otava2_nr15<-test2[15,]
Otava2_nr16<-test2[16,]
Otava2_nr17<-test2[17,]
Otava2_nr18<-test2[18,]
Otava2_nr19<-test2[19,]
Otava2_nr20<-test2[20,]
Otava2_nr21<-test2[21,]
Otava2_nr22<-test2[22,]
Otava2_nr23<-test2[23,]
Otava2_nr24<-test2[24,]
Otava2_nr25<-test2[25,]
Otava2_nr26<-test2[26,]
Otava2_nr27<-test2[27,]
Otava2_nr28<-test2[28,]
Otava2_nr29<-test2[29,]
Otava2_nr30<-test2[30,]
Otava2_nr31<-test2[31,]
Otava2_nr32<-test2[32,]
Otava2_nr33<-test2[33,]
Otava2_nr34<-test2[34,]
Otava2_nr35<-test2[35,]
Otava2_nr36<-test2[36,]
Otava2_nr37<-test2[37,]
Otava2_nr38<-test2[38,]
Otava2_nr39<-test2[39,]
Otava2_nr40<-test2[40,]
Otava2_nr41<-test2[41,]
Otava2_nr42<-test2[42,]
Otava2_nr43<-test2[43,]
Otava2_nr44<-test2[44,]
Otava2_nr45<-test2[45,]
Otava2_nr46<-test2[46,]
Otava2_nr47<-test2[47,]
Otava2_nr48<-test2[48,]
Otava2_nr49<-test2[49,]
Otava2_nr50<-test2[50,]
Otava2_nr51<-test2[51,]
Otava2_nr52<-test2[52,]
Otava2_nr53<-test2[53,]
Otava2_nr54<-test2[54,]
Otava2_nr55<-test2[55,]
```

```
Otava2_nr56<-test2[56,]
Otava2_nr57<-test2[57,]
Otava2_nr58<-test2[58,]
Otava2_nr59<-test2[59,]
Otava2_nr60<-test2[60,]
Otava2_nr61<-test2[61,]
Otava2_nr62<-test2[62,]
Otava2_nr63<-test2[63,]
Otava2_nr64<-test2[64,]
Otava2_nr65<-test2[65,]
Otava2_nr66<-test2[66,]
Otava2_nr67<-test2[67,]
Otava2_nr68<-test2[68,]
Otava2_nr69<-test2[69,]
Otava2_nr70<-test2[70,]
Otava2_nr71<-test2[71,]
Otava2_nr72<-test2[72,]
Otava2_nr73<-test2[73,]
Otava2_nr74<-test2[74,]
Otava2_nr75<-test2[75,]
Otava2_nr76<-test2[76,]
Otava2_nr77<-test2[77,]
Otava2_nr78<-test2[78,]
Otava2_nr79<-test2[79,]
Otava2_nr80<-test2[80,]
Otava2_nr81<-test2[81,]
Otava2_nr82<-test2[82,]
Otava2_nr83<-test2[83,]
Otava2_nr84<-test2[84,]
Otava2_nr85<-test2[85,]
Otava2_nr86<-test2[86,]
Otava2_nr87<-test2[87,]
Otava2_nr88<-test2[88,]
Otava2_nr89<-test2[89,]
Otava2_nr90<-test2[90,]
Otava2_nr91<-test2[91,]
Otava2_nr92<-test2[92,]
Otava2_nr93<-test2[93,]
Otava2_nr94<-test2[94,]
Otava2_nr95<-test2[95,]
Otava2_nr96<-test2[96,]
Otava2_nr97<-test2[97,]
Otava2_nr98<-test2[98,]
Otava2_nr99<-test2[99,]
Otava2_nr100<-test2[100,]
Otava2_nr101<-test2[101,]
Otava2_nr102<-test2[102,]
Otava2_nr103<-test2[103,]
Otava2_nr104<-test2[104,]
Otava2_nr105<-test2[105,]
Otava2_nr106<-test2[106,]
Otava2_nr107<-test2[107,]
Otava2_nr108<-test2[108,]
Otava2_nr109<-test2[109,]
Otava2_nr110<-test2[110,]
Otava2_nr111<-test2[111,]
Otava2_nr112<-test2[112,]
Otava2_nr113<-test2[113,]
Otava2_nr114<-test2[114,]
Otava2_nr115<-test2[115,]


#nr.3 Volyňka
Otava3_nr1<-test3[1,]
Otava3_nr2<-test3[2,]
Otava3_nr3<-test3[3,]
Otava3_nr4<-test3[4,]
Otava3_nr5<-test3[5,]
Otava3_nr6<-test3[6,]
Otava3_nr7<-test3[7,]
Otava3_nr8<-test3[8,]
Otava3_nr9<-test3[9,]
Otava3_nr10<-test3[10,]
Otava3_nr11<-test3[11,]
Otava3_nr12<-test3[12,]
Otava3_nr13<-test3[13,]
Otava3_nr14<-test3[14,]
Otava3_nr15<-test3[15,]
Otava3_nr16<-test3[16,]
Otava3_nr17<-test3[17,]
Otava3_nr18<-test3[18,]
Otava3_nr19<-test3[19,]
Otava3_nr20<-test3[20,]
Otava3_nr21<-test3[21,]
Otava3_nr22<-test3[22,]
Otava3_nr23<-test3[23,]
Otava3_nr24<-test3[24,]
Otava3_nr25<-test3[25,]
Otava3_nr26<-test3[26,]
Otava3_nr27<-test3[27,]
Otava3_nr28<-test3[28,]
Otava3_nr29<-test3[29,]
Otava3_nr30<-test3[30,]
```

```
Otava3_nr31<-test3[31,]
Otava3_nr32<-test3[32,]
Otava3_nr33<-test3[33,]
Otava3_nr34<-test3[34,]
Otava3_nr35<-test3[35,]
Otava3_nr36<-test3[36,]
Otava3_nr37<-test3[37,]
Otava3_nr38<-test3[38,]
Otava3_nr39<-test3[39,]
Otava3_nr40<-test3[40,]
Otava3_nr41<-test3[41,]
Otava3_nr42<-test3[42,]
Otava3_nr43<-test3[43,]
Otava3_nr44<-test3[44,]

#nr.5 Černíčský potok
Otava5_nr1<-test5[1,]
Otava5_nr2<-test5[2,]
Otava5_nr3<-test5[3,]
Otava5_nr4<-test5[4,]
Otava5_nr5<-test5[5,]


#nr.9 Volsovkou
Otava9_nr1<-test9[1,]
Otava9_nr2<-test9[2,]
Otava9_nr3<-test9[3,]
Otava9_nr4<-test9[4,]
Otava9_nr5<-test9[5,]
Otava9_nr6<-test9[6,]
Otava9_nr7<-test9[7,]
Otava9_nr8<-test9[8,]
Otava9_nr9<-test9[9,]
Otava9_nr10<-test9[10,]
Otava9_nr11<-test9[11,]
Otava9_nr12<-test9[12,]
Otava9_nr13<-test9[13,]
Otava9_nr14<-test9[14,]
Otava9_nr15<-test9[15,]
Otava9_nr16<-test9[16,]
Otava9_nr17<-test9[17,]
Otava9_nr18<-test9[18,]
Otava9_nr19<-test9[19,]
Otava9_nr20<-test9[20,]
Otava9_nr21<-test9[21,]
Otava9_nr22<-test9[22,]
Otava9_nr23<-test9[23,]
Otava9_nr24<-test9[24,]
Otava9_nr25<-test9[25,]
Otava9_nr26<-test9[26,]
Otava9_nr27<-test9[27,]
Otava9_nr28<-test9[28,]
Otava9_nr29<-test9[29,]
Otava9_nr30<-test9[30,]
Otava9_nr31<-test9[31,]
Otava9_nr32<-test9[32,]
Otava9_nr33<-test9[33,]
Otava9_nr34<-test9[34,]
Otava9_nr35<-test9[35,]
Otava9_nr36<-test9[36,]
Otava9_nr37<-test9[37,]
Otava9_nr38<-test9[38,]
Otava9_nr39<-test9[39,]
Otava9_nr40<-test9[40,]
Otava9_nr41<-test9[41,]
Otava9_nr42<-test9[42,]
Otava9_nr43<-test9[43,]
Otava9_nr44<-test9[44,]
Otava9_nr45<-test9[45,]
Otava9_nr46<-test9[46,]
Otava9_nr47<-test9[47,]
Otava9_nr48<-test9[48,]
Otava9_nr49<-test9[49,]
Otava9_nr50<-test9[50,]
Otava9_nr51<-test9[51,]
Otava9_nr52<-test9[52,]
Otava9_nr53<-test9[53,]
Otava9_nr54<-test9[54,]
Otava9_nr55<-test9[55,]

#nr.10 Locenice
Otava10_nr1<-test10[1,]
Otava10_nr2<-test10[2,]
Otava10_nr3<-test10[3,]
Otava10_nr4<-test10[4,]
Otava10_nr5<-test10[5,]

#nr.14 Podedvory
Otava14_nr1<-test14[1,]
Otava14_nr2<-test14[2,]
Otava14_nr3<-test14[3,]
Otava14_nr4<-test14[4,]
Otava14_nr5<-test14[5,]
```

```
Otava14_nr6<-test14[6,]
Otava14_nr7<-test14[7,]
Otava14_nr8<-test14[8,]
Otava14_nr9<-test14[9,]
Otava14_nr10<-test14[10,]
Otava14_nr11<-test14[11,]
Otava14_nr12<-test14[12,]
Otava14_nr13<-test14[13,]
Otava14_nr14<-test14[14,]
Otava14_nr15<-test14[15,]
Otava14_nr16<-test14[16,]
Otava14_nr17<-test14[17,]
Otava14_nr18<-test14[18,]
Otava14_nr19<-test14[19,]
Otava14_nr20<-test14[20,]
Otava14_nr21<-test14[21,]
Otava14_nr22<-test14[22,]
Otava14_nr23<-test14[23,]
Otava14_nr24<-test14[24,]
Otava14_nr25<-test14[25,]


#Nummer 1 Pisek
table1_1 <- mean_of_shapefile(Otava1_nr1,2000,2019)
mean1_1 <- annual_NDVI(table1_1)
mean1_1$geometry <- Otava1_nr1$geometry
mean1_1$id <- "Otava1_nr1"

#2 Blanice - Putim pod
table1_2 <- mean_of_shapefile(Otava2_nr1,2000,2019)
mean1_2 <- annual_NDVI(table1_2)
mean1_2$geometry <- Otava2_nr1$geometry
mean1_2$id <- "Otava2_nr1"

table2_2 <- mean_of_shapefile(Otava2_nr2,2000,2019)
mean2_2 <- annual_NDVI(table2_2)
mean2_2$geometry <- Otava2_nr2$geometry
mean2_2$id <- "Otava2_nr2"

table3_2 <- mean_of_shapefile(Otava2_nr3,2000,2019)
mean3_2 <- annual_NDVI(table3_2)
mean3_2$geometry <- Otava2_nr3$geometry
mean3_2$id <- "Otava2_nr3"

table4_2 <- mean_of_shapefile(Otava2_nr4,2000,2019)
mean4_2 <- annual_NDVI(table4_2)
mean4_2$geometry <- Otava2_nr4$geometry
mean4_2$id <- "Otava2_nr4"

table5_2 <- mean_of_shapefile(Otava2_nr5,2000,2019)
mean5_2 <- annual_NDVI(table5_2)
mean5_2$geometry <- Otava2_nr5$geometry
mean5_2$id <- "Otava2_nr5"

table6_2 <- mean_of_shapefile(Otava2_nr6,2000,2019)
mean6_2 <- annual_NDVI(table6_2)
mean6_2$geometry <- Otava2_nr6$geometry
mean6_2$id <- "Otava2_nr6"

table7_2 <- mean_of_shapefile(Otava2_nr7,2000,2019)
mean7_2 <- annual_NDVI(table7_2)
mean7_2$geometry <- Otava2_nr7$geometry
mean7_2$id <- "Otava2_nr7"

table8_2 <- mean_of_shapefile(Otava2_nr8,2000,2019)
mean8_2 <- annual_NDVI(table8_2)
mean8_2$geometry <- Otava2_nr8$geometry
mean8_2$id <- "Otava2_nr8"

table9_2 <- mean_of_shapefile(Otava2_nr9,2000,2019)
mean9_2 <- annual_NDVI(table9_2)
mean9_2$geometry <- Otava2_nr9$geometry
mean9_2$id <- "Otava2_nr9"

table10_2 <- mean_of_shapefile(Otava2_nr10,2000,2019)
mean10_2 <- annual_NDVI(table10_2)
mean10_2$geometry <- Otava2_nr10$geometry
mean10_2$id <- "Otava2_nr10"

table11_2 <- mean_of_shapefile(Otava2_nr11,2000,2019)
mean11_2 <- annual_NDVI(table11_2)
mean11_2$geometry <- Otava2_nr11$geometry
mean11_2$id <- "Otava2_nr11"

table12_2 <- mean_of_shapefile(Otava2_nr12,2000,2019)
mean12_2 <- annual_NDVI(table12_2)
mean12_2$geometry <- Otava2_nr12$geometry
mean12_2$id <- "Otava2_nr12"

table13_2 <- mean_of_shapefile(Otava2_nr13,2000,2019)
mean13_2 <- annual_NDVI(table13_2)
mean13_2$geometry <- Otava2_nr13$geometry
mean13_2$id <- "Otava2_nr13"
```

```
table14_2 <- mean_of_shapefile(Otava2_nr14,2000,2019)
mean14_2 <- annual_NDVI(table14_2)
mean14_2$geometry <- Otava2_nr14$geometry
mean14_2$id <- "Otava2_nr14"

table15_2 <- mean_of_shapefile(Otava2_nr15,2000,2019)
mean15_2 <- annual_NDVI(table15_2)
mean15_2$geometry <- Otava2_nr15$geometry
mean15_2$id <- "Otava2_nr15"

table16_2 <- mean_of_shapefile(Otava2_nr16,2000,2019)
mean16_2 <- annual_NDVI(table16_2)
mean16_2$geometry <- Otava2_nr16$geometry
mean16_2$id <- "Otava2_nr16"

table17_2 <- mean_of_shapefile(Otava2_nr17,2000,2019)
mean17_2 <- annual_NDVI(table17_2)
mean17_2$geometry <- Otava2_nr17$geometry
mean17_2$id <- "Otava2_nr17"

table18_2 <- mean_of_shapefile(Otava2_nr18,2000,2019)
mean18_2 <- annual_NDVI(table18_2)
mean18_2$geometry <- Otava2_nr18$geometry
mean18_2$id <- "Otava2_nr18"

table19_2 <- mean_of_shapefile(Otava2_nr19,2000,2019)
mean19_2 <- annual_NDVI(table19_2)
mean19_2$geometry <- Otava2_nr19$geometry
mean19_2$id <- "Otava2_nr19"

table20_2 <- mean_of_shapefile(Otava2_nr20,2000,2019)
mean20_2 <- annual_NDVI(table20_2)
mean20_2$geometry <- Otava2_nr20$geometry
mean20_2$id <- "Otava2_nr20"

table21_2 <- mean_of_shapefile(Otava2_nr21,2000,2019)
mean21_2 <- annual_NDVI(table21_2)
mean21_2$geometry <- Otava2_nr21$geometry
mean21_2$id <- "Otava2_nr21"

table22_2 <- mean_of_shapefile(Otava2_nr22,2000,2019)
mean22_2 <- annual_NDVI(table22_2)
mean22_2$geometry <- Otava2_nr22$geometry
mean22_2$id <- "Otava2_nr22"

table23_2 <- mean_of_shapefile(Otava2_nr23,2000,2019)
mean23_2 <- annual_NDVI(table23_2)
mean23_2$geometry <- Otava2_nr23$geometry
mean23_2$id <- "Otava2_nr23"

table24_2 <- mean_of_shapefile(Otava2_nr24,2000,2019)
mean24_2 <- annual_NDVI(table24_2)
mean24_2$geometry <- Otava2_nr24$geometry
mean24_2$id <- "Otava2_nr24"

table25_2 <- mean_of_shapefile(Otava2_nr25,2000,2019)
mean25_2 <- annual_NDVI(table25_2)
mean25_2$geometry <- Otava2_nr25$geometry
mean25_2$id <- "Otava2_nr25"

table26_2 <- mean_of_shapefile(Otava2_nr26,2000,2019)
mean26_2 <- annual_NDVI(table26_2)
mean26_2$geometry <- Otava2_nr26$geometry
mean26_2$id <- "Otava2_nr26"

table27_2 <- mean_of_shapefile(Otava2_nr27,2000,2019)
mean27_2 <- annual_NDVI(table27_2)
mean27_2$geometry <- Otava2_nr27$geometry
mean27_2$id <- "Otava2_nr27"

table28_2 <- mean_of_shapefile(Otava2_nr28,2000,2019)
mean28_2 <- annual_NDVI(table28_2)
mean28_2$geometry <- Otava2_nr28$geometry
mean28_2$id <- "Otava2_nr28"

table29_2 <- mean_of_shapefile(Otava2_nr29,2000,2019)
mean29_2 <- annual_NDVI(table29_2)
mean29_2$geometry <- Otava2_nr29$geometry
mean29_2$id <- "Otava2_nr29"

table30_2 <- mean_of_shapefile(Otava2_nr30,2000,2019)
mean30_2 <- annual_NDVI(table30_2)
mean30_2$geometry <- Otava2_nr30$geometry
mean30_2$id <- "Otava2_nr30"

table31_2 <- mean_of_shapefile(Otava2_nr31,2000,2019)
mean31_2 <- annual_NDVI(table31_2)
mean31_2$geometry <- Otava2_nr31$geometry
mean31_2$id <- "Otava2_nr31"

table32_2 <- mean_of_shapefile(Otava2_nr32,2000,2019)
mean32_2 <- annual_NDVI(table32_2)
```

```
mean32_2$geometry <- Otava2_nr32$geometry
mean32_2$id <- "Otava2_nr32"

table33_2 <- mean_of_shapefile(Otava2_nr33,2000,2019)
mean33_2 <- annual_NDVI(table33_2)
mean33_2$geometry <- Otava2_nr33$geometry
mean33_2$id <- "Otava2_nr33"

table34_2 <- mean_of_shapefile(Otava2_nr34,2000,2019)
mean34_2 <- annual_NDVI(table34_2)
mean34_2$geometry <- Otava2_nr34$geometry
mean34_2$id <- "Otava2_nr34"

table35_2 <- mean_of_shapefile(Otava2_nr35,2000,2019)
mean35_2 <- annual_NDVI(table35_2)
mean35_2$geometry <- Otava2_nr35$geometry
mean35_2$id <- "Otava2_nr35"

table36_2 <- mean_of_shapefile(Otava2_nr36,2000,2019)
mean36_2 <- annual_NDVI(table36_2)
mean36_2$geometry <- Otava2_nr36$geometry
mean36_2$id <- "Otava2_nr36"

table37_2 <- mean_of_shapefile(Otava2_nr37,2000,2019)
mean37_2 <- annual_NDVI(table37_2)
mean37_2$geometry <- Otava2_nr37$geometry
mean37_2$id <- "Otava2_nr37"

table38_2 <- mean_of_shapefile(Otava2_nr38,2000,2019)
mean38_2 <- annual_NDVI(table38_2)
mean38_2$geometry <- Otava2_nr38$geometry
mean38_2$id <- "Otava2_nr38"

table39_2 <- mean_of_shapefile(Otava2_nr39,2000,2019)
mean39_2 <- annual_NDVI(table39_2)
mean39_2$geometry <- Otava2_nr39$geometry
mean39_2$id <- "Otava2_nr39"

table40_2 <- mean_of_shapefile(Otava2_nr40,2000,2019)
mean40_2 <- annual_NDVI(table40_2)
mean40_2$geometry <- Otava2_nr40$geometry
mean40_2$id <- "Otava2_nr40"

table41_2 <- mean_of_shapefile(Otava2_nr41,2000,2019)
mean41_2 <- annual_NDVI(table41_2)
mean41_2$geometry <- Otava2_nr41$geometry
mean41_2$id <- "Otava2_nr41"

table42_2 <- mean_of_shapefile(Otava2_nr42,2000,2019)
mean42_2 <- annual_NDVI(table42_2)
mean42_2$geometry <- Otava2_nr42$geometry
mean42_2$id <- "Otava2_nr42"

table43_2 <- mean_of_shapefile(Otava2_nr43,2000,2019)
mean43_2 <- annual_NDVI(table43_2)
mean43_2$geometry <- Otava2_nr43$geometry
mean43_2$id <- "Otava2_nr43"

table44_2 <- mean_of_shapefile(Otava2_nr44,2000,2019)
mean44_2 <- annual_NDVI(table44_2)
mean44_2$geometry <- Otava2_nr44$geometry
mean44_2$id <- "Otava2_nr44"

table45_2 <- mean_of_shapefile(Otava2_nr45,2000,2019)
mean45_2 <- annual_NDVI(table45_2)
mean45_2$geometry <- Otava2_nr45$geometry
mean45_2$id <- "Otava2_nr45"

table46_2 <- mean_of_shapefile(Otava2_nr46,2000,2019)
mean46_2 <- annual_NDVI(table46_2)
mean46_2$geometry <- Otava2_nr46$geometry
mean46_2$id <- "Otava2_nr46"

table47_2 <- mean_of_shapefile(Otava2_nr47,2000,2019)
mean47_2 <- annual_NDVI(table47_2)
mean47_2$geometry <- Otava2_nr47$geometry
mean47_2$id <- "Otava2_nr47"

table48_2 <- mean_of_shapefile(Otava2_nr48,2000,2019)
mean48_2 <- annual_NDVI(table48_2)
mean48_2$geometry <- Otava2_nr48$geometry
mean48_2$id <- "Otava2_nr48"

table49_2 <- mean_of_shapefile(Otava2_nr49,2000,2019)
mean49_2 <- annual_NDVI(table49_2)
mean49_2$geometry <- Otava2_nr49$geometry
mean49_2$id <- "Otava2_nr49"

table50_2 <- mean_of_shapefile(Otava2_nr50,2000,2019)
mean50_2 <- annual_NDVI(table50_2)
mean50_2$geometry <- Otava2_nr50$geometry
mean50_2$id <- "Otava2_nr50"
```

```
table51_2 <- mean_of_shapefile(Otava2_nr51,2000,2019)
mean51_2 <- annual_NDVI(table51_2)
mean51_2$geometry <- Otava2_nr51$geometry
mean51_2$id <- "Otava2_nr51"

table52_2 <- mean_of_shapefile(Otava2_nr52,2000,2019)
mean52_2 <- annual_NDVI(table52_2)
mean52_2$geometry <- Otava2_nr52$geometry
mean52_2$id <- "Otava2_nr52"

table53_2 <- mean_of_shapefile(Otava2_nr53,2000,2019)
mean53_2 <- annual_NDVI(table53_2)
mean53_2$geometry <- Otava2_nr53$geometry
mean53_2$id <- "Otava2_nr53"

table54_2 <- mean_of_shapefile(Otava2_nr54,2000,2019)
mean54_2 <- annual_NDVI(table54_2)
mean54_2$geometry <- Otava2_nr54$geometry
mean54_2$id <- "Otava2_nr54"

table55_2 <- mean_of_shapefile(Otava2_nr55,2000,2019)
mean55_2 <- annual_NDVI(table55_2)
mean55_2$geometry <- Otava2_nr55$geometry
mean55_2$id <- "Otava2_nr55"

table56_2 <- mean_of_shapefile(Otava2_nr56,2000,2019)
mean56_2 <- annual_NDVI(table56_2)
mean56_2$geometry <- Otava2_nr56$geometry
mean56_2$id <- "Otava2_nr56"

table57_2 <- mean_of_shapefile(Otava2_nr57,2000,2019)
mean57_2 <- annual_NDVI(table57_2)
mean57_2$geometry <- Otava2_nr57$geometry
mean57_2$id <- "Otava2_nr57"

table58_2 <- mean_of_shapefile(Otava2_nr58,2000,2019)
mean58_2 <- annual_NDVI(table58_2)
mean58_2$geometry <- Otava2_nr58$geometry
mean58_2$id <- "Otava2_nr58"

table59_2 <- mean_of_shapefile(Otava2_nr59,2000,2019)
mean59_2 <- annual_NDVI(table59_2)
mean59_2$geometry <- Otava2_nr59$geometry
mean59_2$id <- "Otava2_nr59"

table60_2 <- mean_of_shapefile(Otava2_nr60,2000,2019)
mean60_2 <- annual_NDVI(table60_2)
mean60_2$geometry <- Otava2_nr60$geometry
mean60_2$id <- "Otava2_nr60"

table61_2 <- mean_of_shapefile(Otava2_nr61,2000,2019)
mean61_2 <- annual_NDVI(table61_2)
mean61_2$geometry <- Otava2_nr61$geometry
mean61_2$id <- "Otava2_nr61"

table62_2 <- mean_of_shapefile(Otava2_nr62,2000,2019)
mean62_2 <- annual_NDVI(table62_2)
mean62_2$geometry <- Otava2_nr62$geometry
mean62_2$id <- "Otava2_nr62"

table63_2 <- mean_of_shapefile(Otava2_nr63,2000,2019)
mean63_2 <- annual_NDVI(table63_2)
mean63_2$geometry <- Otava2_nr63$geometry
mean63_2$id <- "Otava2_nr63"

table64_2 <- mean_of_shapefile(Otava2_nr64,2000,2019)
mean64_2 <- annual_NDVI(table64_2)
mean64_2$geometry <- Otava2_nr64$geometry
mean64_2$id <- "Otava2_nr64"

table65_2 <- mean_of_shapefile(Otava2_nr65,2000,2019)
mean65_2 <- annual_NDVI(table65_2)
mean65_2$geometry <- Otava2_nr65$geometry
mean65_2$id <- "Otava2_nr65"

table66_2 <- mean_of_shapefile(Otava2_nr66,2000,2019)
mean66_2 <- annual_NDVI(table66_2)
mean66_2$geometry <- Otava2_nr66$geometry
mean66_2$id <- "Otava2_nr66"

table67_2 <- mean_of_shapefile(Otava2_nr67,2000,2019)
mean67_2 <- annual_NDVI(table67_2)
mean67_2$geometry <- Otava2_nr67$geometry
mean67_2$id <- "Otava2_nr67"

table68_2 <- mean_of_shapefile(Otava2_nr68,2000,2019)
mean68_2 <- annual_NDVI(table68_2)
mean68_2$geometry <- Otava2_nr68$geometry
mean68_2$id <- "Otava2_nr68"

table69_2 <- mean_of_shapefile(Otava2_nr69,2000,2019)
mean69_2 <- annual_NDVI(table69_2)
mean69_2$geometry <- Otava2_nr69$geometry
```

```
mean69_2$id <- "Otava2_nr69"

table70_2 <- mean_of_shapefile(Otava2_nr70,2000,2019)
mean70_2 <- annual_NDVI(table70_2)
mean70_2$geometry <- Otava2_nr70$geometry
mean70_2$id <- "Otava2_nr70"

table71_2 <- mean_of_shapefile(Otava2_nr71,2000,2019)
mean71_2 <- annual_NDVI(table71_2)
mean71_2$geometry <- Otava2_nr71$geometry
mean71_2$id <- "Otava2_nr71"

table72_2 <- mean_of_shapefile(Otava2_nr72,2000,2019)
mean72_2 <- annual_NDVI(table72_2)
mean72_2$geometry <- Otava2_nr72$geometry
mean72_2$id <- "Otava2_nr72"

table73_2 <- mean_of_shapefile(Otava2_nr73,2000,2019)
mean73_2 <- annual_NDVI(table73_2)
mean73_2$geometry <- Otava2_nr73$geometry
mean73_2$id <- "Otava2_nr73"

table74_2 <- mean_of_shapefile(Otava2_nr74,2000,2019)
mean74_2 <- annual_NDVI(table74_2)
mean74_2$geometry <- Otava2_nr74$geometry
mean74_2$id <- "Otava2_nr74"

table75_2 <- mean_of_shapefile(Otava2_nr75,2000,2019)
mean75_2 <- annual_NDVI(table75_2)
mean75_2$geometry <- Otava2_nr75$geometry
mean75_2$id <- "Otava2_nr75"

table76_2 <- mean_of_shapefile(Otava2_nr76,2000,2019)
mean76_2 <- annual_NDVI(table76_2)
mean76_2$geometry <- Otava2_nr76$geometry
mean76_2$id <- "Otava2_nr76"

table77_2 <- mean_of_shapefile(Otava2_nr77,2000,2019)
mean77_2 <- annual_NDVI(table77_2)
mean77_2$geometry <- Otava2_nr77$geometry
mean77_2$id <- "Otava2_nr77"

table78_2 <- mean_of_shapefile(Otava2_nr78,2000,2019)
mean78_2 <- annual_NDVI(table78_2)
mean78_2$geometry <- Otava2_nr78$geometry
mean78_2$id <- "Otava2_nr78"

table79_2 <- mean_of_shapefile(Otava2_nr79,2000,2019)
mean79_2 <- annual_NDVI(table79_2)
mean79_2$geometry <- Otava2_nr79$geometry
mean79_2$id <- "Otava2_nr79"

table80_2 <- mean_of_shapefile(Otava2_nr80,2000,2019)
mean80_2 <- annual_NDVI(table80_2)
mean80_2$geometry <- Otava2_nr80$geometry
mean80_2$id <- "Otava2_nr80"

table81_2 <- mean_of_shapefile(Otava2_nr81,2000,2019)
mean81_2 <- annual_NDVI(table81_2)
mean81_2$geometry <- Otava2_nr81$geometry
mean81_2$id <- "Otava2_nr81"

table82_2 <- mean_of_shapefile(Otava2_nr82,2000,2019)
mean82_2 <- annual_NDVI(table82_2)
mean82_2$geometry <- Otava2_nr82$geometry
mean82_2$id <- "Otava2_nr82"

table83_2 <- mean_of_shapefile(Otava2_nr83,2000,2019)
mean83_2 <- annual_NDVI(table83_2)
mean83_2$geometry <- Otava2_nr83$geometry
mean83_2$id <- "Otava2_nr83"

table84_2 <- mean_of_shapefile(Otava2_nr84,2000,2019)
mean84_2 <- annual_NDVI(table84_2)
mean84_2$geometry <- Otava2_nr84$geometry
mean84_2$id <- "Otava2_nr84"

table85_2 <- mean_of_shapefile(Otava2_nr85,2000,2019)
mean85_2 <- annual_NDVI(table85_2)
mean85_2$geometry <- Otava2_nr85$geometry
mean85_2$id <- "Otava2_nr85"

table86_2 <- mean_of_shapefile(Otava2_nr86,2000,2019)
mean86_2 <- annual_NDVI(table86_2)
mean86_2$geometry <- Otava2_nr86$geometry
mean86_2$id <- "Otava2_nr86"

table87_2 <- mean_of_shapefile(Otava2_nr87,2000,2019)
mean87_2 <- annual_NDVI(table87_2)
mean87_2$geometry <- Otava2_nr87$geometry
mean87_2$id <- "Otava2_nr87"

table88_2 <- mean_of_shapefile(Otava2_nr88,2000,2019)
```

```
mean88_2 <- annual_NDVI(table88_2)
mean88_2$geometry <- Otava2_nr88$geometry
mean88_2$id <- "Otava2_nr88"

table89_2 <- mean_of_shapefile(Otava2_nr89,2000,2019)
mean89_2 <- annual_NDVI(table89_2)
mean89_2$geometry <- Otava2_nr89$geometry
mean89_2$id <- "Otava2_nr89"

table90_2 <- mean_of_shapefile(Otava2_nr90,2000,2019)
mean90_2 <- annual_NDVI(table90_2)
mean90_2$geometry <- Otava2_nr90$geometry
mean90_2$id <- "Otava2_nr90"

table91_2 <- mean_of_shapefile(Otava2_nr91,2000,2019)
mean91_2 <- annual_NDVI(table91_2)
mean91_2$geometry <- Otava2_nr91$geometry
mean91_2$id <- "Otava2_nr91"

table92_2 <- mean_of_shapefile(Otava2_nr92,2000,2019)
mean92_2 <- annual_NDVI(table92_2)
mean92_2$geometry <- Otava2_nr92$geometry
mean92_2$id <- "Otava2_nr92"

table93_2 <- mean_of_shapefile(Otava2_nr93,2000,2019)
mean93_2 <- annual_NDVI(table93_2)
mean93_2$geometry <- Otava2_nr93$geometry
mean93_2$id <- "Otava2_nr93"

table94_2 <- mean_of_shapefile(Otava2_nr94,2000,2019)
mean94_2 <- annual_NDVI(table94_2)
mean94_2$geometry <- Otava2_nr94$geometry
mean94_2$id <- "Otava2_nr94"

table95_2 <- mean_of_shapefile(Otava2_nr95,2000,2019)
mean95_2 <- annual_NDVI(table95_2)
mean95_2$geometry <- Otava2_nr95$geometry
mean95_2$id <- "Otava2_nr95"

table96_2 <- mean_of_shapefile(Otava2_nr96,2000,2019)
mean96_2 <- annual_NDVI(table96_2)
mean96_2$geometry <- Otava2_nr96$geometry
mean96_2$id <- "Otava2_nr96"

table97_2 <- mean_of_shapefile(Otava2_nr97,2000,2019)
mean97_2 <- annual_NDVI(table97_2)
mean97_2$geometry <- Otava2_nr97$geometry
mean97_2$id <- "Otava2_nr97"

table98_2 <- mean_of_shapefile(Otava2_nr98,2000,2019)
mean98_2 <- annual_NDVI(table98_2)
mean98_2$geometry <- Otava2_nr98$geometry
mean98_2$id <- "Otava2_nr98"

table99_2 <- mean_of_shapefile(Otava2_nr99,2000,2019)
mean99_2 <- annual_NDVI(table99_2)
mean99_2$geometry <- Otava2_nr99$geometry
mean99_2$id <- "Otava2_nr99"

table100_2 <- mean_of_shapefile(Otava2_nr100,2000,2019)
mean100_2 <- annual_NDVI(table100_2)
mean100_2$geometry <- Otava2_nr100$geometry
mean100_2$id <- "Otava2_nr100"

table101_2 <- mean_of_shapefile(Otava2_nr101,2000,2019)
mean101_2 <- annual_NDVI(table101_2)
mean101_2$geometry <- Otava2_nr101$geometry
mean101_2$id <- "Otava2_nr101"

table102_2 <- mean_of_shapefile(Otava2_nr102,2000,2019)
mean102_2 <- annual_NDVI(table102_2)
mean102_2$geometry <- Otava2_nr102$geometry
mean102_2$id <- "Otava2_nr102"

table103_2 <- mean_of_shapefile(Otava2_nr103,2000,2019)
mean103_2 <- annual_NDVI(table103_2)
mean103_2$geometry <- Otava2_nr103$geometry
mean103_2$id <- "Otava2_nr103"

table104_2 <- mean_of_shapefile(Otava2_nr104,2000,2019)
mean104_2 <- annual_NDVI(table104_2)
mean104_2$geometry <- Otava2_nr104$geometry
mean104_2$id <- "Otava2_nr104"

table105_2 <- mean_of_shapefile(Otava2_nr105,2000,2019)
mean105_2 <- annual_NDVI(table105_2)
mean105_2$geometry <- Otava2_nr105$geometry
mean105_2$id <- "Otava2_nr105"

table106_2 <- mean_of_shapefile(Otava2_nr106,2000,2019)
mean106_2 <- annual_NDVI(table106_2)
mean106_2$geometry <- Otava2_nr106$geometry
mean106_2$id <- "Otava2_nr106"
```

```
table107_2 <- mean_of_shapefile(Otava2_nr107,2000,2019)
mean107_2 <- annual_NDVI(table107_2)
mean107_2$geometry <- Otava2_nr107$geometry
mean107_2$id <- "Otava2_nr107"

table108_2 <- mean_of_shapefile(Otava2_nr108,2000,2019)
mean108_2 <- annual_NDVI(table108_2)
mean108_2$geometry <- Otava2_nr108$geometry
mean108_2$id <- "Otava2_nr108"

table109_2 <- mean_of_shapefile(Otava2_nr109,2000,2019)
mean109_2 <- annual_NDVI(table109_2)
mean109_2$geometry <- Otava2_nr109$geometry
mean109_2$id <- "Otava2_nr109"

table110_2 <- mean_of_shapefile(Otava2_nr110,2000,2019)
mean110_2 <- annual_NDVI(table110_2)
mean110_2$geometry <- Otava2_nr110$geometry
mean110_2$id <- "Otava2_nr110"

table111_2 <- mean_of_shapefile(Otava2_nr111,2000,2019)
mean111_2 <- annual_NDVI(table111_2)
mean111_2$geometry <- Otava2_nr111$geometry
mean111_2$id <- "Otava2_nr111"

table112_2 <- mean_of_shapefile(Otava2_nr112,2000,2019)
mean112_2 <- annual_NDVI(table112_2)
mean112_2$geometry <- Otava2_nr112$geometry
mean112_2$id <- "Otava2_nr112"

table113_2 <- mean_of_shapefile(Otava2_nr113,2000,2019)
mean113_2 <- annual_NDVI(table113_2)
mean113_2$geometry <- Otava2_nr113$geometry
mean113_2$id <- "Otava2_nr113"

table114_2 <- mean_of_shapefile(Otava2_nr114,2000,2019)
mean114_2 <- annual_NDVI(table114_2)
mean114_2$geometry <- Otava2_nr114$geometry
mean114_2$id <- "Otava2_nr114"

table115_2 <- mean_of_shapefile(Otava2_nr115,2000,2019)
mean115_2 <- annual_NDVI(table115_2)
mean115_2$geometry <- Otava2_nr115$geometry
mean115_2$id <- "Otava2_nr115"

#nr 3 Volyňka
table1_3 <- mean_of_shapefile(Otava3_nr1,2000,2019)
mean1_3 <- annual_NDVI(table1_3)
mean1_3$geometry <- Otava3_nr1$geometry
mean1_3$id <- "Otava3_nr1"

table2_3 <- mean_of_shapefile(Otava3_nr2,2000,2019)
mean2_3 <- annual_NDVI(table2_3)
mean2_3$geometry <- Otava3_nr2$geometry
mean2_3$id <- "Otava3_nr2"

table3_3 <- mean_of_shapefile(Otava3_nr3,2000,2019)
mean3_3 <- annual_NDVI(table3_3)
mean3_3$geometry <- Otava3_nr3$geometry
mean3_3$id <- "Otava3_nr3"

table4_3 <- mean_of_shapefile(Otava3_nr4,2000,2019)
mean4_3 <- annual_NDVI(table4_3)
mean4_3$geometry <- Otava3_nr4$geometry
mean4_3$id <- "Otava3_nr4"

table5_3 <- mean_of_shapefile(Otava3_nr5,2000,2019)
mean5_3 <- annual_NDVI(table5_3)
mean5_3$geometry <- Otava3_nr5$geometry
mean5_3$id <- "Otava3_nr5"

table6_3 <- mean_of_shapefile(Otava3_nr6,2000,2019)
mean6_3 <- annual_NDVI(table6_3)
mean6_3$geometry <- Otava3_nr6$geometry
mean6_3$id <- "Otava3_nr6"

table7_3 <- mean_of_shapefile(Otava3_nr7,2000,2019)
mean7_3 <- annual_NDVI(table7_3)
mean7_3$geometry <- Otava3_nr7$geometry
mean7_3$id <- "Otava3_nr7"

table8_3 <- mean_of_shapefile(Otava3_nr8,2000,2019)
mean8_3 <- annual_NDVI(table8_3)
mean8_3$geometry <- Otava3_nr8$geometry
mean8_3$id <- "Otava3_nr8"

table9_3 <- mean_of_shapefile(Otava3_nr9,2000,2019)
mean9_3 <- annual_NDVI(table9_3)
mean9_3$geometry <- Otava3_nr9$geometry
mean9_3$id <- "Otava3_nr9"

table10_3 <- mean_of_shapefile(Otava3_nr10,2000,2019)
```

```
mean10_3 <- annual_NDVI(table10_3)
mean10_3$geometry <- Otava3_nr10$geometry
mean10_3$id <- "Otava3_nr10"

table11_3 <- mean_of_shapefile(Otava3_nr11,2000,2019)
mean11_3 <- annual_NDVI(table11_3)
mean11_3$geometry <- Otava3_nr11$geometry
mean11_3$id <- "Otava3_nr11"

table12_3 <- mean_of_shapefile(Otava3_nr12,2000,2019)
mean12_3 <- annual_NDVI(table12_3)
mean12_3$geometry <- Otava3_nr12$geometry
mean12_3$id <- "Otava3_nr12"

table13_3 <- mean_of_shapefile(Otava3_nr13,2000,2019)
mean13_3 <- annual_NDVI(table13_3)
mean13_3$geometry <- Otava3_nr13$geometry
mean13_3$id <- "Otava3_nr13"

table14_3 <- mean_of_shapefile(Otava3_nr14,2000,2019)
mean14_3 <- annual_NDVI(table14_3)
mean14_3$geometry <- Otava3_nr14$geometry
mean14_3$id <- "Otava3_nr14"

table15_3 <- mean_of_shapefile(Otava3_nr15,2000,2019)
mean15_3 <- annual_NDVI(table15_3)
mean15_3$geometry <- Otava3_nr15$geometry
mean15_3$id <- "Otava3_nr15"

table16_3 <- mean_of_shapefile(Otava3_nr16,2000,2019)
mean16_3 <- annual_NDVI(table16_3)
mean16_3$geometry <- Otava3_nr16$geometry
mean16_3$id <- "Otava3_nr16"

table17_3 <- mean_of_shapefile(Otava3_nr17,2000,2019)
mean17_3 <- annual_NDVI(table17_3)
mean17_3$geometry <- Otava3_nr17$geometry
mean17_3$id <- "Otava3_nr17"

table18_3 <- mean_of_shapefile(Otava3_nr18,2000,2019)
mean18_3 <- annual_NDVI(table18_3)
mean18_3$geometry <- Otava3_nr18$geometry
mean18_3$id <- "Otava3_nr18"

table19_3 <- mean_of_shapefile(Otava3_nr19,2000,2019)
mean19_3 <- annual_NDVI(table19_3)
mean19_3$geometry <- Otava3_nr19$geometry
mean19_3$id <- "Otava3_nr19"

table20_3 <- mean_of_shapefile(Otava3_nr20,2000,2019)
mean20_3 <- annual_NDVI(table20_3)
mean20_3$geometry <- Otava3_nr20$geometry
mean20_3$id <- "Otava3_nr20"

table21_3 <- mean_of_shapefile(Otava3_nr21,2000,2019)
mean21_3 <- annual_NDVI(table21_3)
mean21_3$geometry <- Otava3_nr21$geometry
mean21_3$id <- "Otava3_nr21"

table22_3 <- mean_of_shapefile(Otava3_nr22,2000,2019)
mean22_3 <- annual_NDVI(table22_3)
mean22_3$geometry <- Otava3_nr22$geometry
mean22_3$id <- "Otava3_nr22"

table23_3 <- mean_of_shapefile(Otava3_nr23,2000,2019)
mean23_3 <- annual_NDVI(table23_3)
mean23_3$geometry <- Otava3_nr23$geometry
mean23_3$id <- "Otava3_nr23"

table24_3 <- mean_of_shapefile(Otava3_nr24,2000,2019)
mean24_3 <- annual_NDVI(table24_3)
mean24_3$geometry <- Otava3_nr24$geometry
mean24_3$id <- "Otava3_nr24"

table25_3 <- mean_of_shapefile(Otava3_nr25,2000,2019)
mean25_3 <- annual_NDVI(table25_3)
mean25_3$geometry <- Otava3_nr25$geometry
mean25_3$id <- "Otava3_nr25"

table26_3 <- mean_of_shapefile(Otava3_nr26,2000,2019)
mean26_3 <- annual_NDVI(table26_3)
mean26_3$geometry <- Otava3_nr26$geometry
mean26_3$id <- "Otava3_nr26"

table27_3 <- mean_of_shapefile(Otava3_nr27,2000,2019)
mean27_3 <- annual_NDVI(table27_3)
mean27_3$geometry <- Otava3_nr27$geometry
mean27_3$id <- "Otava3_nr27"

table28_3 <- mean_of_shapefile(Otava3_nr28,2000,2019)
mean28_3 <- annual_NDVI(table28_3)
mean28_3$geometry <- Otava3_nr28$geometry
mean28_3$id <- "Otava3_nr28"
```

```
table29_3 <- mean_of_shapefile(Otava3_nr29,2000,2019)
mean29_3 <- annual_NDVI(table29_3)
mean29_3$geometry <- Otava3_nr29$geometry
mean29_3$id <- "Otava3_nr29"

table30_3 <- mean_of_shapefile(Otava3_nr30,2000,2019)
mean30_3 <- annual_NDVI(table30_3)
mean30_3$geometry <- Otava3_nr30$geometry
mean30_3$id <- "Otava3_nr30"

table31_3 <- mean_of_shapefile(Otava3_nr31,2000,2019)
mean31_3 <- annual_NDVI(table31_3)
mean31_3$geometry <- Otava3_nr31$geometry
mean31_3$id <- "Otava3_nr31"

table32_3 <- mean_of_shapefile(Otava3_nr32,2000,2019)
mean32_3 <- annual_NDVI(table32_3)
mean32_3$geometry <- Otava3_nr32$geometry
mean32_3$id <- "Otava3_nr32"

table33_3 <- mean_of_shapefile(Otava3_nr33,2000,2019)
mean33_3 <- annual_NDVI(table33_3)
mean33_3$geometry <- Otava3_nr33$geometry
mean33_3$id <- "Otava3_nr33"

table34_3 <- mean_of_shapefile(Otava3_nr34,2000,2019)
mean34_3 <- annual_NDVI(table34_3)
mean34_3$geometry <- Otava3_nr34$geometry
mean34_3$id <- "Otava3_nr34"

table35_3 <- mean_of_shapefile(Otava3_nr35,2000,2019)
mean35_3 <- annual_NDVI(table35_3)
mean35_3$geometry <- Otava3_nr35$geometry
mean35_3$id <- "Otava3_nr35"

table36_3 <- mean_of_shapefile(Otava3_nr36,2000,2019)
mean36_3 <- annual_NDVI(table36_3)
mean36_3$geometry <- Otava3_nr36$geometry
mean36_3$id <- "Otava3_nr36"

table37_3 <- mean_of_shapefile(Otava3_nr37,2000,2019)
mean37_3 <- annual_NDVI(table37_3)
mean37_3$geometry <- Otava3_nr37$geometry
mean37_3$id <- "Otava3_nr37"

table38_3 <- mean_of_shapefile(Otava3_nr38,2000,2019)
mean38_3 <- annual_NDVI(table38_3)
mean38_3$geometry <- Otava3_nr38$geometry
mean38_3$id <- "Otava3_nr38"

table39_3 <- mean_of_shapefile(Otava3_nr39,2000,2019)
mean39_3 <- annual_NDVI(table39_3)
mean39_3$geometry <- Otava3_nr39$geometry
mean39_3$id <- "Otava3_nr39"

table40_3 <- mean_of_shapefile(Otava3_nr40,2000,2019)
mean40_3 <- annual_NDVI(table40_3)
mean40_3$geometry <- Otava3_nr40$geometry
mean40_3$id <- "Otava3_nr40"

table41_3 <- mean_of_shapefile(Otava3_nr41,2000,2019)
mean41_3 <- annual_NDVI(table41_3)
mean41_3$geometry <- Otava3_nr41$geometry
mean41_3$id <- "Otava3_nr41"

table42_3 <- mean_of_shapefile(Otava3_nr42,2000,2019)
mean42_3 <- annual_NDVI(table42_3)
mean42_3$geometry <- Otava3_nr42$geometry
mean42_3$id <- "Otava3_nr42"

table43_3 <- mean_of_shapefile(Otava3_nr43,2000,2019)
mean43_3 <- annual_NDVI(table43_3)
mean43_3$geometry <- Otava3_nr43$geometry
mean43_3$id <- "Otava3_nr43"

table44_3 <- mean_of_shapefile(Otava3_nr44,2000,2019)
mean44_3 <- annual_NDVI(table44_3)
mean44_3$geometry <- Otava3_nr44$geometry
mean44_3$id <- "Otava3_nr44"

#nr. 5 Černíčský potok
table1_5 <- mean_of_shapefile(Otava5_nr1,2000,2019)
mean1_5 <- annual_NDVI(table1_5)
mean1_5$geometry <- Otava5_nr1$geometry
mean1_5$id <- "Otava5_nr1"

table2_5 <- mean_of_shapefile(Otava5_nr2,2000,2019)
mean2_5 <- annual_NDVI(table2_5)
mean2_5$geometry <- Otava5_nr1$geometry
mean2_5$id <- "Otava5_nr2"

table3_5 <- mean_of_shapefile(Otava5_nr3,2000,2019)
```

```
mean3_5 <- annual_NDVI(table3_5)
mean3_5$geometry <- Otava5_nr1$geometry
mean3_5$id <- "Otava5_nr3"

table4_5 <- mean_of_shapefile(Otava5_nr4,2000,2019)
mean4_5 <- annual_NDVI(table4_5)
mean4_5$geometry <- Otava5_nr1$geometry
mean4_5$id <- "Otava5_nr4"

table5_5 <- mean_of_shapefile(Otava5_nr5,2000,2019)
mean5_5 <- annual_NDVI(table5_5)
mean5_5$geometry <- Otava5_nr1$geometry
mean5_5$id <- "Otava5_nr5"

#nr.9 Volsovkou
table1_9 <- mean_of_shapefile(Otava9_nr1,2000,2019)
mean1_9 <- annual_NDVI(table1_9)
mean1_9$geometry <- Otava9_nr1$geometry
mean1_9$id <- "Otava9_nr1"

table2_9 <- mean_of_shapefile(Otava9_nr2,2000,2019)
mean2_9 <- annual_NDVI(table2_9)
mean2_9$geometry <- Otava9_nr2$geometry
mean2_9$id <- "Otava9_nr2"

table3_9 <- mean_of_shapefile(Otava9_nr3,2000,2019)
mean3_9 <- annual_NDVI(table3_9)
mean3_9$geometry <- Otava9_nr3$geometry
mean3_9$id <- "Otava9_nr3"

table4_9 <- mean_of_shapefile(Otava9_nr4,2000,2019)
mean4_9 <- annual_NDVI(table4_9)
mean4_9$geometry <- Otava9_nr4$geometry
mean4_9$id <- "Otava9_nr4"

table5_9 <- mean_of_shapefile(Otava9_nr5,2000,2019)
mean5_9 <- annual_NDVI(table5_9)
mean5_9$geometry <- Otava9_nr5$geometry
mean5_9$id <- "Otava9_nr5"

table6_9 <- mean_of_shapefile(Otava9_nr6,2000,2019)
mean6_9 <- annual_NDVI(table6_9)
mean6_9$geometry <- Otava9_nr6$geometry
mean6_9$id <- "Otava9_nr6"

table7_9 <- mean_of_shapefile(Otava9_nr7,2000,2019)
mean7_9 <- annual_NDVI(table7_9)
mean7_9$geometry <- Otava9_nr7$geometry
mean7_9$id <- "Otava9_nr7"

table8_9 <- mean_of_shapefile(Otava9_nr8,2000,2019)
mean8_9 <- annual_NDVI(table8_9)
mean8_9$geometry <- Otava9_nr8$geometry
mean8_9$id <- "Otava9_nr8"

table9_9 <- mean_of_shapefile(Otava9_nr9,2000,2019)
mean9_9 <- annual_NDVI(table9_9)
mean9_9$geometry <- Otava9_nr9$geometry
mean9_9$id <- "Otava9_nr9"

table10_9 <- mean_of_shapefile(Otava9_nr10,2000,2019)
mean10_9 <- annual_NDVI(table10_9)
mean10_9$geometry <- Otava9_nr10$geometry
mean10_9$id <- "Otava9_nr10"

table11_9 <- mean_of_shapefile(Otava9_nr11,2000,2019)
mean11_9 <- annual_NDVI(table11_9)
mean11_9$geometry <- Otava9_nr11$geometry
mean11_9$id <- "Otava9_nr11"

table12_9 <- mean_of_shapefile(Otava9_nr12,2000,2019)
mean12_9 <- annual_NDVI(table12_9)
mean12_9$geometry <- Otava9_nr12$geometry
mean12_9$id <- "Otava9_nr12"

table13_9 <- mean_of_shapefile(Otava9_nr13,2000,2019)
mean13_9 <- annual_NDVI(table13_9)
mean13_9$geometry <- Otava9_nr13$geometry
mean13_9$id <- "Otava9_nr13"

table14_9 <- mean_of_shapefile(Otava9_nr14,2000,2019)
mean14_9 <- annual_NDVI(table14_9)
mean14_9$geometry <- Otava9_nr14$geometry
mean14_9$id <- "Otava9_nr14"

table15_9 <- mean_of_shapefile(Otava9_nr15,2000,2019)
mean15_9 <- annual_NDVI(table15_9)
mean15_9$geometry <- Otava9_nr15$geometry
mean15_9$id <- "Otava9_nr15"

table16_9 <- mean_of_shapefile(Otava9_nr16,2000,2019)
mean16_9 <- annual_NDVI(table16_9)
mean16_9$geometry <- Otava9_nr16$geometry
```

```
mean16_9$id <- "Otava9_nr16"

table17_9 <- mean_of_shapefile(Otava9_nr17,2000,2019)
mean17_9 <- annual_NDVI(table17_9)
mean17_9$geometry <- Otava9_nr17$geometry
mean17_9$id <- "Otava9_nr17"

table18_9 <- mean_of_shapefile(Otava9_nr18,2000,2019)
mean18_9 <- annual_NDVI(table18_9)
mean18_9$geometry <- Otava9_nr18$geometry
mean18_9$id <- "Otava9_nr18"

table19_9 <- mean_of_shapefile(Otava9_nr19,2000,2019)
mean19_9 <- annual_NDVI(table19_9)
mean19_9$geometry <- Otava9_nr19$geometry
mean19_9$id <- "Otava9_nr19"

table20_9 <- mean_of_shapefile(Otava9_nr20,2000,2019)
mean20_9 <- annual_NDVI(table20_9)
mean20_9$geometry <- Otava9_nr20$geometry
mean20_9$id <- "Otava9_nr20"

table21_9 <- mean_of_shapefile(Otava9_nr21,2000,2019)
mean21_9 <- annual_NDVI(table21_9)
mean21_9$geometry <- Otava9_nr21$geometry
mean21_9$id <- "Otava9_nr21"

table22_9 <- mean_of_shapefile(Otava9_nr22,2000,2019)
mean22_9 <- annual_NDVI(table22_9)
mean22_9$geometry <- Otava9_nr22$geometry
mean22_9$id <- "Otava9_nr22"

table23_9 <- mean_of_shapefile(Otava9_nr23,2000,2019)
mean23_9 <- annual_NDVI(table23_9)
mean23_9$geometry <- Otava9_nr23$geometry
mean23_9$id <- "Otava9_nr23"

table24_9 <- mean_of_shapefile(Otava9_nr24,2000,2019)
mean24_9 <- annual_NDVI(table24_9)
mean24_9$geometry <- Otava9_nr24$geometry
mean24_9$id <- "Otava9_nr24"

table25_9 <- mean_of_shapefile(Otava9_nr25,2000,2019)
mean25_9 <- annual_NDVI(table25_9)
mean25_9$geometry <- Otava9_nr25$geometry
mean25_9$id <- "Otava9_nr25"

table26_9 <- mean_of_shapefile(Otava9_nr26,2000,2019)
mean26_9 <- annual_NDVI(table26_9)
mean26_9$geometry <- Otava9_nr26$geometry
mean26_9$id <- "Otava9_nr26"

table27_9 <- mean_of_shapefile(Otava9_nr27,2000,2019)
mean27_9 <- annual_NDVI(table27_9)
mean27_9$geometry <- Otava9_nr27$geometry
mean27_9$id <- "Otava9_nr27"

table28_9 <- mean_of_shapefile(Otava9_nr28,2000,2019)
mean28_9 <- annual_NDVI(table28_9)
mean28_9$geometry <- Otava9_nr28$geometry
mean28_9$id <- "Otava9_nr28"

table29_9 <- mean_of_shapefile(Otava9_nr29,2000,2019)
mean29_9 <- annual_NDVI(table29_9)
mean29_9$geometry <- Otava9_nr29$geometry
mean29_9$id <- "Otava9_nr29"

table30_9 <- mean_of_shapefile(Otava9_nr30,2000,2019)
mean30_9 <- annual_NDVI(table30_9)
mean30_9$geometry <- Otava9_nr30$geometry
mean30_9$id <- "Otava9_nr30"

table31_9 <- mean_of_shapefile(Otava9_nr31,2000,2019)
mean31_9 <- annual_NDVI(table31_9)
mean31_9$geometry <- Otava9_nr31$geometry
mean31_9$id <- "Otava9_nr31"

table32_9 <- mean_of_shapefile(Otava9_nr32,2000,2019)
mean32_9 <- annual_NDVI(table32_9)
mean32_9$geometry <- Otava9_nr32$geometry
mean32_9$id <- "Otava9_nr32"

table33_9 <- mean_of_shapefile(Otava9_nr33,2000,2019)
mean33_9 <- annual_NDVI(table33_9)
mean33_9$geometry <- Otava9_nr33$geometry
mean33_9$id <- "Otava9_nr33"

table34_9 <- mean_of_shapefile(Otava9_nr34,2000,2019)
mean34_9 <- annual_NDVI(table34_9)
mean34_9$geometry <- Otava9_nr34$geometry
mean34_9$id <- "Otava9_nr34"

table35_9 <- mean_of_shapefile(Otava9_nr35,2000,2019)
```

```
mean35_9 <- annual_NDVI(table35_9)
mean35_9$geometry <- Otava9_nr35$geometry
mean35_9$id <- "Otava9_nr35"

table36_9 <- mean_of_shapefile(Otava9_nr36,2000,2019)
mean36_9 <- annual_NDVI(table36_9)
mean36_9$geometry <- Otava9_nr36$geometry
mean36_9$id <- "Otava9_nr36"

table37_9 <- mean_of_shapefile(Otava9_nr37,2000,2019)
mean37_9 <- annual_NDVI(table37_9)
mean37_9$geometry <- Otava9_nr37$geometry
mean37_9$id <- "Otava9_nr37"

table38_9 <- mean_of_shapefile(Otava9_nr38,2000,2019)
mean38_9 <- annual_NDVI(table38_9)
mean38_9$geometry <- Otava9_nr38$geometry
mean38_9$id <- "Otava9_nr38"

table39_9 <- mean_of_shapefile(Otava9_nr39,2000,2019)
mean39_9 <- annual_NDVI(table39_9)
mean39_9$geometry <- Otava9_nr39$geometry
mean39_9$id <- "Otava9_nr39"

table40_9 <- mean_of_shapefile(Otava9_nr40,2000,2019)
mean40_9 <- annual_NDVI(table40_9)
mean40_9$geometry <- Otava9_nr40$geometry
mean40_9$id <- "Otava9_nr40"

table41_9 <- mean_of_shapefile(Otava9_nr41,2000,2019)
mean41_9 <- annual_NDVI(table41_9)
mean41_9$geometry <- Otava9_nr41$geometry
mean41_9$id <- "Otava9_nr41"

table42_9 <- mean_of_shapefile(Otava9_nr42,2000,2019)
mean42_9 <- annual_NDVI(table42_9)
mean42_9$geometry <- Otava9_nr42$geometry
mean42_9$id <- "Otava9_nr42"

table43_9 <- mean_of_shapefile(Otava9_nr43,2000,2019)
mean43_9 <- annual_NDVI(table43_9)
mean43_9$geometry <- Otava9_nr43$geometry
mean43_9$id <- "Otava9_nr43"

table44_9 <- mean_of_shapefile(Otava9_nr44,2000,2019)
mean44_9 <- annual_NDVI(table44_9)
mean44_9$geometry <- Otava9_nr44$geometry
mean44_9$id <- "Otava9_nr44"

table45_9 <- mean_of_shapefile(Otava9_nr45,2000,2019)
mean45_9 <- annual_NDVI(table45_9)
mean45_9$geometry <- Otava9_nr45$geometry
mean45_9$id <- "Otava9_nr45"

table46_9 <- mean_of_shapefile(Otava9_nr46,2000,2019)
mean46_9 <- annual_NDVI(table46_9)
mean46_9$geometry <- Otava9_nr46$geometry
mean46_9$id <- "Otava9_nr46"

table47_9 <- mean_of_shapefile(Otava9_nr47,2000,2019)
mean47_9 <- annual_NDVI(table47_9)
mean47_9$geometry <- Otava9_nr47$geometry
mean47_9$id <- "Otava9_nr47"

table48_9 <- mean_of_shapefile(Otava9_nr48,2000,2019)
mean48_9 <- annual_NDVI(table48_9)
mean48_9$geometry <- Otava9_nr48$geometry
mean48_9$id <- "Otava9_nr48"

table49_9 <- mean_of_shapefile(Otava9_nr49,2000,2019)
mean49_9 <- annual_NDVI(table49_9)
mean49_9$geometry <- Otava9_nr49$geometry
mean49_9$id <- "Otava9_nr49"

table50_9 <- mean_of_shapefile(Otava9_nr50,2000,2019)
mean50_9 <- annual_NDVI(table50_9)
mean50_9$geometry <- Otava9_nr50$geometry
mean50_9$id <- "Otava9_nr50"

table51_9 <- mean_of_shapefile(Otava9_nr51,2000,2019)
mean51_9 <- annual_NDVI(table51_9)
mean51_9$geometry <- Otava9_nr51$geometry
mean51_9$id <- "Otava9_nr51"

table52_9 <- mean_of_shapefile(Otava9_nr52,2000,2019)
mean52_9 <- annual_NDVI(table52_9)
mean52_9$geometry <- Otava9_nr52$geometry
mean52_9$id <- "Otava9_nr52"

table53_9 <- mean_of_shapefile(Otava9_nr53,2000,2019)
mean53_9 <- annual_NDVI(table53_9)
mean53_9$geometry <- Otava9_nr53$geometry
mean53_9$id <- "Otava9_nr53"
```

```
table54_9 <- mean_of_shapefile(Otava9_nr54,2000,2019)
mean54_9 <- annual_NDVI(table54_9)
mean54_9$geometry <- Otava9_nr54$geometry
mean54_9$id <- "Otava9_nr54"

table55_9 <- mean_of_shapefile(Otava9_nr55,2000,2019)
mean55_9 <- annual_NDVI(table55_9)
mean55_9$geometry <- Otava9_nr55$geometry
mean55_9$id <- "Otava9_nr55"

#nr. 10 Locenice
table1_10 <- mean_of_shapefile(Otava10_nr1,2000,2019)
mean1_10 <- annual_NDVI(table1_10)
mean1_10$geometry <- Otava10_nr1$geometry
mean1_10$id <- "Otava10_nr1"

table2_10 <- mean_of_shapefile(Otava10_nr2,2000,2019)
mean2_10 <- annual_NDVI(table2_10)
mean2_10$geometry <- Otava10_nr2$geometry
mean2_10$id <- "Otava10_nr2"

table3_10 <- mean_of_shapefile(Otava10_nr3,2000,2019)
mean3_10 <- annual_NDVI(table3_10)
mean3_10$geometry <- Otava10_nr3$geometry
mean3_10$id <- "Otava10_nr3"

table4_10 <- mean_of_shapefile(Otava10_nr4,2000,2019)
mean4_10 <- annual_NDVI(table4_10)
mean4_10$geometry <- Otava10_nr4$geometry
mean4_10$id <- "Otava10_nr4"

table5_10 <- mean_of_shapefile(Otava10_nr5,2000,2019)
mean5_10 <- annual_NDVI(table5_10)
mean5_10$geometry <- Otava10_nr5$geometry
mean5_10$id <- "Otava10_nr5"


#nr. 14 Blanice - Podedvory
table1_14 <- mean_of_shapefile(Otava14_nr1,2000,2019)
mean1_14 <- annual_NDVI(table1_14)
mean1_14$geometry <- Otava14_nr1$geometry
mean1_14$id <- "Otava14_nr1"

table2_14 <- mean_of_shapefile(Otava14_nr2,2000,2019)
mean2_14 <- annual_NDVI(table2_14)
mean2_14$geometry <- Otava14_nr2$geometry
mean2_14$id <- "Otava14_nr2"

table3_14 <- mean_of_shapefile(Otava14_nr3,2000,2019)
mean3_14 <- annual_NDVI(table3_14)
mean3_14$geometry <- Otava14_nr3$geometry
mean3_14$id <- "Otava14_nr3"

table4_14 <- mean_of_shapefile(Otava14_nr4,2000,2019)
mean4_14 <- annual_NDVI(table4_14)
mean4_14$geometry <- Otava14_nr4$geometry
mean4_14$id <- "Otava14_nr4"

table5_14 <- mean_of_shapefile(Otava14_nr5,2000,2019)
mean5_14 <- annual_NDVI(table5_14)
mean5_14$geometry <- Otava14_nr5$geometry
mean5_14$id <- "Otava14_nr5"

table6_14 <- mean_of_shapefile(Otava14_nr6,2000,2019)
mean6_14 <- annual_NDVI(table6_14)
mean6_14$geometry <- Otava14_nr6$geometry
mean6_14$id <- "Otava14_nr6"

table7_14 <- mean_of_shapefile(Otava14_nr7,2000,2019)
mean7_14 <- annual_NDVI(table7_14)
mean7_14$geometry <- Otava14_nr7$geometry
mean7_14$id <- "Otava14_nr7"

table8_14 <- mean_of_shapefile(Otava14_nr8,2000,2019)
mean8_14 <- annual_NDVI(table8_14)
mean8_14$geometry <- Otava14_nr8$geometry
mean8_14$id <- "Otava14_nr8"

table9_14 <- mean_of_shapefile(Otava14_nr9,2000,2019)
mean9_14 <- annual_NDVI(table9_14)
mean9_14$geometry <- Otava14_nr9$geometry
mean9_14$id <- "Otava14_nr9"

table10_14 <- mean_of_shapefile(Otava14_nr10,2000,2019)
mean10_14 <- annual_NDVI(table10_14)
mean10_14$geometry <- Otava14_nr10$geometry
mean10_14$id <- "Otava14_nr10"

table11_14 <- mean_of_shapefile(Otava14_nr11,2000,2019)
mean11_14 <- annual_NDVI(table11_14)
mean11_14$geometry <- Otava14_nr11$geometry
mean11_14$id <- "Otava14_nr11"
```

```
table12_14 <- mean_of_shapefile(Otava14_nr12,2000,2019)
mean12_14 <- annual_NDVI(table12_14)
mean12_14$geometry <- Otava14_nr12$geometry
mean12_14$id <- "Otava14_nr12"

table13_14 <- mean_of_shapefile(Otava14_nr13,2000,2019)
mean13_14 <- annual_NDVI(table13_14)
mean13_14$geometry <- Otava14_nr13$geometry
mean13_14$id <- "Otava14_nr10"

table14_14 <- mean_of_shapefile(Otava14_nr14,2000,2019)
mean14_14 <- annual_NDVI(table14_14)
mean14_14$geometry <- Otava14_nr14$geometry
mean14_14$id <- "Otava14_nr14"

table15_14 <- mean_of_shapefile(Otava14_nr15,2000,2019)
mean15_14 <- annual_NDVI(table15_14)
mean15_14$geometry <- Otava14_nr15$geometry
mean15_14$id <- "Otava14_nr15"

table16_14 <- mean_of_shapefile(Otava14_nr16,2000,2019)
mean16_14 <- annual_NDVI(table16_14)
mean16_14$geometry <- Otava14_nr16$geometry
mean16_14$id <- "Otava14_nr16"

table17_14 <- mean_of_shapefile(Otava14_nr17,2000,2019)
mean17_14 <- annual_NDVI(table17_14)
mean17_14$geometry <- Otava14_nr17$geometry
mean17_14$id <- "Otava14_nr17"

table18_14 <- mean_of_shapefile(Otava14_nr18,2000,2019)
mean18_14 <- annual_NDVI(table18_14)
mean18_14$geometry <- Otava14_nr18$geometry
mean18_14$id <- "Otava14_nr18"

table19_14 <- mean_of_shapefile(Otava14_nr19,2000,2019)
mean19_14 <- annual_NDVI(table19_14)
mean19_14$geometry <- Otava14_nr19$geometry
mean19_14$id <- "Otava14_nr19"

table20_14 <- mean_of_shapefile(Otava14_nr20,2000,2019)
mean20_14 <- annual_NDVI(table20_14)
mean20_14$geometry <- Otava14_nr20$geometry
mean20_14$id <- "Otava14_nr20"

table21_14 <- mean_of_shapefile(Otava14_nr21,2000,2019)
mean21_14 <- annual_NDVI(table21_14)
mean21_14$geometry <- Otava14_nr21$geometry
mean21_14$id <- "Otava14_nr21"

table22_14 <- mean_of_shapefile(Otava14_nr22,2000,2019)
mean22_14 <- annual_NDVI(table22_14)
mean22_14$geometry <- Otava14_nr22$geometry
mean22_14$id <- "Otava14_nr22"

table23_14 <- mean_of_shapefile(Otava14_nr23,2000,2019)
mean23_14 <- annual_NDVI(table23_14)
mean23_14$geometry <- Otava14_nr23$geometry
mean23_14$id <- "Otava14_nr23"

table24_14 <- mean_of_shapefile(Otava14_nr24,2000,2019)
mean24_14 <- annual_NDVI(table24_14)
mean24_14$geometry <- Otava14_nr24$geometry
mean24_14$id <- "Otava14_nr24"

table25_14 <- mean_of_shapefile(Otava14_nr25,2000,2019)
mean25_14 <- annual_NDVI(table25_14)
mean25_14$geometry <- Otava14_nr25$geometry
mean25_14$id <- "Otava14_nr25"

#nr.1 Pisek
total_1 <- rbind(mean1_1)
total2_1 <- total_1 %>% group_by(years) %>% summarize(ndvi = mean(NDVI), sd = mean(NDVI_SD))

ggplot(total2_1,aes(x=as.numeric(years),y=ndvi))+geom_point()+geom_errorbar(aes(ymin =ndvi, ymax = ndvi))+
  geom_smooth(se=FALSE)+labs(x="Year",y="NDVI", title = "Pisek nad")+theme_light()

#nr.2 Blanice - Putim pod
total_2 <- rbind(mean1_2, mean2_2, mean3_2,mean4_2, mean5_2, mean6_2, mean7_2, mean8_2, mean9_2, mean10_2, mean11_2, mean12_2, mean13_2, mean15_2,
mean16_2, mean17_2, mean18_2, mean19_2, mean20_2, mean21_2, mean22_2, mean23_2,mean24_2, mean25_2, mean26_2, mean27_2, mean28_2, mean29_2,
mean30_2, mean31_2, mean32_2, mean33_2, mean34_2, mean35_2, mean36_2, mean37_2, mean38_2, mean39_2, mean40_2, mean41_2, mean42_2, mean43_2,
mean44_2, mean45_2, mean46_2, mean47_2, mean48_2, mean49_2, mean50_2, mean51_2, mean52_2, mean53_2, mean54_2, mean55_2, mean56_2, mean57_2,
mean58_2, mean59_2, mean60_2, mean61_2, mean62_2, mean63_2, mean64_2, mean65_2, mean66_2, mean67_2, mean68_2, mean69_2, mean70_2, mean71_2,
mean72_2, mean73_2, mean74_2, mean75_2, mean76_2, mean77_2, mean78_2, mean79_2, mean80_2,mean81_2, mean82_2, mean83_2, mean84_2, mean85_2,
mean86_2, mean87_2, mean88_2, mean89_2, mean99_2,mean100_2, mean101_2, mean102_2, mean103_2, mean104_2, mean105_2, mean106_2, mean107_2,
mean108_2, mean109_2, mean110_2,mean111_2, mean112_2, mean113_2, mean114_2, mean115_2)
total2_2 <- total_2 %>% group_by(years) %>% summarize(ndvi = mean(NDVI), sd = mean(NDVI_SD))

ggplot(total2_2,aes(x=as.numeric(years),y=ndvi))+geom_point()+geom_errorbar(aes(ymin =ndvi-sd, ymax = ndvi+sd))+
  geom_smooth(se=FALSE)+labs(x="Year",y="NDVI", title = "Blanice - Putim pod")+theme_light()

#nr.3 Volyňka
```

```
total_3 <- rbind(mean1_3, mean2_3, mean3_3, mean4_3, mean5_3, mean6_3, mean7_3, mean8_3, mean9_3,mean10_3, mean11_3, mean12_3, mean13_3, mean14_3,
mean15_3,  mean16_3, mean17_3, mean18_3, mean19_3, mean20_3, mean21_3, mean22_3, mean23_3,mean24_3,mean25_3, mean26_3, mean27_3, mean28_3,
mean29_3, mean30_3, mean31_3, mean32_3, mean33_3, mean34_3, mean35_3, mean36_3, mean37_3, mean38_3, mean39_3, mean40_3, mean41_3, mean42_3,
mean43_3, mean44_3)
total2_3 <- total_3 %>% group_by(years) %>% summarize(ndvi = mean(NDVI), sd=mean(NDVI_SD))

ggplot(total2_3,aes(x=as.numeric(years),y=ndvi))+geom_point()+geom_errorbar(aes(ymin =ndvi, ymax = ndvi))+
  geom_smooth(se=FALSE)+labs(x="Year",y="NDVI", title = "Volyňka")+theme_light()

#nr.5 Černíčský potok
total_5 <- rbind(mean1_5,mean2_5, mean3_5, mean4_5, mean5_5)
total2_5 <- total_5 %>% group_by(years) %>% summarize(ndvi = mean(NDVI), sd = mean(NDVI_SD))

ggplot(total2_5,aes(x=as.numeric(years),y=ndvi))+geom_point()+geom_errorbar(aes(ymin =ndvi-sd, ymax = ndvi+sd))+
  geom_smooth(se=FALSE)+labs(x="Year",y="NDVI", title = "Černíčský potok")+theme_light()

#nr.9 Volšovkou
total_9 <- rbind(mean1_9, mean2_9, mean3_9,mean4_9, mean5_9, mean6_9, mean7_9, mean8_9, mean9_9, mean10_9, mean11_9, mean12_9, mean13_9, mean15_9,
mean16_9, mean17_9, mean18_9, mean19_9, mean20_9, mean21_9, mean22_9, mean23_9,mean24_9, mean25_9, mean26_9, mean27_9, mean28_9, mean29_9,
mean30_9, mean31_9, mean32_9, mean33_9, mean34_9, mean35_9, mean36_9, mean37_9, mean38_9, mean39_9, mean40_9, mean41_9, mean42_9, mean43_9,
mean44_9, mean45_9, mean46_9, mean47_9, mean48_9, mean49_9, mean50_9, mean51_9, mean52_9, mean53_9, mean54_9, mean55_9)
total2_9 <- total_9 %>% group_by(years) %>% summarize(ndvi = mean(NDVI), sd = mean(NDVI_SD))

ggplot(total2_9,aes(x=as.numeric(years),y=ndvi))+geom_point()+geom_errorbar(aes(ymin =ndvi, ymax = ndvi))+
  geom_smooth(se=FALSE)+labs(x="Year",y="NDVI", title = "Volšovkou")+theme_light()

#nr.10 Losenice
total_10 <- rbind(mean1_10,mean2_10, mean3_10, mean4_10, mean5_10)
total2_10 <- total_10 %>% group_by(years) %>% summarize(ndvi = mean(NDVI), sd = mean(NDVI_SD))

ggplot(total2_10,aes(x=as.numeric(years),y=ndvi))+geom_point()+geom_errorbar(aes(ymin = ndvi, ymax = ndvi))+
  geom_smooth(se=FALSE)+labs(x="Year",y="NDVI", title = "Losenice")+theme_light()

#nr.14 Blanice - Podedvory
total_14 <- rbind(mean1_14,mean2_14, mean3_14, mean4_14, mean5_14, mean6_14,mean7_14, mean8_14, mean9_14, mean10_14,mean11_14,mean12_14,
mean13_14, mean14_14, mean15_14, mean16_14,mean17_14, mean18_14, mean19_14, mean20_14, mean21_14, mean22_14, mean23_14, mean24_14, mean25_14)
total2_14 <- total_14 %>% group_by(years) %>% summarize(ndvi = mean(NDVI), sd = mean(NDVI_SD))

ggplot(total2_14,aes(x=as.numeric(years),y=ndvi))+geom_point()+geom_errorbar(aes(ymin =ndvi-sd, ymax = ndvi+sd))+
  geom_smooth(se=FALSE)+labs(x="Year",y="NDVI", title = "Blanice - Podedvory")+theme_light()

save.image(file = "martine_data.Rdata")
```